Application of Local Post-Tensioning to New and Existing Structures

by

Assaad Taoum

B.Eng (Hons)(Civil)
M.Eng (Civil)
MIEAust

Submitted in fulfilment of the requirements for the degree of Doctor of Philosophy

School of Engineering and ICT

University of Tasmania

February 2016

Supervisors:

Dr Hui Jiao

Dr Damien Holloway

DECLARATIONS

This thesis contains no material which has been accepted for a degree or diploma by the University or any other institution, except by way of background information and duly acknowledged in the thesis, and to the best of my knowledge and belief no material previously published or written by another person except where due acknowledgement is made in the text of the thesis, nor does the thesis contain any material that infringes copyright.

Assaad Taoum

Date: 06/07/2015

This thesis may be made available for loan and limited copying and communication in accordance with the Copyright Act 1968.

Assaad Taoum

Date: 06/07/2015

ACKNOWLEDGEMENTS

I would like to thank my supervisors, Dr Hui Jiao and Dr Damien Holloway for their uncountable advices and constant support over the whole period of my candidacy. Thanks are extended to the workshop staff at the School of Engineering and ICT for their technical support and to all those who helped me complete this project.

This research would not have been possible without the support of my family, to whom I dedicate this thesis.

Statement of Co-Authorship

The following people and institutions contributed to the publication of work undertaken as part of this thesis:

Assaad Taoum, *School of Engineering and ICT* = **Candidate**

Hui Jiao, *School of Engineering and ICT* = **Author 1**

Damien Holloway, *School of Engineering and ICT* = **Author 2**

Jon Shanks, *BuroHappold Engineering, Bath, UK* = **Author 3**

Author details and their roles:

Paper 1, *Flexural Behaviour of Locally Post-Tensioned Reinforced Concrete Beams:*

Located in Chapter 3

Paper 2, *Upgrading Steel I-Beams Using Local Post-Tensioning:*

Located in Chapter 4

Paper 3, *Using Locally Pre-stressed Reinforcing Bars to Restore the Capacity of Severely Damaged Steel Beams:*

Located in Chapter 5

For the above three papers, candidate was the primary author. The idea of local post-tensioning using a manual screw jack arose out of his Masters thesis, and he came up with the idea of applying it to a variety of beam types, including concrete, steel and timber. He designed and performed the experiments, analysed and presented the results.

Author 1 contributed towards developing the conceptual design of the jacking arrangement and design of the experiments.

Author 1 and author 2 provided technical consultation, particularly with the theoretical analysis, and assisted with refinement and final presentation.

Paper 4, *Behaviour of Locally Post-Tensioned Timber Panels under Serviceability Loads:*

Located in Chapter 6

The question of loss of stiffness of a panel made from low grade timber with joints arose out of previous work of Author 3. The Candidate, who was the primary author of this paper, proposed local post-tensioning as a solution to this problem. He designed the tensioning

strap arrangement in consultation with Author 3, and designed and performed the experiments, analysed and presented the results

Author 1 and Author 3 contributed towards developing the conceptual design. Author 3 has particular expertise and experience with timber.

Author 1 and author 2 provided technical consultation as for papers 1-3, and assisted with refinement and final presentation.

We the undersigned agree with the above stated "proportion of work undertaken" for each of the above published (or submitted) peer-reviewed manuscripts contributing to this thesis:

Signed: _____

Hui Jiao	*Andrew Chan*
Supervisor	*Head of School*
School Of Engineering and ICT	*School of Engineering and ICT*
University of Tasmania	University of Tasmania

Date: 9/06/2015

ABSTRACT

While the technology of post-tensioning has been widely used and well developed in concrete structures, it has also been applied to other structures, such as timber frame construction. In addition, post-tensioning, along with other strengthening techniques such as retrofitting and carbon fibre reinforced polymers (CFRP), has been used to strengthen and upgrade existing steel structures using similar materials and setup as in post-tensioned concrete beams. However the technology required for prestressed members can be very expensive and not widely available in many developing countries, or even in remote areas of developed countries such as Australia, and, if specified, may prove to be uneconomical if for example personnel and equipment have to be imported or relocated. The objective of this thesis is therefore to introduce and investigate *local post-tensioning* (LPT) as a simple and low-cost alternative to modern high-tech post-tensioning techniques. LPT uses conventional reinforcing bars and a manual screw jack (in the case of concrete or steel members) or bracing straps and bracing tensioners (in the case of timber members), instead of tendons and hydraulic jacks, to apply post-tensioning to the new or existing structure. This research investigated LPT reinforced concrete, timber and steel beams, resulting in the following findings:

- Four large-scale concrete beams were locally post-tensioned and tested. Theoretical predictions were made based on AS 3600-2009 and a new theoretical approach was proposed to determine the cracking moment of tested beams, since the current design guide was not applicable to this post-tensioning method.
- LPT timber panels were investigated as an application to new structures. Six identical panels made of butt jointed and nailed timber beams were post-tensioned and

tested under four-point bending. These were compared with equivalent panels made from continuous unjointed beams. In addition, the dynamic behaviour of these panels was experimentally investigated. Results showed that the post-tensioning created hogging deflections and decreased the overall serviceability deflections by almost half of their values; moreover, LPT affected the dynamic behaviour of these panels, in particular the damping ratio, which significantly decreased but remained within the acceptable limits.

- The effectiveness of LPT to enhance the repair of damaged steel beams was studied. Six repaired beams with different bar diameters and levels of pre-stress were tested under three-points bending. The level of post-tensioning controlled the beams' stiffness, while restoration of their ultimate load-carrying capacity was governed by the bar size. Significantly higher repaired capacities were achieved by this method than by other published methods used for the strengthening of steel beams.
- Upgrading of intact steel beams using LPT was also investigated. In total, seven beams were upgraded and tested under three-point bending, using different configurations of reinforcing steel. The level of post-tensioning, the type of LPT (internal or external) and the diameter of reinforcing bars used significantly affected the beams' stiffness and their ultimate load-carrying capacity. The results obtained in this study compared favourably with those of other methods used for upgrading steel beams.

List of Symbols

A Cross-sectional area of reinforcing bar, *[mm^2]*

A_g Gross-sectional area of concrete beam, *[mm^2]*

d Distance from the bottom of the void to the centre of post-tensioned bar, *[mm]*

D Total depth of cross-section, *[mm]*

E Young's modulus of steel, *[MPa]*

e Eccentricity from centroidal axis, *[mm]*

F Jacking force, *[kN]*

f Vertical displacement (jacking distance), *[mm]*

f'_c Compressive strength of concrete at 28 days, *[MPa]*

f_{cp} Concrete Strength at transfer, *[MPa]*

$f'_{ct.f}$ Characteristic flexural strength of concrete, *[MPa]*

I_g Gross second moment of area, *[mm^4]*

l Length of exposed section of reinforcing bar (equal to the length of the void), *[mm]*

M_{cr} Cracking moment, *[kN.m]*

M_{dec} Decompression moment, *[kN.m]*

M_u Ultimate moment, *[kN.m]*

N Tensile force within the reinforcing bar, *[kN]*

P Axial stressing force, *[kN]*

P_e Effective prestressing force, *[kN]*

P_i Initial prestressing force, *[kN]*

t Time, *[s]*

R Force applied on the beam by the testing machine, *[kN]*

Z Elastic section modulus, *[mm^3]*

δ Damping ratio, *[%]*

ε Strain, *[mm/mm]*

σ Stress, *[MPa]*

ω Frequency, *[Hz]*

Table of Contents

List of Figures

List of Tables

1. Introduction

1.1. Background

Post-tensioned concrete is the most recent of the major forms of construction being introduced into structural engineering. Within the field of building structures, most post-tensioned concrete applications are in the form of cast-in-situ continuous floor, beams and slabs. When compared to ordinary reinforced concrete, prestressing provides improved service load behaviour, high span-to-depth ratios and increased stiffness and crack resistance. While the technology of post-tensioning has been widely used and well developed in concrete structures, it has also been applied to other structures, such as timber frame construction, to allow increased span-to-depth ratios and decreased deflections under service loads. In addition, post-tensioning, along with other strengthening techniques such as retrofitting and carbon fibre reinforced polymers (CFRP), were used to strengthen and upgrade existing steel structures by using similar materials and setup as in post-tensioned concrete beams.

1.2. Problem definition

According to Hurst and Spon (1998), the technology required for prestressed members can be very expensive and widely not available in many developing countries or even in remote areas of developed countries such as Australia, and, if specified, may prove to be uneconomical if for example personnel and equipment have to be imported or relocated. The erection of in situ post-tensioned structures requires special technologies and equipment, which are relatively expensive and may not be available in all cases or simply cannot be used in particular cases such as in strengthening and reconstruction.

This thesis therefore seeks alternative low cost and low technology methods of post-tensioning, suitable for developing countries or remote locations.

1.3. Objectives of work

The objective of this thesis was to introduce and investigate local post-tensioning (LPT), as a simple and low-cost alternative to the above-mentioned post-tensioning techniques. The idea of LPT consists of adopting conventional reinforcing bars tensioned using a manual screw jack (in the case of concrete and steel members) and bracing straps and bracing tensioners (in the case of timber members), instead of tendons and hydraulic jacks, to apply post-tensioning to the new or existing structure.

1.4. Research outline

The outline of the thesis is considered below.

Chapter 2 reviews and summarises existing literature related to LPT in 3 main areas: post-tensioned concrete beams, post-tensioned and mass timber panels and existing repair and upgrading techniques of steel girders.

Chapter 3 investigates the behaviour of locally post-tensioned reinforced concrete beams. Four large-scale concrete beams were locally post-tensioned and tested. The theoretical predictions were made based on AS 3600-2009. A new theoretical approach was proposed to determine the cracking moment of tested beams, since the current design guide was not applicable to this post-tensioning method. The findings of this chapter were published in the *Australian Journal of Structural Engineering* 16(2): 1-7 (2015).

In **Chapter 4**, the behaviour of locally post-tensioned timber panels was investigated as part of applying LPT to new structures. Six identical panels made of butt jointed and nailed

timber beams were post-tensioned and tested under four-point bending. These were compared with equivalent panels made from continuous unjointed beams. In addition, the dynamic behaviour of these panels was experimentally investigated. The findings of this chapter were submitted for review and publication in *Engineering Structures* journal.

Chapter 5 investigated the behaviour of damaged steel beams repaired using LPT. Six beams with different bar diameters and levels of pre-stress were repaired and tested under three-points bending. Significantly higher repaired capacities were achieved by this method than by other published methods used for the strengthening of steel beams. The results were published in the *International Journal of Steel Structures* 15(1): 125-134 (2015).

Chapter 6 investigates the behaviour of steel beams upgraded using LPT. The results obtained in this study were compared to those of other methods used for upgrading steel beams. The outcomes of this chapter were published in the *Journal of Constructional Steel Research* 113: 127-134 (2015).

Chapter 7 summarises the major outcomes of this research and the possibilities for future research using LPT.

2. Literature Review

2.1. Post-tensioned continuous concrete beams

2.1.1. Background

Like reinforced concrete, prestressed concrete is a composite material that uses to advantage the compressive strength of concrete, while circumventing its weakness in tension. Prestressed concrete is made from structural concrete, usually of high strength, and small quantities of very-high-strength tendons, which are often grouped together to form cables. Prestressing involves the application of an initial compressive load on the concrete structure to reduce or eliminate the internal tensile forces and thereby control or eliminate cracking. Usually, some ordinary reinforcing steel is also included, both as subsidiary longitudinal reinforcement and as transverse stirrups to resist shear (Gilbert & Mickleborough, 1990; Warner & Faulkes, 1988).

Prestressed concrete has many advantages over ordinary reinforced concrete, including improved behaviour under service load, efficient use of high strength steel and concrete, higher span-to-depth ratios, improved recovery after overload, improved strength in shear and torsion and improved fatigue resistance (Loo & Chowdhury, 2010; Sengupta & Menon, 2007; Warner & Faulkes, 1988).

In the field of building structures, most prestressed concrete applications are in the form of simply supported precast floor and roof beams. These are usually factory-made, where the advantages of controlled mass production can be realised. Where large spans are required, in situ prestressed concrete beams are sometimes used, and in situ prestressed concrete flat slab construction is increasingly being employed (Hurst & Spon, 1998).

Despite its obvious advantages over ordinary reinforced concrete, prestressed concrete requires sophisticated and expensive technology to be implemented, as mentioned previously. In addition, post-tensioning continuous members require the prestress cable duct to sag in the span and hog over the support, which makes this process even more costly and complicated.

2.1.2. Externally post-tensioned beams

Externally post-tensioned beams, or beams with external tendons have been used in the construction of new structures and in strengthening existing ones. External tendons may be rectilinear (Figure 2.1) or draped with a path fixed by end anchorages and by intermediate saddle points (Figure 2.2) in order to induce a set of forces on the beam which opposes the external loads (Dall'Asta & Zona, 2005). The main advantage of such technique is the simplicity of installation and the ease of inspection compared to the internal tendons system (Alkhairi & Naaman, 1993; Harajli, Khairallah, & Nassif, 1999; Tan, 2014).

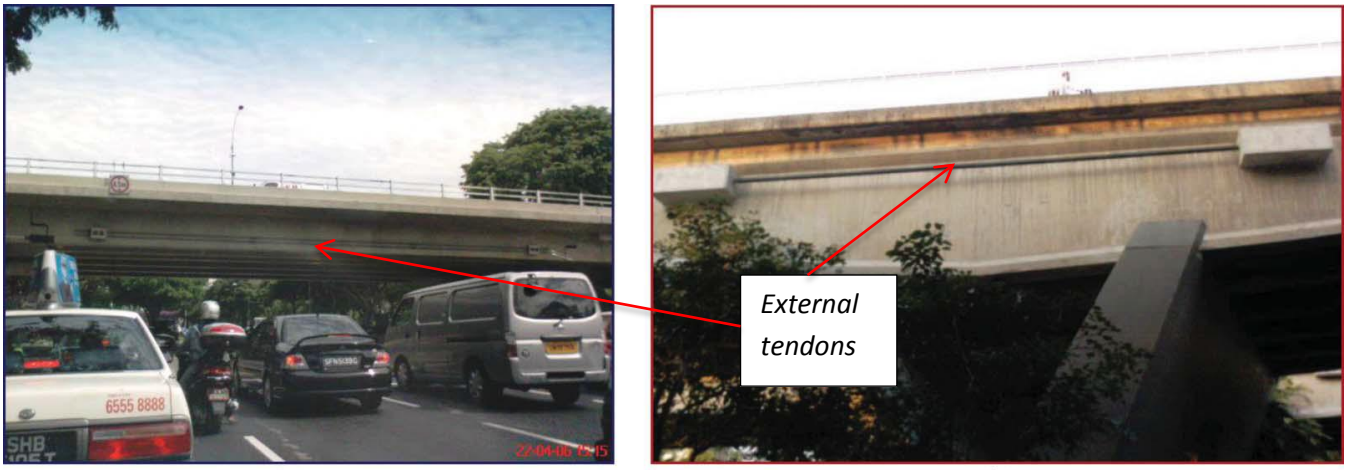

Figure 2.1. Strengthening of girders with external tendons. (a) Positive moment region. (b) Negative moment region (Tan, 2014).

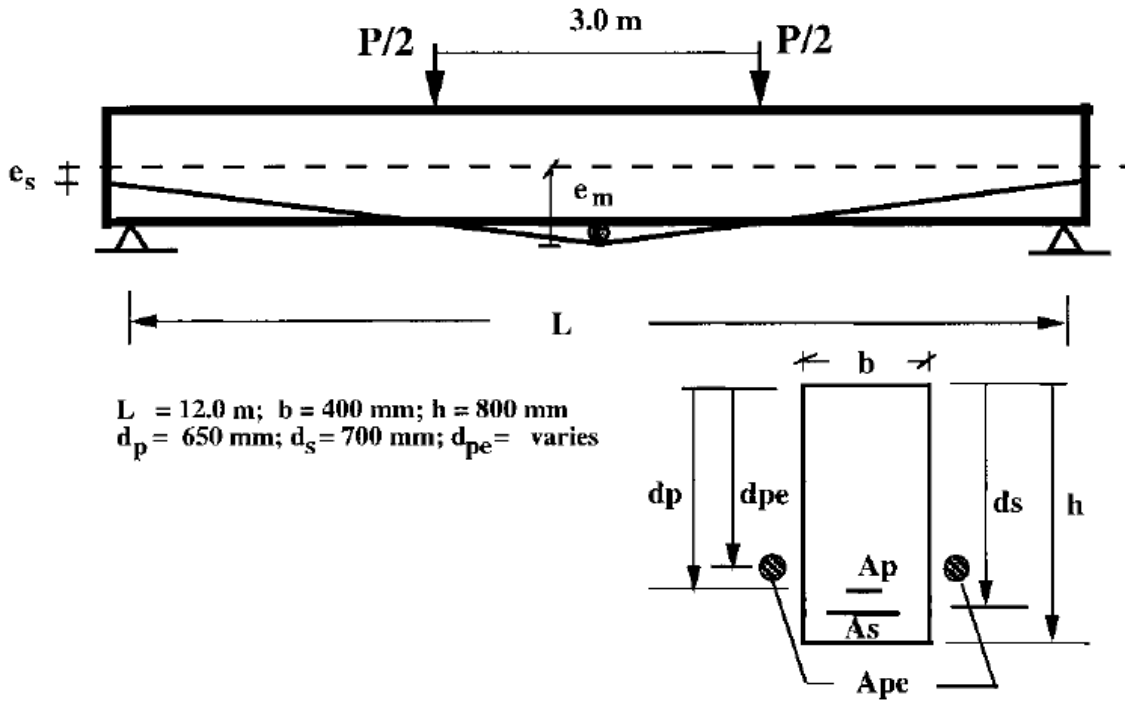

Figure 2.2. Dimensions of an externally post-tensioned beam evaluated by (Harajli et al., 1999).

Ibrahim (2010); Rao and Mathew (1996) suggest that the analysis of externally prestressed member is similar to the internally prestressed one with unbounded tendons except for 2 points: the possible slip at a deviation point and shift of tendon eccentricity due to the deformation of structure, which can have a considerable effect on the ultimate load behaviour.

Shagin (1996, 2005, 2008) suggested local post-tensioning to replace expensive prestressing tendons that require sophisticated equipment and training, to be installed by ordinary reinforcing bars and a manual screw jack that are both cheap and require no special skills or training to be implemented (Figure 2.3).

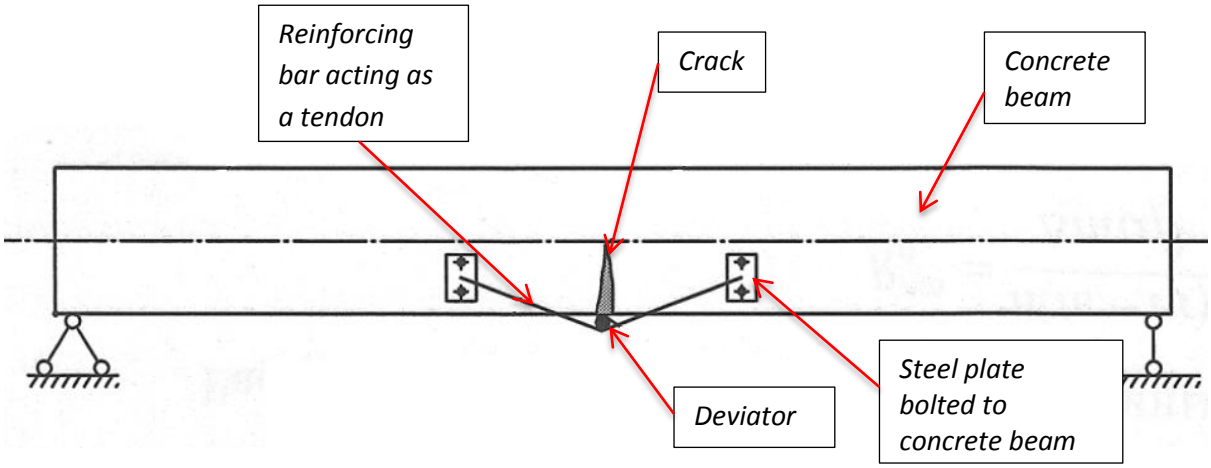

Figure 2.3. Strengthening cracked concrete beams using local post-tensioning (Shagin, 2008).

2.2. Post-tensioned mass timber panels

2.2.1. Post-tensioned timber structures

Post-tensioned timber beams and frames have been used to reduce the depth of timber beams opening up the way for multi-storey timber office and commercial buildings (van Breeschoten et al., 2012). According to Buchanan, Palermo, Carradine, and Pampanin (2011) recent developments in New Zealand and Australia have resulted in the development of unbonded post-tensioned timber frames for use in multi-storey and long-span structures. Initially, this system was developed as moment-resisting frames to resist earthquake loading (Palermo, Pampanin, Buchanan, & Newcombe, 2005), following developments in precast concrete seismic design (Priestley, Sritharan, Conley, & Pampanin, 1999). Unbonded post-tensioned concrete frames have further evolved to non-seismic frames, known as the "Brooklyn system" (Pampanin, Pagani, & Zambelli, 2004). The same design principles were later applied to timber with research focusing on gravity design of post-tensioned frames for

multi-storey timber buildings. Among many sections developed, core box sections form the most efficient cross-section and allow for easy application of internal posttensioning (van Beerschoten et al., 2012).

Design of long span timber beams and roof systems is often governed by deflection criteria, resulting in an underutilisation of the strength of timber. This can partly be resolved by adding a precamber which can be achieved during fabrication of glulam beams, but is difficult for Laminated Veneer Lumber (LVL) beams. Analogously to post-tensioned concrete beams, the use of post-tensioning induces a precamber to hollow core box beams resulting in decreased deflections. Either straight tendons, anchored at the bottom of the beam, or draped tendons, anchored centrically can be used (Figure 2.4, Figure 2.5, Figure 2.6). Beams can be manufactured and stressed off-site, similar to precast concrete beams (Lago & Dibenedetto, 2009; van Beerschoten et al., 2012).

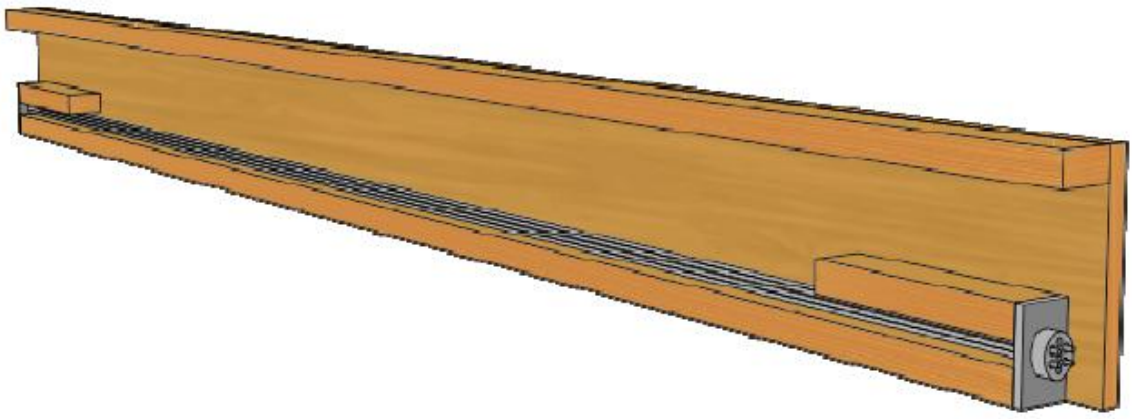

Figure 2.4. Longitudinal section of timber box beams with straight post-tensioning tendons (van Beerschoten et al., 2012).

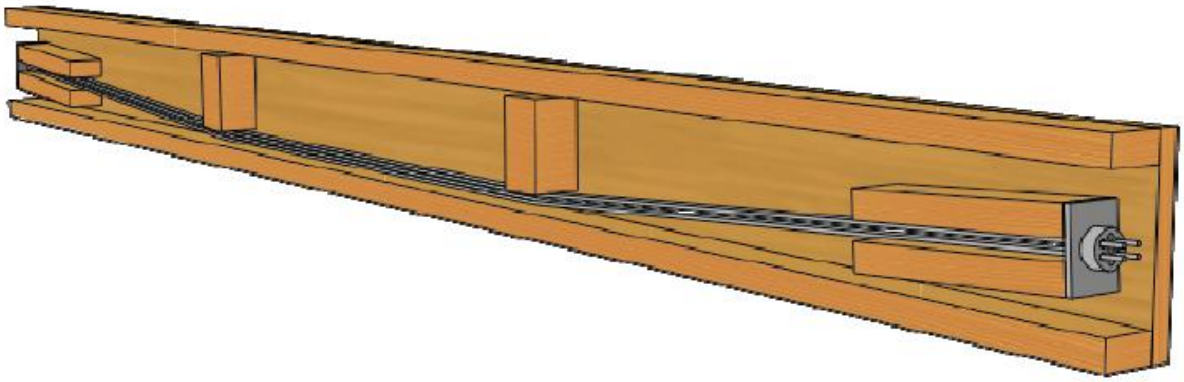

Figure 2.5. Longitudinal section of timber box beams with drapped post-tensioning tendons (van Beerschoten et al., 2012).

Figure 2.6. Experimental testing of 9m post-tensioned timber box beam, (top) side view, (bottom left) deviator and (bottom right) end view (van Beerschoten et al., 2012).

It is worth to mentioning that developing moment resisting connections in timber is difficult and usually large steel components are necessary (Buchanan & Fairweather, 1993), compromising cost-efficiency of the structural system (van Beerschoten et al., 2012).

2.2.2. Mass timber panels

Mass timber panels have been used in the residential construction industry for a long time. One of the relevant examples is the Brettstapel timber flooring panel that uses hardwood dowels to connect vertically laminated timber (Figure 2.7). The dowels have a moisture content lower than that of the posts, and due to moisture equilibrum over time, they expand and and lock the posts together creating a structural load-bearing system (Henderson, Foster, & Bridgstock, 2012a)

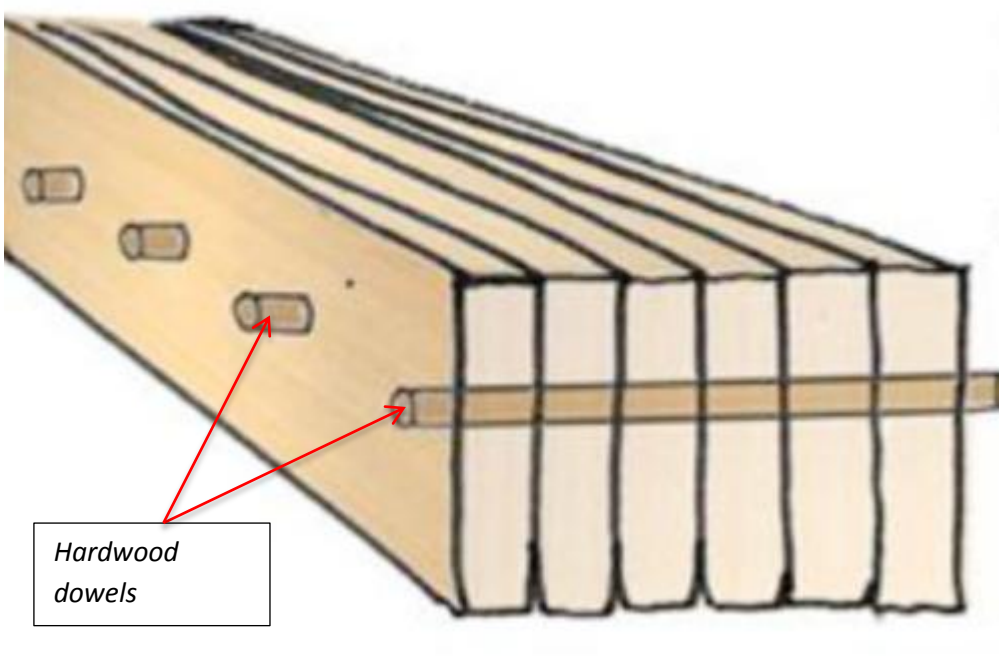

Figure 2.7. Horizontally dowelled Brettstapel (Henderson et al., 2012a; Henderson, Foster, & Bridgstock, 2012b)

According to Henderson et al. (2012b) this system can be prefabricated offsite and then erected relativly quickly on the construction site, with spans ranging from 3 to 15 m in one direction.

Another example is the O'portune, or staggered timber slabs, developed at the Suiss Federal Institut of Technology Lusanne in the late 1990's (Figure 2.8). This system achieved greater rigidity, due to its increased depth, than standard mass timber panels, while reducing the amount of required timber (CBS & CBT, 2011b; Sandoz & des Jordils, 2004).

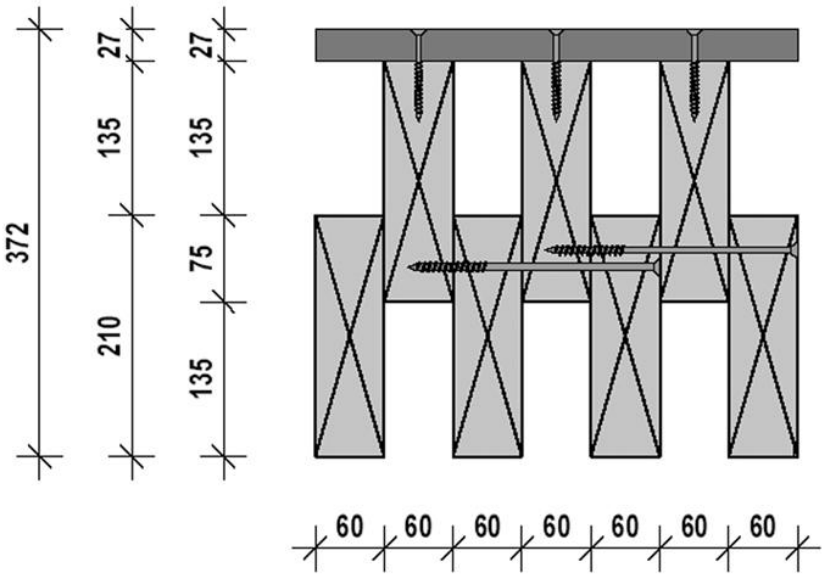

Figure 2.8. Final cross-section of the O'portue system (CBS & CBT, 2011b; Sandoz & des Jordils, 2004).

For spans between 9 and 12 m, this system is used as complete slab, however, when smaller spans are involved (typicaly 6-8m), O'portune is used as a conventional beam occupying half to a third of the floor area, with planar elements between the down stand members (Figure 2.9).

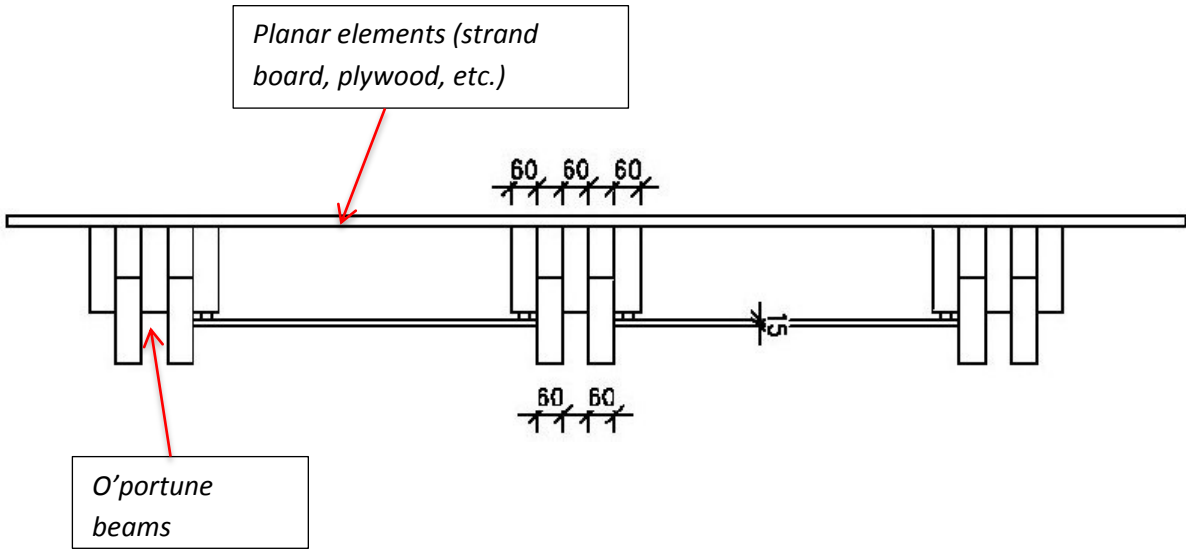

Figure 2.9. Partial O'portune slab used as beams for 6-8 m spans (Sandoz & des Jordils, 2004).

To achieve even greater spans (up to 18 m), the O'porune system can be improved by adding a concrete filling on the top (Figure 2.10). In this case, the concrete bears all the compression stresses while the timber panels counter the tensile stresses (CBS & CBT, 2011a; Sandoz & des Jordils, 2004).

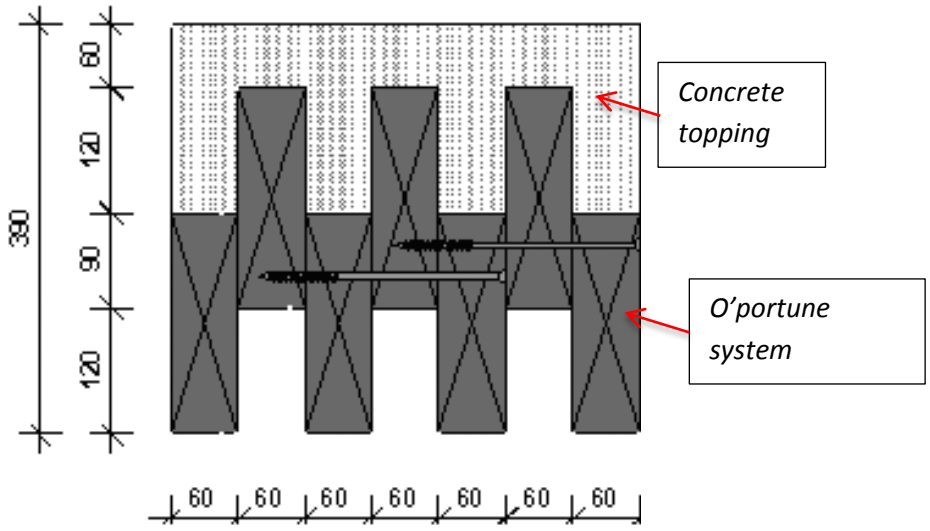

Figure 2.10. Cross section of the wood-concrete composite slab for spans up to 18 m (CBS & CBT, 2011a; Sandoz & des Jordils, 2004).

2.2.3. Composite timber panels

The Centre for Sustainable Architecture with Wood (CSAW), a research department of the University of Tasmania, investigated the use of composite timber panel as an alternative to a reinforced concrete beam. In this suggested system, low grade timber carries the compression in bending and a soffit, attached to the panel, acts as a tensile element (Baxter, 2014; Hamilton, 2014; Schaap, 2012; Snowball, 2013).

Many systems were proposed and tested, including systems similar to O'portune made of low-grade timber with a plywood tension element (Figure 2.11), and fiber reinforced cement sheets (Figure 2.12) attached to soffit (Baxter, 2014; Hamilton, 2014).

Figure 2.11. Plywood tension element attached to panel's soffit (Baxter, 2014)

Figure 2.12. Fibre reinforced cement sheet attached to the panel's soffit (Baxter, 2014).

Experimental results showed that low-grade non-structural timber can be used in large-span residential structural applications if it is a part of a composite panel approach, and although the proposed systems met the Australian Standard performance criteria for serviceability (mid-span deflection and natural frequency of vibration) at a span of 4.2 m, it was recommended to reduce the span in order for the system to be accepted by residential home owners (Baxter, 2014).

As it can be concluded, there is a potential to apply post-tensioning to the mass timber systems for improved performance under serviceability loading condition.

2.3. Repairing and upgrading steel beams

2.3.1. Background

Due to the aging of structures and the increase of traffic loads many steel bridges are experiencing corrosion damage and fatigue cracks in areas of high stress concentration.

Moreover, many steel bridges are rendered structurally inadequate with the increase of traffic loads, or simply due to upgrading existing design standards (Colombi & Poggi, 2006; Deng & Lee, 2009; Kim, Green M F., & J., 2008; Kim & Yoon, 2010; Shahrooz, Saraf, Godbole, & Miller, 2002; Wardhana & Hadipriono, 2003). It is estimated that in the United States alone, 25% of bridges, of which 50% are made of steel, are structurally deficient or functionally obsolete (ASCE, 2005; Deng & Lee, 2009; Kim & Brunell, 2011; Klaiber, Dunker, Wipf, & Sanders Jr, 1988).

The replacement of these structures is costly and will lead to the interruption to traffic. Therefore various structural repair techniques and strengthening mechanism have been used to mitigate this issue (Hmidan, Kim, & Yazdani, 2011; Kim & Brunell, 2011; Kim & Harries, 2012; Photiou, Hollaway, & Chryssanthopoulos, 2006).

2.3.2. Existing repair and upgrading techniques

Bolting or welding of steel plates to existing steel beams is one of the most widely used repair techniques (Kim & Brunell, 2011; Tavakkolizadeh & Saadatmanesh, 2003). However there are issues related to this method. For example, the added plates increase the self-weight of the structure. In addition, the welding or bolting process may introduce new stress concentrations in the repaired region, causing a reduction of structural fatigue life (Colombi & Poggi, 2006; Hmidan et al., 2011; Kim & Brunell, 2011; Lenwari, 2006; Nozaka, Shield, & Hajjar, 2005; Roy, Lang, & May, 2009). Another strengthening method involves applying carbon-fibre reinforced polymer (CFRP), adding sheets bonded to the web or soffit of steel beams. Due to the features of light weight, good durability and ease of handling (Nozaka et al., 2005; Tavakkolizadeh & Saadatmanesh, 2003), use of FRP materials appears to be a convenient and efficient method for increasing the load carrying capacity of the

existing beams (Jiao, Mashiri, & Zhao, 2012; Kim & Brunell, 2011; Kim & Harries, 2012; Lenwari, 2006; Tavakkolizadeh & Saadatmanesh, 2003).

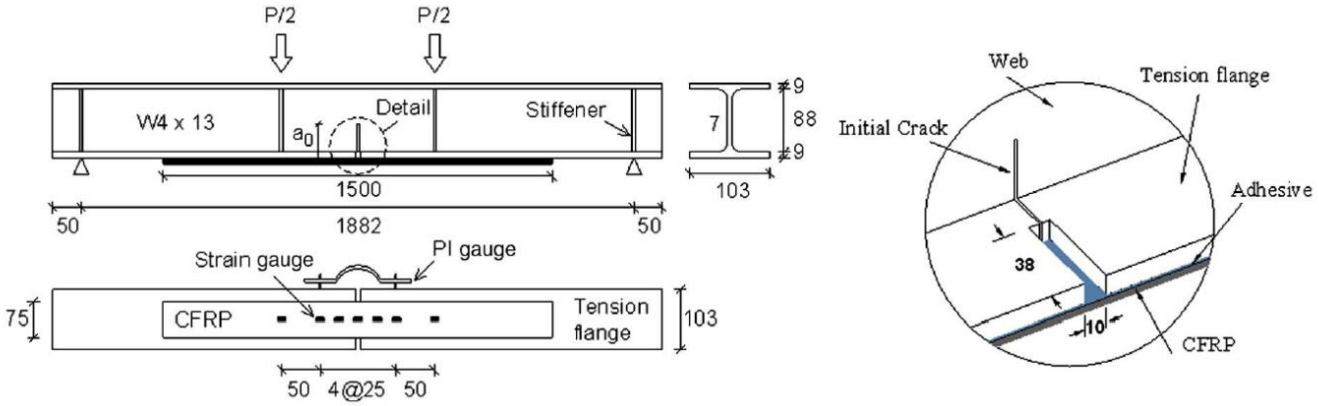

Figure 2.13. Beam details and test setup by Hmidan et al. (2011).

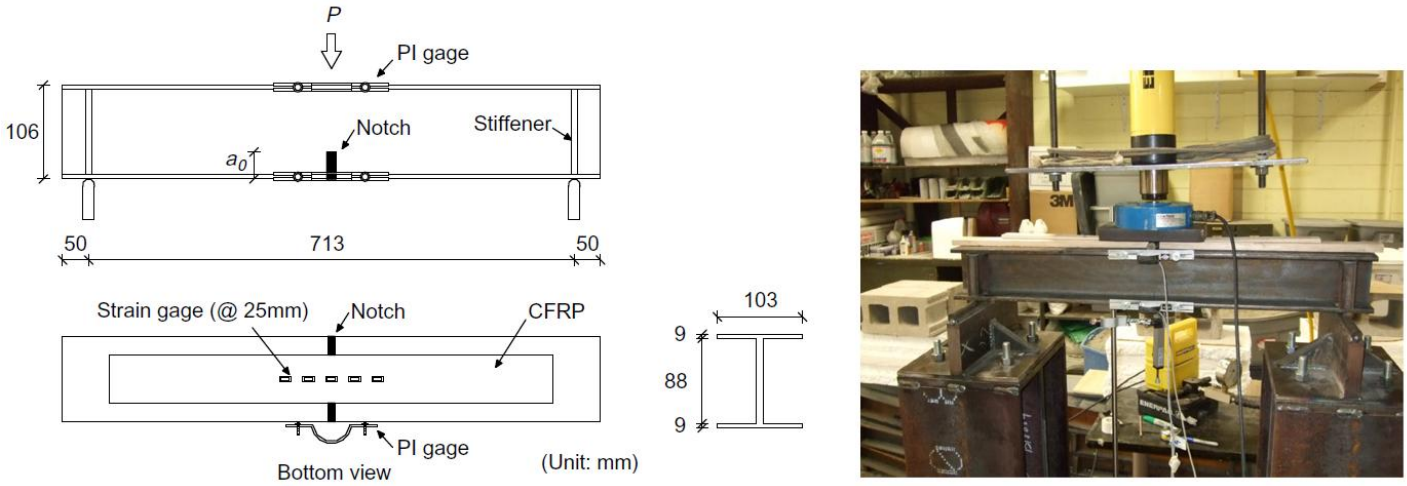

Figure 2.14. Test beams and test setup by Kim and Brunell (2011).

Figures 2.13 and 2.14 show the test setups of two researches on using CFRP sheets to strengthen steel beams that have an initial induced damage. Results of these studies showed that the CFRP repair increased the load-carrying capacity of the damaged beams by almost 23% and effectively reduced crack-opening of the damaged beams while delaying the crack formation across the steel section (Kim & Brunell, 2011). Nevertheless, Hmidan et al. (2011) noticed that the load carrying capacity and serviceability of tested repaired beams

were significantly affected by the level of initial induced damage. The effectiveness of the repair, measured through the experimental ultimate moment dropped by more than 50% when the ratio of the crack depth to the depth of the beam, a_0/h, was increased from 0.1 to 0.5.

The use of CFRP for upgrading steel beams was investigated by many researchers. Among the studies made, were those conducted by Colombi and Poggi (2006); Linghoff, Al-Emrani, and Kliger (2010); Narmashiri, Sulong, and Jumaat (2011); Yu, Chiew, and Lee (2011). In all these studies, CFRP was used to strengthen steel I-beams, which were subject to 3-point and 4-point bending tests (Figure 2.15).

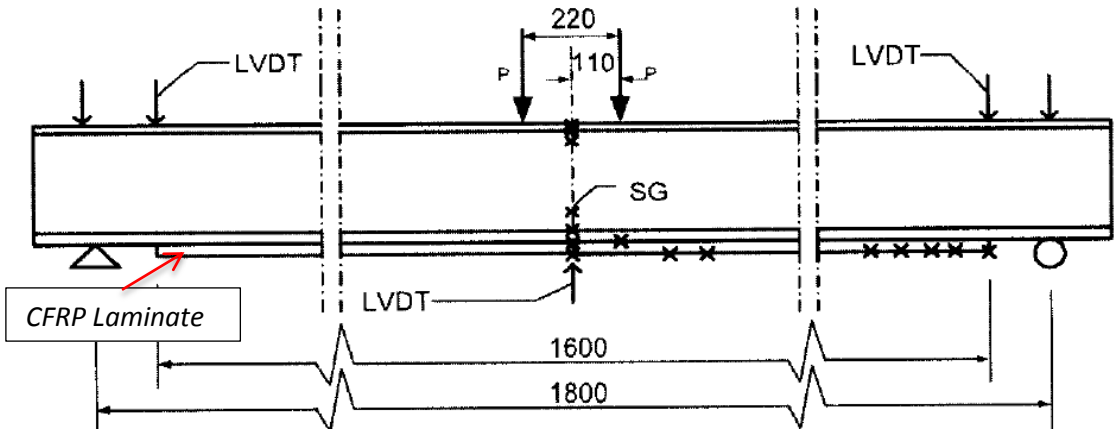

Figure 2.15. Sketch of the test setup and strain gauges locations used by Linghoff et al. (2010).

Test results showed that the flexural behaviour of upgraded beams was significantly improved by the CFRP. Linghoff et al. (2010) stated that a 20% increase of bending stress is possible by applying CFRP to the tension flange of an I-beam. Increased stiffness was obtained by using a larger amount of CFRP. Narmashiri et al. (2011) stated that applying a thicker CFRP layer resulted in an increase of the load carrying capacity; however, results

from these 2 studies showed that when increasing the thinness of CFRP, the fibre showed brittle behaviour and premature debonding.

Yu et al. (2011) outlined that, when using CFRP for upgrading steel beams, the most important strengthening parameter is the bond length, because when compared to other parameters, it could be much more easily changed in engineering practice. They also stated that longer bond length will lead to a higher bond failure load and larger effective tension area of the beam.

Finally, experiments conducted by Colombi and Poggi (2006) showed that reinforcing beams with CFRP strips produces an improvement in the load-carrying capacity and in the yield load of the strengthened beams. Such increments in yield loads reached almost 24% for the beams strengthened with 2 layers of CFRP and around 20% for those strengthened with only 1 layer of the same CFRP material. Nevertheless, no significant differences in load-deflection curves or yield loads were observed strengthened using the same CFRP setup but different epoxy adhesives.

2.3.3. Using post-tensioning to strengthen and upgrade existing composite structures

In addition to these methods, external prestressed tendons have been used to strengthen existing composite steel-concrete beam structures (Albercht & Lenwari, 2008; Ayyub, Sohn, & Saadatmanesh, 1992; Chen, 2005; Chen & Gu, 2004; Nie, Tao, Cai, & Li, 2011; Qader, Agarwal, & Ibrahim, 2013; Uy, 2007; W. Xue, Ding, He, & Li, 2008; W. C. Xue & Li, 2001). This technique involves welding end anchorages and using conventional high-strength post-tensioning cables (Figure 2.16). Results proved that the initial force in the tendon and its eccentricity significantly affect the strength and stiffness of tested beams (Uy & Craine,

2004), and in some cases, this type of strengthening lead to a 25% increase in load carrying capacity (Lorenc & Kubica, 2006).

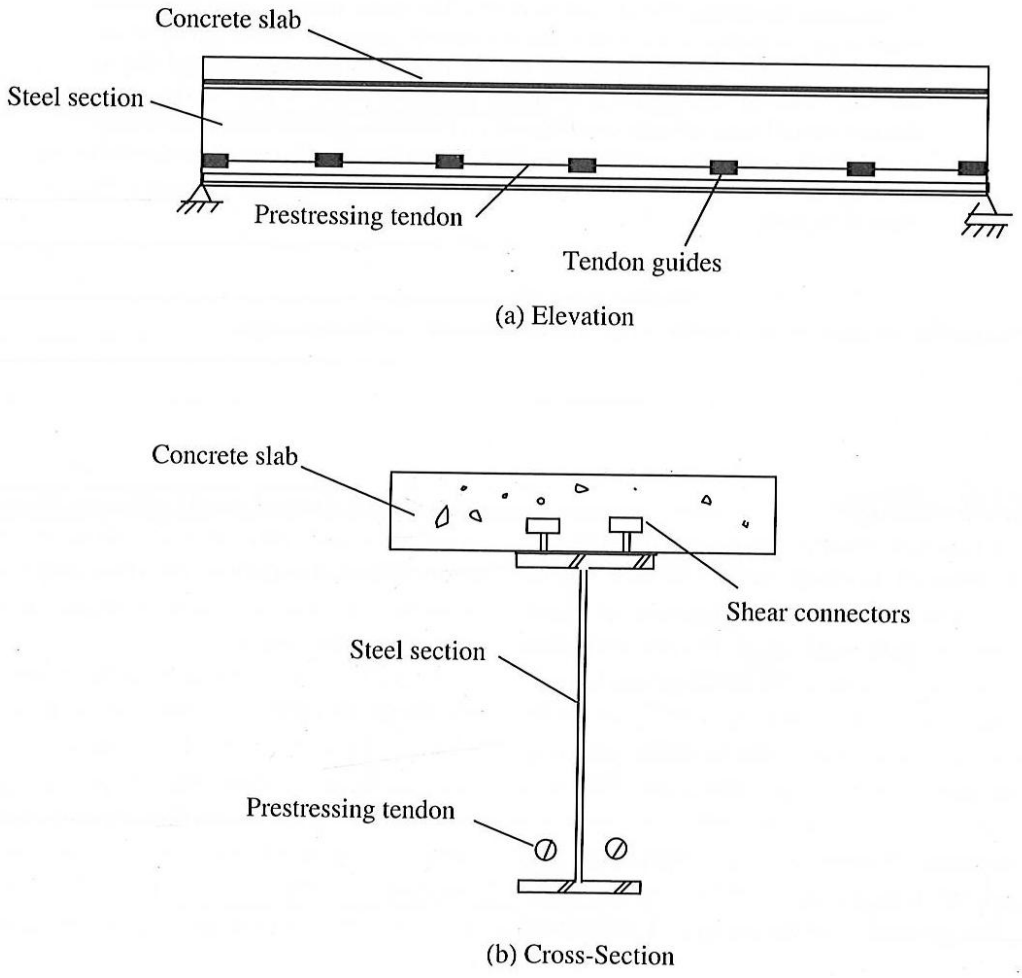

Figure 2.16. Elevation and cross section of post-tensioned composite beam (Uy & Craine, 2004).

3. Flexural Behaviour of Locally Post-Tensioned Reinforced Concrete Beams

3.1. Introduction

As mentioned previously, prestressed concrete has many advantages over ordinary reinforced concrete, including improved behaviour under service load, efficient use of high strength steel and concrete, higher span-to-depth ratios, improved recovery after overload, improved strength in shear and torsion and improved fatigue resistance (Loo & Chowdhury, 2010; Sengupta & Menon, 2007; Warner & Faulkes, 1988).

However, the technology required for prestressing (in particular post-tensioning) concrete can be very expensive and not readily available in many developing countries or even in remote areas of large countries such as Australia, and, if specified, may prove to be uneconomical since all personnel and equipment have to be imported or relocated (Hurst & Spon, 1998). In addition, post-tensioning continuous members requires the prestress cable duct to sag in the span and hog over the support, which makes this process even more costly and complicated (See Section 2.1)

As an alternative to the existing post-tensioning methods, this chapter presents an experimental and theoretical study incorporating locally post-tensioned continuous concrete beams, a subject that has not been explored in the past. The aim of this chapter is to investigate the behaviour of locally post-tensioned concrete beams and to examine the effect of different levels of post-tensioning on the stiffness and crack-resistance of concrete beams.

3.2. Specimen preparation and test setup

3.2.1. Specimens

It would be ideal to perform continuous beam tests to study the complete performance of concrete beams under loading, however due to the limitation of testing facilities the effect of local post-tensioning in continuous beams in the above-support area with the negative bending moment was investigated. This is particularly important since the negative bending moments in these areas of the beams are typically 1.5-1.75 higher than the positive bending moments in the mid-span of the beam. Also, it is worth noting that three point bending tests have been widely used by many researchers as a standard testing method of the behaviour of beam elements.

To study the effect of post-tensioning, four beams with different levels of post-tensioning were tested. As shown in Figure 3.1, the reinforced concrete beams used in this testing had a cross section of 250 mm in depth by 300 mm in width and length of 3m. Four N16 grade 500 deformed reinforced steel bars were used as the main tensile reinforcement (including 2 partially exposed) and four N12 grade 500 deformed bars were used as the secondary reinforcement in the compression section. Also, 10 mm diameter plain reinforcing steel grade 250N, were provided as the shear reinforcement with a spacing of 150 mm. A void 116 mm deep, 150 mm wide and 1500 mm long was cast in the concrete to partially expose two 16 mm diameter bars (to be post-tensioned later). In real construction, this void is to be filled with concrete after finishing the post-tensioning process, however, in this study, the void was not filled, in order to avoid any complications in the process of installation and data acquisition from steel reinforcing bars strain gauges. All reinforcing bars have a normal yield strength of 500 MPa specified in AS/NZS 4671:2001 (Standards Australia Limited,

2001). The reinforcement had a distinctive plastic zone with a uniform strain of 0.05 and an ultimate fracture strain of 0.2. The concrete used was of grade 40 ($f_c^{'}$=40 *MPa*). The concrete properties were verified through compressive tests according to AS 1012.9-1999 (Standards Australia Limited).

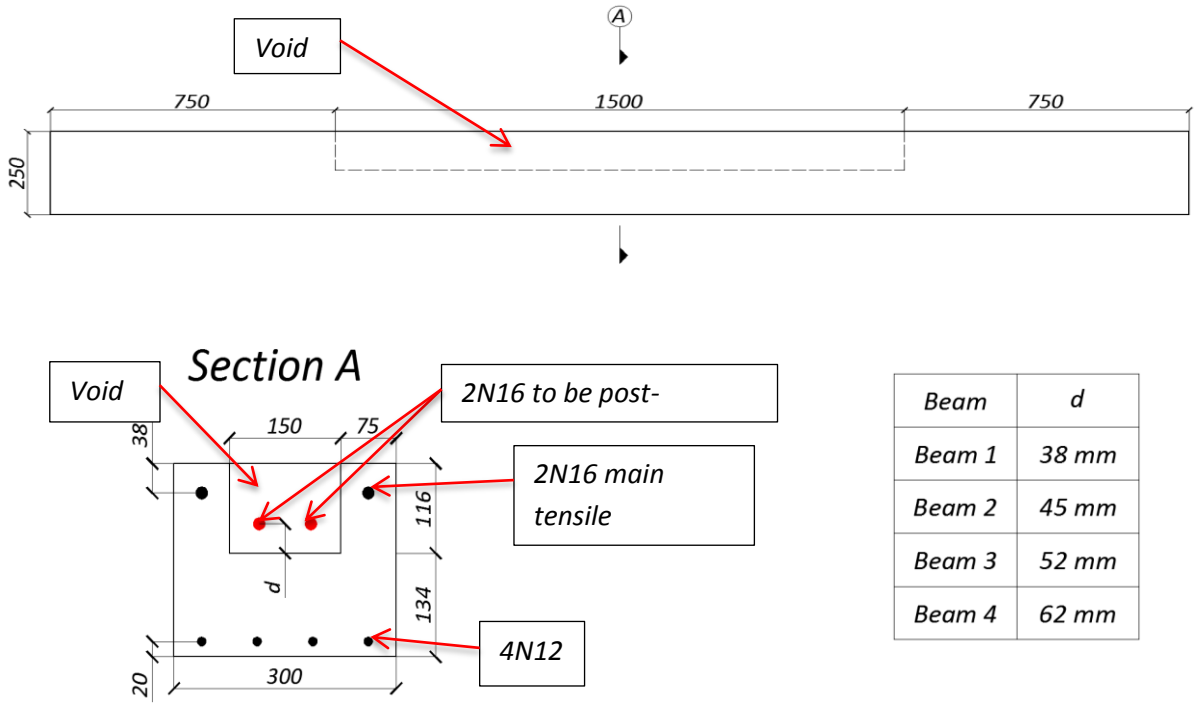

Beam	d
Beam 1	38 mm
Beam 2	45 mm
Beam 3	52 mm
Beam 4	62 mm

Figure 3.1 Dimensional drawing of the specimens.

Local post-tensioning was achieved through the vertical displacement of the exposed N16 reinforcing bars in the tensile section using a screw and plate apparatus (Figure 3.2). A Dimensional drawing of the beams after post-tensioning is provided in Figure 3.3 The displacement of the reinforcing bars created axial strain which was transferred to the concrete beam through the bonded part of the bars, also, the eccentricity of the bars about the neutral axis creates a decompression moment in the beam prior to loading and, generated pre-stress in the beam due to the post-tensioning.

The variation of post-tensioning level was achieved through the variation of vertical displacement (jacking distance).

Based on the elastic stress-strain relationship, ($E=\sigma/\varepsilon$), the vertical displacement (jacking distance) f is calculated using Equation 3.1 (see Appendix 2):

$$f = l\sqrt{\frac{\sigma}{2E}}, \tag{3.1}$$

where σ = the value of prestressing (less than or equal to 500 MPa, the yield strength of the reinforcing bar)

l = The length of exposed section of the reinforcing bar

E = Young's modulus of steel

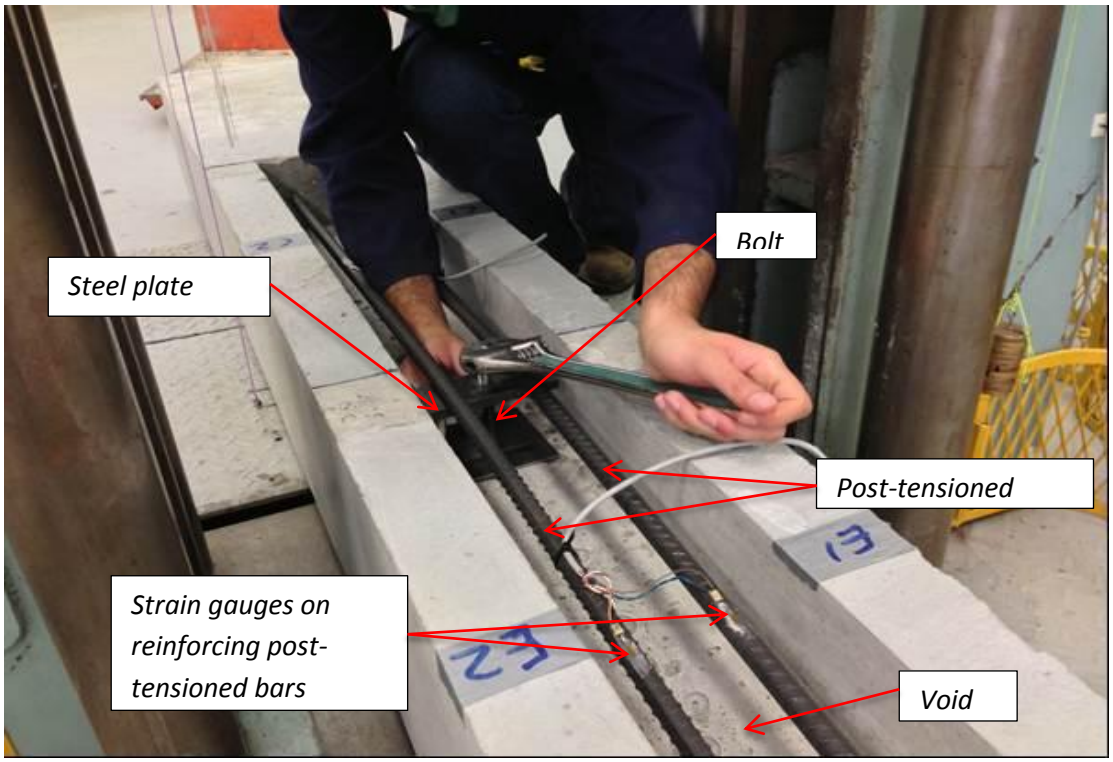

Figure 3.2. Tensioning the reinforcing bars.

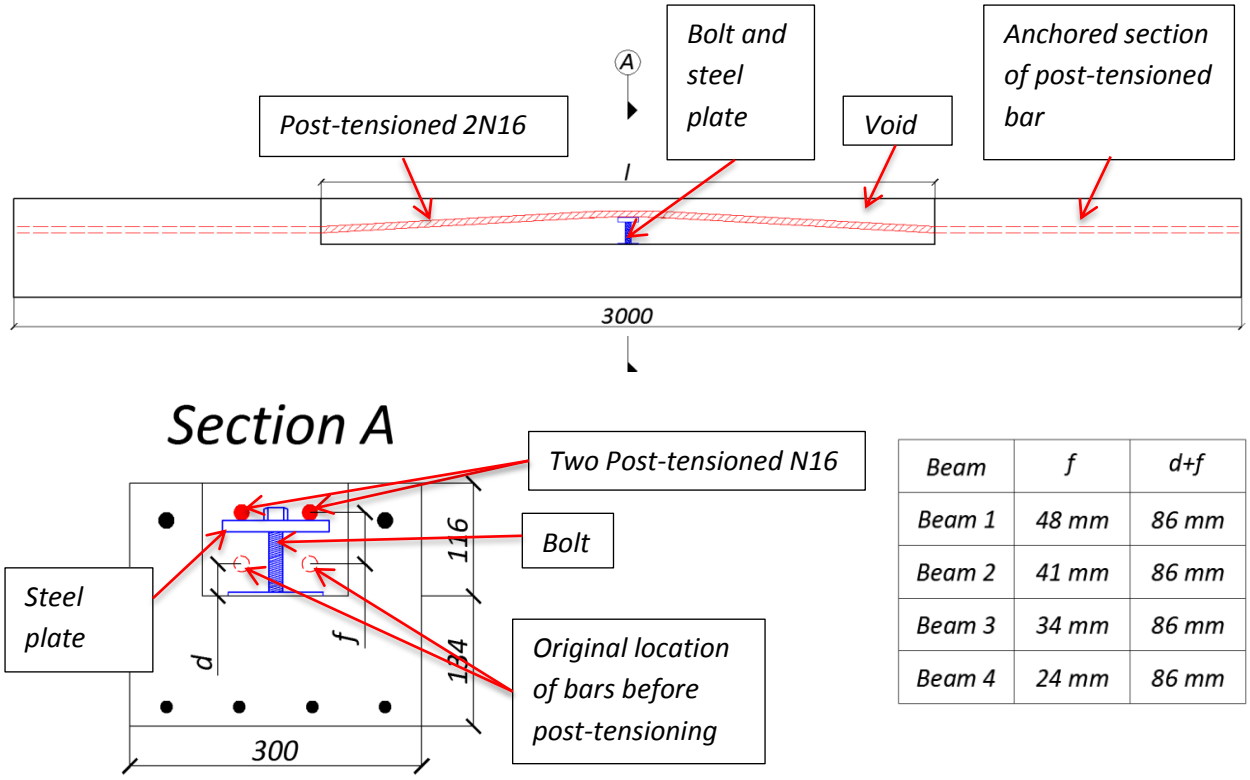

Beam	f	d+f
Beam 1	48 mm	86 mm
Beam 2	41 mm	86 mm
Beam 3	34 mm	86 mm
Beam 4	24 mm	86 mm

Figure 3.3. Dimensional drawing of specimen's void area after achieving the local post-tensioning.

3.2.2. Magnitude of tensioning force in reinforcing bars

The tensile force *N* within the reinforcement bars that was generated by the post-tensioning process can be calculated through the tensile stress and the reinforcing bar cross-sectional area using Equation 3.2:

$$N = \sigma A \tag{3.2}$$

Figure 3.4 shows the relationship between the jacking force, *F,* and the tensile force, *N,* in a post-tensioned beam. The jacking force *F*, required to generate the tensioning force *N*, can be calculated using Equation 3.3 (see Appendix 3), when a displacement is applied in the centre of the reinforcing bar:

$$F = N\sqrt{\frac{8\sigma}{E}} \tag{3.3}$$

It is worth mentioning that based on Equation 3.3, the jacking force is typically an order of magnitude less than the prestress force.

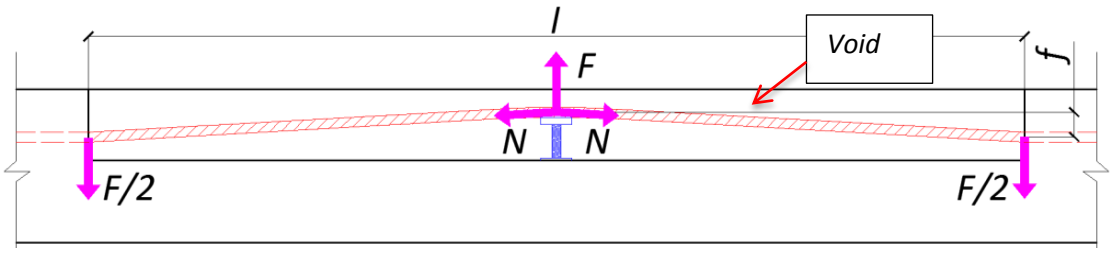

Figure 3.4. Distribution of forces within the beam after completion of post-tensioning.

3.2.3. Tests

Detailed information about prestresses and jacking forces of each beam are listed in Table 3.1. Three-point bending tests were conducted in a universal testing machine with a loading capacity of 1000 kN as shown in Figure 3.5. The beam was simply supported with a span of 2900 mm. The beam was supported by two roller support from both ends and the force *R* was applied from the testing machine at mid span. This test setup simulates the support area of a beam with a negative bending moment and allows an easier access to strain monitoring in the post-tensioned steel bars. Four strain gauges (S1, S2, S3 and S4) were fixed against the middle section of the beams to monitor the strain change in concrete during the post-tensioning and loading phases (their locations are shown on Figure 3.7). Strain gauges were also installed on the reinforced steel bars for the same purpose. All strain gauges were connected to an amplifier and a data acquisition system. All data was stored on the hard drive using software written in Labview 2012 (Refer to Appendix 1).

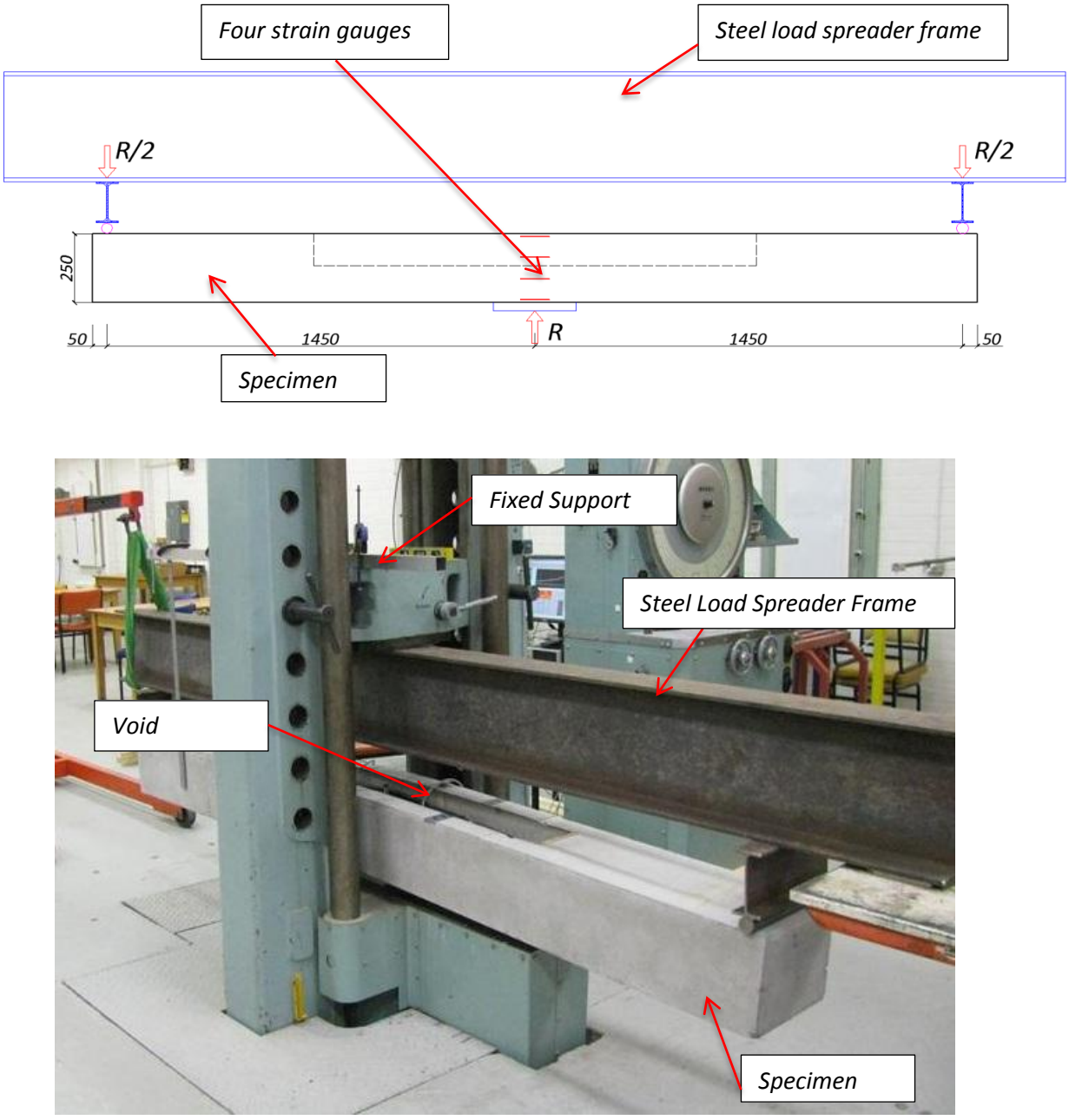

Figure 3.5 Test setup.

In order to study the effect of post-tensioning on the beams, all beams were designed in such a way that the reinforcing bars were in the same eccentricity at mid span after post-tensioning. To achieve this, the untensioned position of post-tensioned bars was varied vertically so that *d+f* was a constant and equal to 86 mm (refer to Table 3.1 and Figure 3.1).

Table 3.1. Jacking details of the beams.

Beam	Level of post-tensioning, % of *500 MPa*	Calculated Prestress Value, *σ, MPa*	Measured Prestress Value *σ, MPa*	Tensioning Force *N*, for both reinforcing bars, *kN (Based on 400 mm^2)* (Equation 3.2)	Jacking Force, *F, kN* (Equation 3.3)	Vertical Jacking Displacement, *f (mm),* (Equation 3.1)
Beam 1	80	400	410	160	20.2	48
Beam 2	60	300	295	120	13.1	42
Beam 3	40	200	205	80	7.1	34
Beam 4	20	100	100	40	2.5	24

3.3. Test results

3.3.1. Behaviour during post-tensioning

As mentioned before, the post-tensioning was achieved by vertically displacing 2N16 reinforcing bars. During this process, the strains in the concrete at mid span and at different heights within the cross section were monitored using the strain gauges (measured strains shown in Figure 3.6). It can be seen from Table 3.1 that with the increase of the vertical prestress jacking displacement, significant pre-stresses were applied in the mid-section of the beam. This was achieved by increasing the axial stress within the reinforcing bars, *N*, and increasing the decompression moment imposed on the section which caused compression

in the top section and tension in the bottom section. The jacking process was completed when the bars were elevated to a position of *f=48mm* for Beam 1. As can be seen from Figure 3.6, the strain gauges S1, S2 and S3 were in compression and S4 was in tension. Based on the data provided by these strain gauges, the stress distribution was drawn in Figure 3.7 (the concrete's Young modulus was taken to be 32800 MPa as per AS 3600-2009). The maximum compressive stress reached 5.7 MPa in the top layer of the tensile section and the maximum tensile stress of 1.8 MPa in the lower layer of the compressive section. The position of the neutral axis at this stage indicates that almost 80% of the section's depth was under compression.

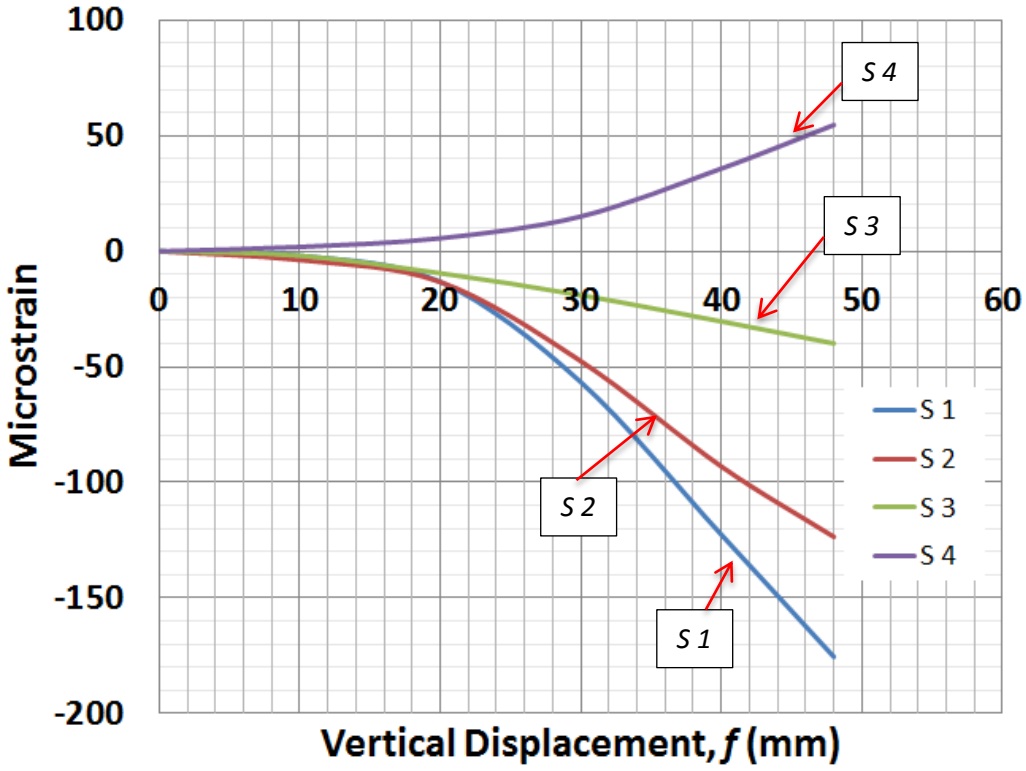

Figure 3.6. Strain development in the concrete mid-section during the post-tensioning process (Beam 1).

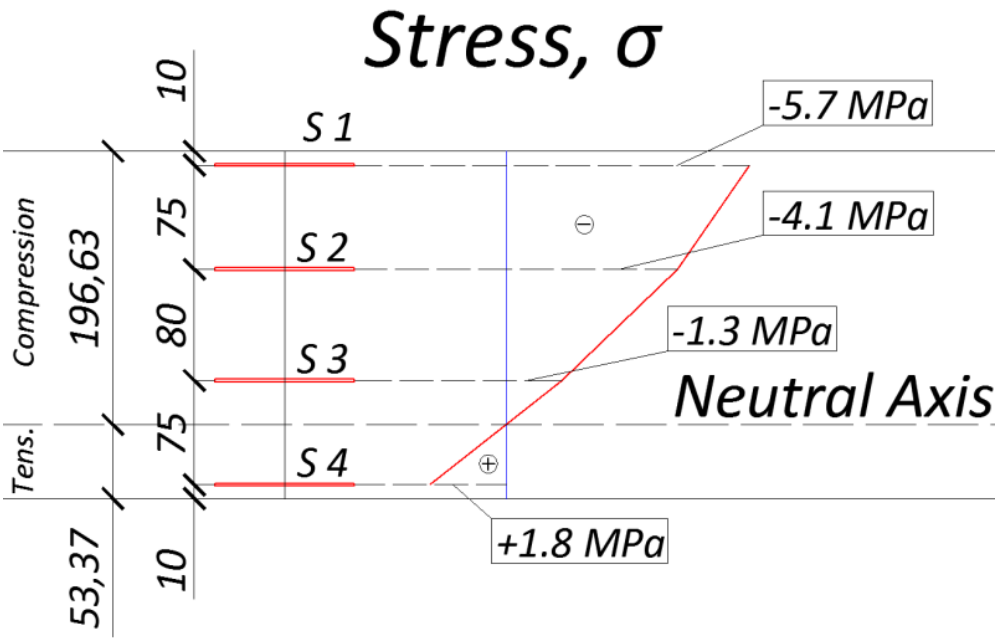

Figure 3.7. Stress distribution in the concrete mid-section after post-tensioning.

3.3.2. Failure modes

Figure 3.8 shows Beam 1 and Beam 2 at failure. All tested beams had almost the same failure mode. Initially, flexural cracks appeared in the top tensile section in the mid-section, then these cracks widened with the increment of the applied load. Flexural shear cracks appeared only when the applied load was approaching the ultimate load, in case of Beam 2 and Beam 4; the failure occurred without noticeable flexural shear cracks.

Figure 3.9 shows the strain behaviour of the beam during loading. Initially, S1, S2 and S3 were in compression, while S4 was in tension. This was due to the post-tensioning applied before loading. As the loading increased, the neutral axis moved up towards the tensile section as a result of the increment of the negative moment. The initial crack was detected by the failure of S1, marked by the sudden increment of strain reading from around *ε=170* microstrain to *ε=7000* microstrain. S2 and S3 also stopped working with further increment of loading. The cracking moment, M_{cr} for tested beams can be calculated from the

corresponding applied load when the crack was detected by the strain gauge. The cracking moment of Beam 1 determined using this method was M_{cr}=*30.5 kN.m*. The ultimate and cracking moments for tested beams are listed in Table 3.2.

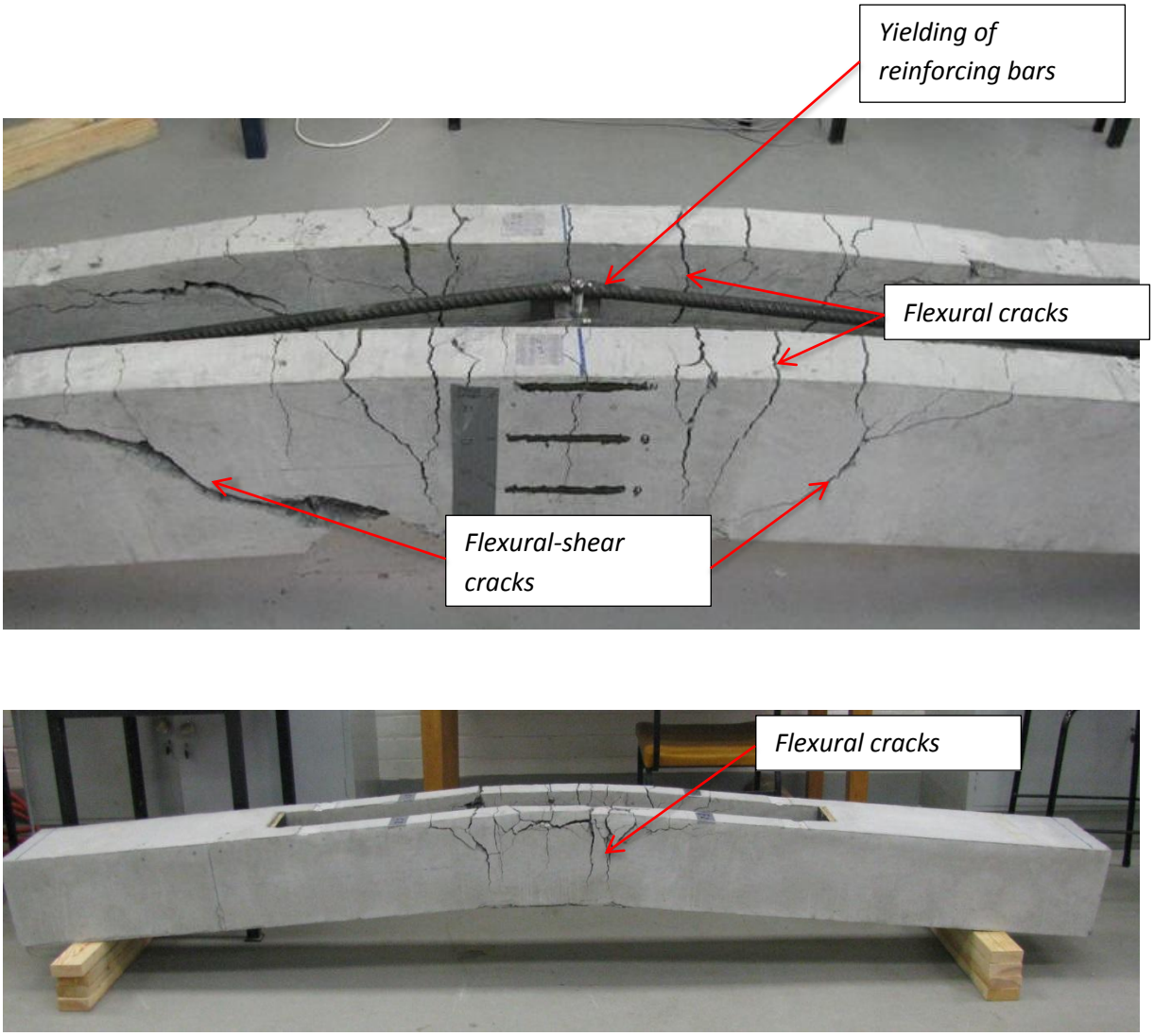

Figure 3.8. Typical failure of Beam 1 (top) and Beam 2 (bottom).

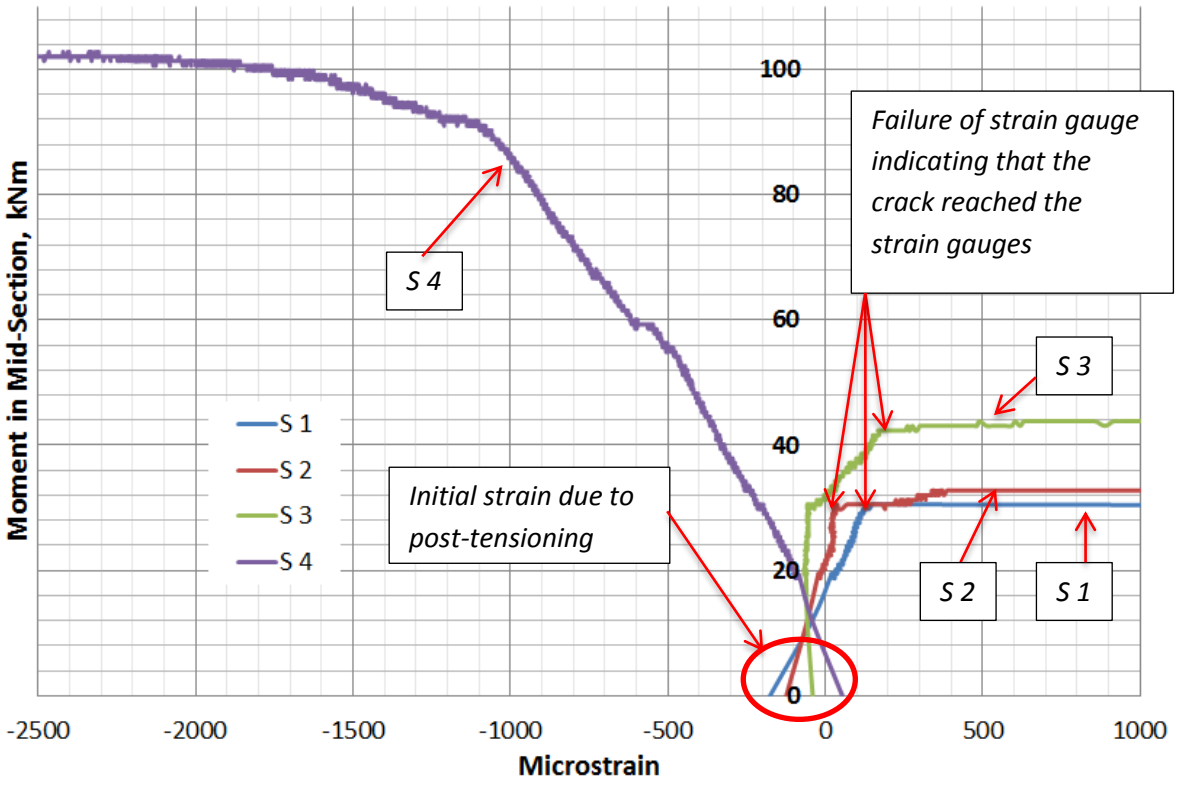

Figure 3.9. Strain development in concrete mid-section during loading (Beam 1).

Table 3.2 Experimental cracking moments, theoretical cracking moments and ultimate loads for tested beams.

Beam	Measured Cracking Moment, M_{cr}, *kN.m*	Theoretical M_{cr} *(kNm)* (AS 3600 2009)	Theoretical M_{cr} *(kNm)* (suggested method)	Measured Ultimate Moment, M_u, *kN.m*
Beam 1	30.5	22.6	32.7	102.1
Beam 2	21.2	20.6	28.3	102.6
Beam 3	26.8	17.6	23.7	101.3
Beam 4	24.1	15.3	19.1	103.9

As can be seen from Table 3.2, all four tested beams had almost the same ultimate moment (within a range of 2%) although different levels of post-tensioning were applied. This is due to the fact that post-tensioning did not increase the load-carrying capacity of prestressed beams. On the other hand, it is clear that the post-tensioning had increased the cracking moment. For Beam 1 and Beam 4 the increment was about 27%.

Figure 3.10 shows the strain development in the reinforcing steel bar during testing. The initial recorded strain was due to the post-tensioning process. In the case of Beam 2 it was around 1500 microstrain based on $\sigma = \varepsilon.E = 300\ MPa$ which was 60% of the Reinforcing bars nominal yield strength. The strain increased with the increment of the applied moment. The reinforcing bar started to yield when the applied moment reached about 90% of the ultimate moment. It should be noted that separate tests on the reinforcing bars showed a distinctive plastic zone with a uniform strain of 5,000 microstrain and an ultimate fracture strain of 20,000 microstrain, therefore, the reinforcing bars would not break even with higher levels of initial post-tensioning (80% or even 100% of the nominal yield strength). This increment of strain in reinforcing bars was mainly due to the post-tensioning mechanism setup. Any increment in the applied load would lead to a stress increment in the post-tensioned bars. The local post-tensioning did not show any friction losses that are common to almost all post-tensioned members (Hurst & Spon, 1998; Nawy, 2003).

3.4. Effect of secondary moments

Secondary moments are additional moments induced at a section of a continuous prestressed member when using prestressing cables. However, due to the localised nature of LPT and the discontinuity of tendons (reinforcing bars) used in mid-span and above support areas, the conventional methods of determining these moments, such as three

moment theorem, consistent deformation and tendon reaction are not applicable to locally post tensioned continuous concrete beams. Alternatively, an innovative theoretical approach can be adopted to predict these moments, in which, jacking forces *F* (having opposite directions), will create a couple that counters the bending moment from loading and therefore, further delay the cracking of the beam. For example, if Beam 1 is considered with a span of 6 m between the supports, the secondary moment would be then equal to the force *F* (20.2 kN) applied to in the above support area, multiplied by the half-distance to the other jacking force applied in the mid-span area (1.5 m) which is approximately equal to 31 kN. Please note that, further research and testing are required to fully understand these moments and their magnitude, which were not conducted in this study due to the limitation of testing facilities as mentioned in Section 3.2.1.

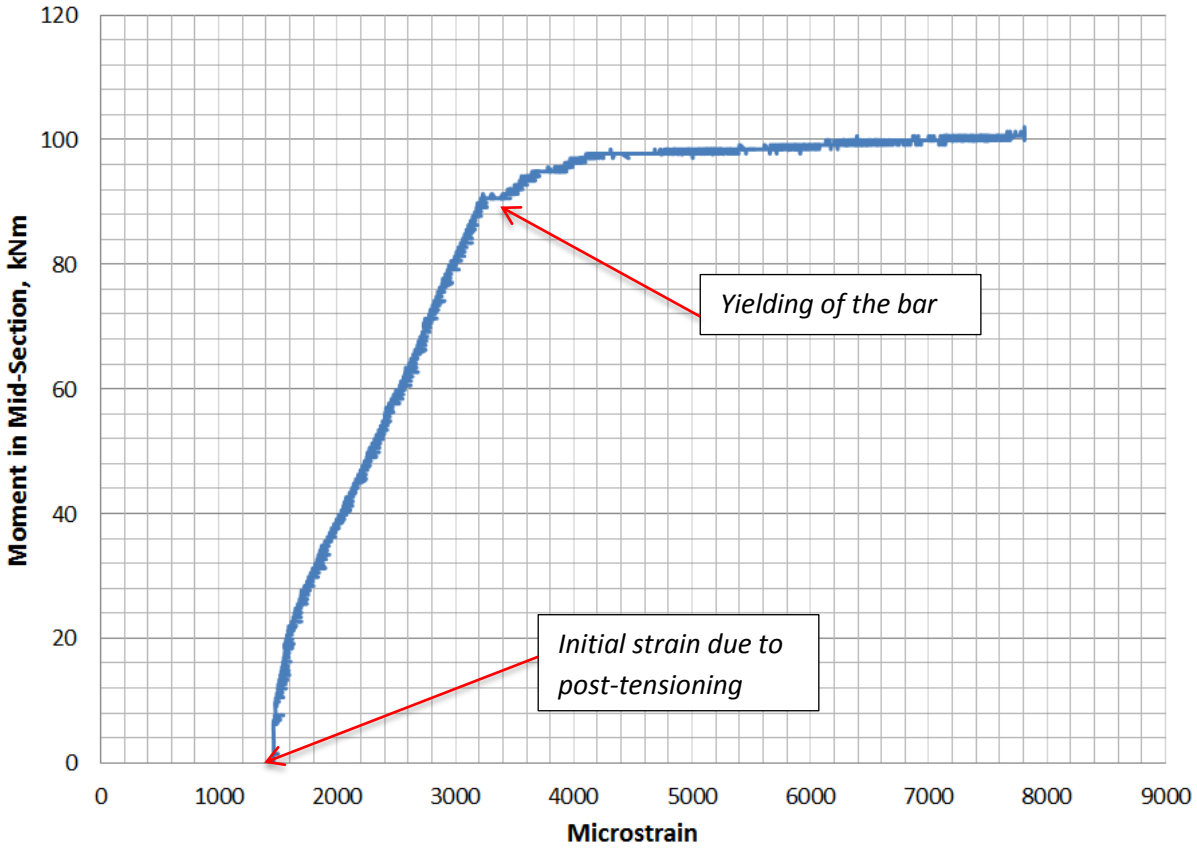

Figure 3.10. Strain development in post-tensioning bars during testing (Beam 2).

3.5. Comparison of results

The theoretical cracking moment M_{cr} was calculated based on the linear elastic beam theory. Current Australian concrete design standard AS 3600-2009 presents the following Equation 3.4 (section 8.5.3.1.c) for the cracked moment of a pre-stressed section with axial stressing force, *P*, gross sectional area , A_g , and eccentricity from centroidal axis, *e* (Standards Australia Limited, 2009)

$$M_{cr} = Z.\left(f'_{ct.f} + \frac{P}{A_g}\right) + P.e, \tag{3.4}$$

where,

Z = elastic section modulus and

$f'_{ct.f}$ = characteristic flexural strength of concrete as defined in section 3.1.1.3 of AS 3600-2009.

Using Equation 3.4 and the values of internal forces provided in Table 3.1, the predicted (theoretical) cracking moment can be calculated. The results are provided in Table 3.2.

As it can be seen from Table 3.2 the experimental cracking moments far exceeded the predicted theoretical ones (except for the case of Beam 2). This was due to the fact that the cracking moment equation, adopted from AS 3600-2009 was based on the action of the prestressing force *P*, in which the interaction of vertical forces is not considered (the effect of the mid-span point load introduced by the LPT process – force *F*). As a result, the vertical reaction forces shown in Figure 3.4 in the bonded lengths of post-tensioning bars were not included. Empirical formulae from AS 3600-2009 were then used to estimate the elastic modulus and uniaxial tensile strength of concrete. It was previously found that there is a

±20% range of accuracy when applying the formula presented in AS 3600-2009 section 3.1.2 (Loo & Chowdhury, 2010).

Based on these results, a new approach was adopted to predict the cracking moments of the beams, based on the sum of decompression moment and the cracking moment of non-post-tensioned section. The decompression moment (M_{dec}) is calculated for each beam based on the equilibrium in the middle section using Equation 3.5:

$$M_{dec} = N.e + \frac{F}{2}.\frac{l}{2} \quad (3.5)$$

The cracking moment of non-post-tensioned beam can be calculated using linear elastic beam theory presented in Equation 3.6:

$$M_{cr} = Z.f'_{ct.f} \quad (3.6)$$

The predicted cracking moments using this approach proved to be more realistic (except for beam 2). This can be explained by the fact that the suggested method includes the jacking force *F.*

Also, regarding the stresses in the steel bars, Figure 3.11 shows the axial stress, σ (experimental and theoretical) in post-tensioned bars after achieving the post-tensioning process. It is worth noting that these values also match the design prestress calculated theoretically using Equations 3.1 and 3.2 (400, 300, 200 and 100 MPa for Beams 1, 2, 3 and 4 respectively).

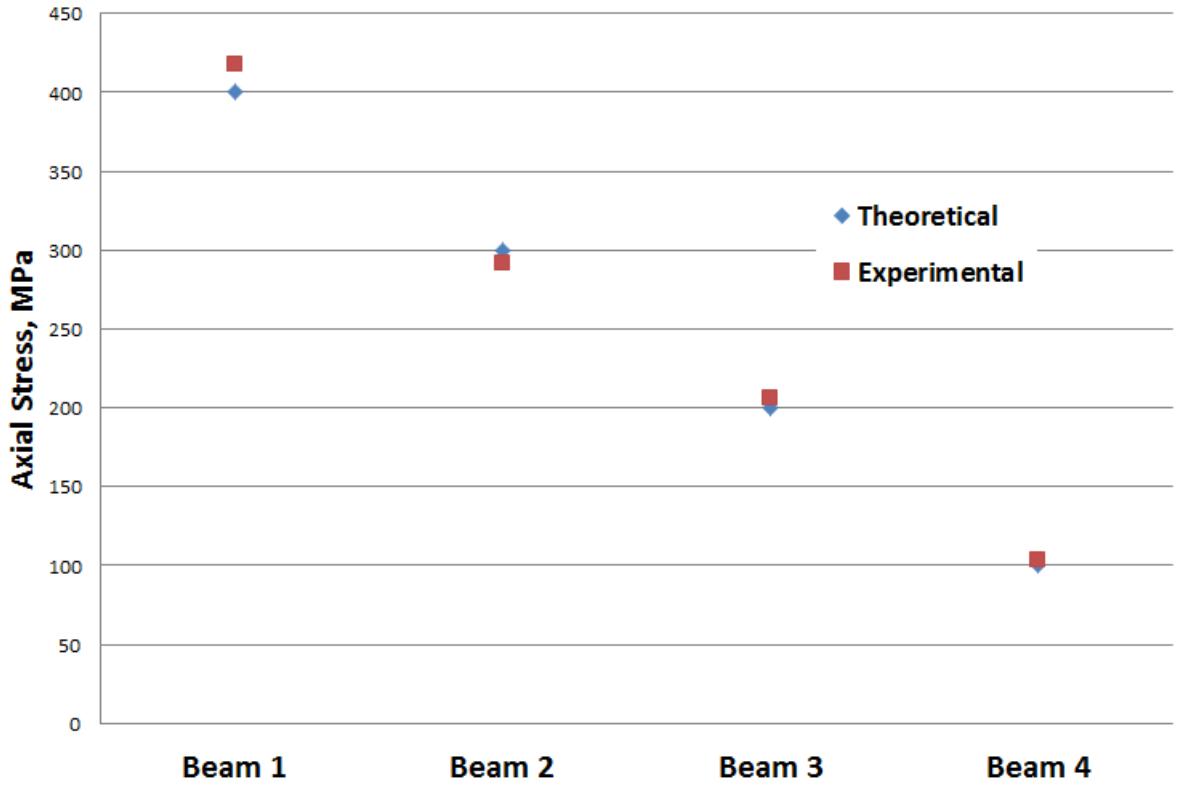

Figure 3.11. Comparison of axial stresses in bars after completion of post-tensioning.

3.6. Design steps of locally post-tensioned beam with a numerical example

The design steps of beams with LPT are similar to those with conventional post-tensioning. However, there are minor diffrences, such as determing the void dimensions, jacking force and jacking distance. There is no need to design an anchorage area or choose a cable profile, as they do not exist in such type of beams.

The design steps below are based on Example given by Warner, Rangan, Hall, and Faulkes (1998):

(1) Make an initial estimate of beam self-weight, and determine maximum bending moments and shear forces due to all loads.

(2) Calculate the design ultimate moments M^* at critical sections for bending; choose a cross-section, and then check the moment and shears due to self-weight.

(3) Choose the serviceability design criterion: either

(a) Choose the load which is to be balanced by the prestress, i.e. the load for which zero deflection is desired; or

(b) Choose the load at which decompression is to occur; or

(c) Choose the design for full prestress if it is necessary to prevent cracking from occurring under all service loads.

(4) Calculate the losses and determine the needed cross section area of steel bars

(5) Calculate the *N* and *f* (Figures 3.3 and 3.4)

(6) Calculate the void dimensions

(7) Check ultimate strength in bending at critical sections and provide additional tensile reinforcement as required

(8) Check for safety of critical cross-section at transfer; either by estimating the section strength against concrete crushing due to overprestressing, or by using the "deemed to comply" extreme fibre stress check permitted in AS 3600-2009.

(9) Check for strength in shear at critical sections and provide stirrups where needed.

(10) Check short-term and long-term deflections and crack widths under full service loading and also at transfer. If necessary, adjust the proportions of prestressing steel and reinforcing steel.

(11) Check for any special requirements such as torsion, fatigue etc.

A numerical example is provided here below.

A simply supported beam spanning *10m* is located in an office for general use, therefore, according to AS/NZS 1170.1 2002, the LL = 3 kPa. The beam has a cross-section of 300x500 mm and is covered by an 80 mm concrete slab, the spacing between the beams is 3m, so in this case, LL = 9 kN/m and DL = 6 kN/m.

Concrete 28-day strength: $f_c' = 40$ MPa.

Concrete strength at transfer: $f_{cp} = 32$ MPa.

The cross-section is rectangular with dimensions of *300x500 mm*. The section area is $A_g = 150000$ mm^2.

(1) Calculation of self-weight:

Self-weight *= 0,3x0,5x25 = 3,75* kN/m

(2) Choose the serviceability criterion:

The beam is initially designed for decompression at mid-span under full dead load, so that the beam will be free of flexural cracks under the permanent load.

Total dead load *= 6+3,75 = 9,75* kN/m. The required decompression moment at mid-span is therefore:

$$M_{dec} = \frac{9{,}75.10^2}{8} = 122\ kN.m$$

(3) Determine prestressing force and eccentricity:

Assuming that the maximum available eccentricity will be approximately *e=200 mm*.

The section modulus is calculated:

$$Z = \frac{bD^2}{6} = \frac{300.500^2}{6} = 12{,}5.10^6 mm^3$$

Then the required effective prestressing force is:

$$P_e = \frac{M_{dec}}{e + \frac{Z}{A_g}} = \frac{122.10^6}{200 + \frac{12{,}5.10^6}{150000}} = 430kN$$

(4) Prestress losses and selection of bars:

Assuming that deferred losses total 20 per cent, the initial prestressing force required at mid-span is:

$$P_i = \frac{430}{0{,}8} = 538kN$$

Considering that the maximum prestressing level is 80% of the steel's yield strength we obtain:

$$\sigma = 0{,}8.500 = 400MPa$$

Therefore, the required cross section area of prestressed steel bars will be:

$$A = \frac{P_i}{\sigma} = \frac{538.10^3}{400} = 1345mm^2$$

Provide *2N32 bars (A_{sp}=1600mm^2)*

(5) Calculation of *N* and *f*:

The total stressing force *N* will be:

$$N = \sigma.A = 400.1600 = 640kN$$

The required manual force which will be provided by a manual screw jack is

$$F = N\sqrt{\frac{8.\sigma}{E}} = 80kN$$

Where *E* is the modulus of elasticity of steel bars as mentioned previously.

Considering that the length of the void (which is equal to the length of the exposed section of the reinforcing bars) is half the span, then *l=5000mm*

The vertical displacement of bars (jacking distance), *f*, is calculated:

$$f = l\sqrt{\frac{\sigma}{2E}} = 158mm$$

(6) Design of void dimensions:

Given that the diameter of bars is 32 mm and that *f = 158* mm, the overall depth of the void, taking in consideration a 20 mm cover and 20 mm clearance for the steel plate will be equal to:

H = 32+20+20+158 = 230 mm The width is taken as *150mm*

(7) Design reinforcement for M_u at mid-span:

$w^* = 1,2.9,75+1,5.9 = 25,2$ kN/m

$M^* = (25,2.10^2)/8 = 315$ kN.m $M_u = M^*/\varphi = 315/0,8 = 394$ kN.m

Given that the lever arm *z=415mm*, the total tensile force required at M_u is:

$$T_{py} + T_{sy} = \frac{M_u}{z} = \frac{394.10^3}{415} = 950kN$$

T_{py}=640kN

Required *T_{sy}=950-640=310kN*

$$A_s = \frac{310.10^3}{500} = 620mm^2$$

Consider *2N20, A_s=620mm^2*

Analysis of the section gives the following results:

A_g = 115200 mm^2 *I_g = 2,35.10^9* mm^4 *e = 200* mm

To calculate the cracking moment *M_{cr}*, it is necessary to calculate the extreme fibre stress due to prestress:

$$\sigma_{bp} = \frac{640000}{115200} + \frac{640000.200.250}{2{,}35.10^9} = 19{,}16MPa$$

$$f'_{cf} = 0{,}6\sqrt{40} = 3{,}79MPa$$

And *σ_{bp}=9,76MPa*

Therefore,

$$M_{cr} = \frac{(3{,}79 + 19{,}16)2{,}35.10^9}{250} = 216kN.m$$

(8) Check strength at transfer at mid-span section:

The self-weight moment at mid-span is *M_G = 3,75.10^2/8 = 47* kN.m. The initial prestressing force at mid-span, i.e. the force immediately after transfer is *575* kN. During the jacking

operation the prestressing force at the section ma temporarily exceed this value, and it will be assumed that the maximum jacking force at mid-span is $P_{jm} = 600$ kN.

The extreme fibre stresses are checked first. The tensile stress in the top fibre is:

$$\sigma_a = \frac{-640000}{115200} + \frac{640000.190.250}{2{,}35.10^9} - \frac{47.10^6.250}{2{,}35.10^9} = +2{,}9MPa$$

$$\sigma_b = \frac{-640000}{115200} - \frac{640000.190.250}{2{,}35.10^9} + \frac{47.10^6.250}{2{,}35.10^9} = -14{,}3MPa < 0{,}5f_{cp}$$

The section therefore satisfies the AS 3600-2009 approximate “deemed to comply” provision for strength at transfer.

Materials for post-tensioning: 2 reinforcement bars N32.

Equipment for post-tensioning: Simple manual screw jack.

Table 3.3. Design parameters comparison for locally post-tensioned beam and conventional post-tensioned beam.

Conventional Post-tensioned Beam	Locally Post-Tensioned Beam
Mid-Span Section Characteristics	
$M_{cr} = 170$ kN.m	$M_{cr} = 216$ kN.m
$M_u = 394$ kN.m	$M_u = 394$ kN.m
Materials for Prestressing	
3 Strands 15,2 mm EHT	*2N32*
Stressing Anchorage Type Gc Live End	
Dead End Anchorage Type P	
Duct Type Pt-Plus	
Additional Reinforcement	
2N16	*2N20*
Equipment for Prestressing	
Stressing Jack VSLB7	Manual Screw Jack
Combined Mixer and Pump Unit	
Cost of Materials (Excluding Concrete) in AUD	
1300	410 (based on a price of 2400 AUD/tonne)

Please note that the Prestressing materials and equipment are provided here as per VSL® Catalogues. Costs were estimated using current VSL® catalogues (As per December 2015) and do not include the cost of workmanship, which is significantly higher for the conventional post-tensioned beam, due to the need for special equipment, specially trained staff and higher degree of quality control. For the design of the same beam using conventional post-tensioning, please refer to Appendix 4. The higher cracking moment for

the LPT beam can be explained by the fact that, although the 15.2 mm strands have a greater yield strength than the conventional steel bars (1640 MPa against only 500 MPa), the cross-sectional area of the bars used in LPT beam (2N32) is by far greater than that of the post-tensioning strands used in the conventional post-tensioned beam (1608 against 544 mm only), and therefore, the prestressing force in the LPT beam is higher than in the conventional one, resulting in a higher cracking moment.

3.7. Conclusion

This chapter has presented an experimental and theoretical investigation to understand the behaviour of locally post-tensioned beams. The following can be concluded from the limited test results:

Local post-tensioning has proved to be an effective method of prestressing concrete beams and increasing their crack-resistance.

The local post-tensioning is applied only in critical areas where the bending moments reach the maximum values e.g. at a support area or mid-span.

The post-tensioning setup allows to eliminate the friction losses in prestressing which is common to almost all post-tensioned members. In fact, the level of post-tensioning increases with further loading of the beam.

It was found that the approach adopted in AS 3600-2009 to predict the cracking moment was not applicable for locally post-tensioned beams, since the forces involved in this process were not included, therefore, a new approach was adopted to predict these moments, which proved to give more accurate results.

A design approach for locally post-tensioned beams was proposed. This approach is based on the design of average post-tensioned beams with modifications made to take in consideration all the differences between the two concepts.

LPT proved to be a low-cost and simple method to post-tension concrete beams (both simple and continuous) when compared with traditional post-tensioning techniques.

4. Behaviour of Locally Post-Tensioned Timber Panels under Serviceability Loads

4.1. Introduction

As discussed previously in Section 2.2, post-tensioned timber beams and frames have been used to reduce the depth of timber beams opening up the way for multi-storey timber office and commercial buildings (van Beerschoten et al., 2012). Initially, these beams and frames were designed to resist earthquake loading (Palermo et al., 2005), however, following the developments in precast concrete seismic design (Priestley et al., 1999) these frames have further evolved to non-seismic frames, known as the "Brooklyn system" (Pampanin et al., 2004)., On the other hand, mass timber panels have been used in residential construction industry for a long time. One of the relevant examples is the Brettstapel timber flooring panel that uses hardwood dowels to connect vertically laminated timber(Henderson et al., 2012a). Another example is the O'portune, or staggered timber slabs that achieve greater rigidity, due to their increased depth, than standard mass timber panels (Sandoz & des Jordils, 2004). The Centre for Sustainable Architecture with Wood (CSAW), a research department of the University of Tasmania, investigated the use of composite timber panel as an alternative to a reinforced concrete beam. In this suggested system, low grade timber carries the compression in bending and a soffit, attached to the panel, acts as a tensile element (Baxter, 2014; Hamilton, 2014; Schaap, 2012; Snowball, 2013). Based on these concepts, a composite timber panel was created and investigated in this study. The tensile soffit was replaced by a bracing strap, usually used to counter the in-plane lateral loads in timber frames. In order to increase the efficiency of this system, the bracing strap was locally post-tensioned using bracing tensioners.

This chapter presents an experimental study on the use of the LPT method to create a composite timber panels for residential construction. The aims were to investigate the effect of post-tensioning on the serviceability behaviour of locally prestressed timber panels in four-point-bending and to experimentally investigate the dynamic performance of these timber slabs.

4.2. Material properties

4.2.1. Timber panels

The timber lamellas were grade MGP 10 and had a cross section of 35 x 90 mm. they were supplied by a local trader and originate from locally grown radiata pine. This type of timber has bending strength of 16.2 MPa, a compressive strength of 23.6 MPa and a characteristic minimum design modulus of elasticity of 10000 MPa at 12 percent moisture content.

4.2.2. Bracing straps

The bracing straps used to induce post-tensioning were G300 Vuetrade Bracing Straps, made of steel 30 mm wide and 0.8 mm thick. The maximum tension strength claimed by the manufacturer was 4.75 kN, however, laboratory tensile tests showed a maximum strength of 6.1 kN.

4.3. Specimen preparation and serviceability deflections test setup

As shown in Figures 4.1 and 4.2, each panel consisted of eight lamellas placed side by side and oriented vertically. The edge lamellas were raised by 45 mm to allow for strap installation and clearance for the post-tensioning process. All specimens had identical configurations and dimensions. The slabs were one-way, simply supported in the

longitudinal direction at a span of 4.2 m and therefore had dimensions of 135 D x 280 mm W x 4400 mm L (allowing 100mm overhang at each end to allow adequate bearing).

The test rig consisted of a four-points bending test frame with 3 spans of 1.4 m each (Figure 4.1). Blocks were inserted at the load and support points to ensure that the load was applied uniformly across the width of the panel and equally resisted by both the raised and the non-raised lamellas (see for example Figure 4.5). Vertical deflection was measured using a LVDT at mid-span, as can be seen in Figure 4.5.

The specimens were tested in 3 conditions: (i) clamped (see Figure 4.2), a reference configuration in which the eight full length (4.4m) lamellas were held together just by three clamps, one at each end and one in the middle; (ii) jointed (nailed), in which the lamellas were cut and butt jointed, then nailed together according to the jointing and nailing patterns in Figures 4.3. and 4.4.; and (iii) nailed post-tensioned, in which the bracing straps were added (see Figures 4.1 and 4.5). All slabs were tested under serviceability load which, in this case consisted of 1.32 kN (See Appendix 5). At each of the three testing stages, the specimen were subject to five loading and unloading cycles to approximately 130% of the serviceability loading.

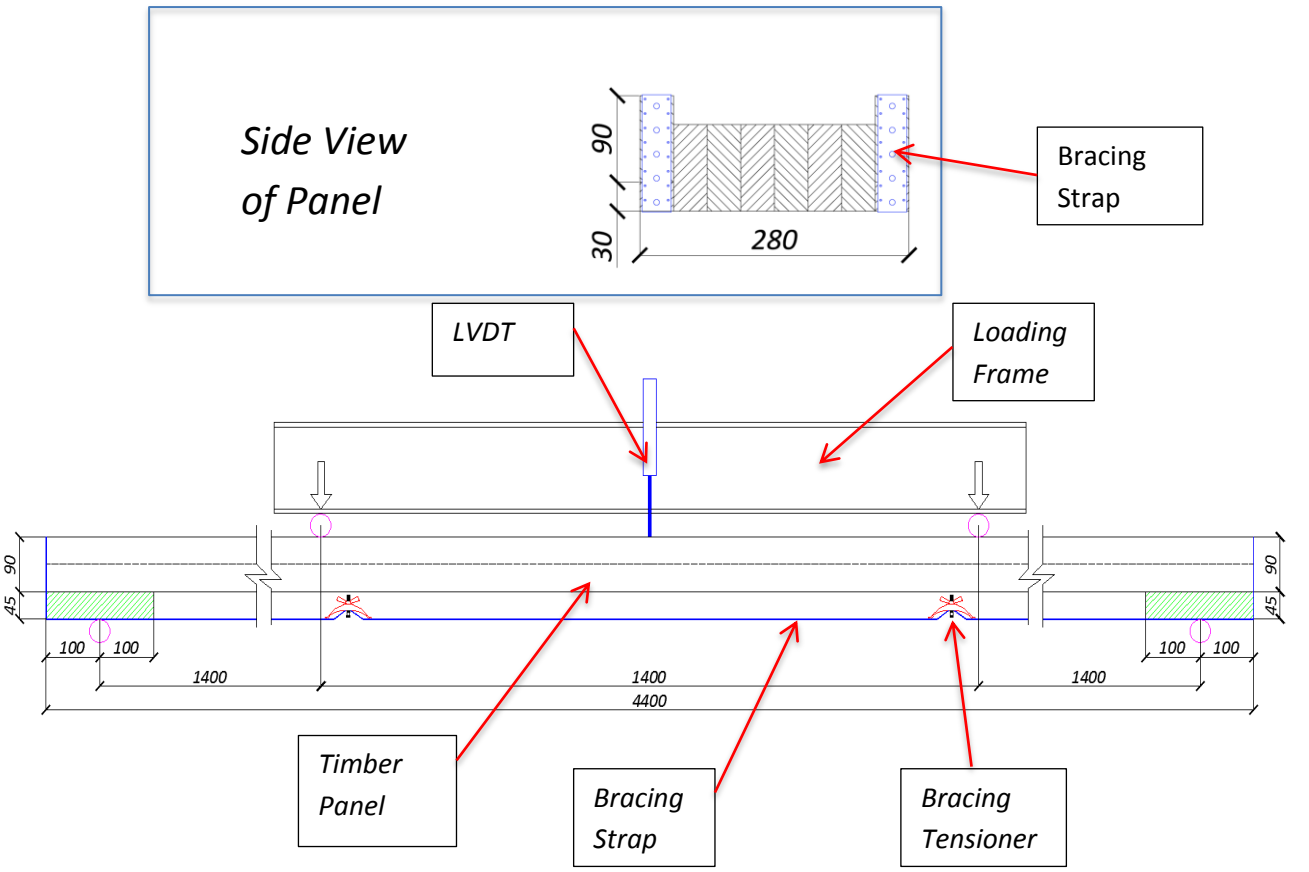

Figure 4.1. Test setup and dimensions.

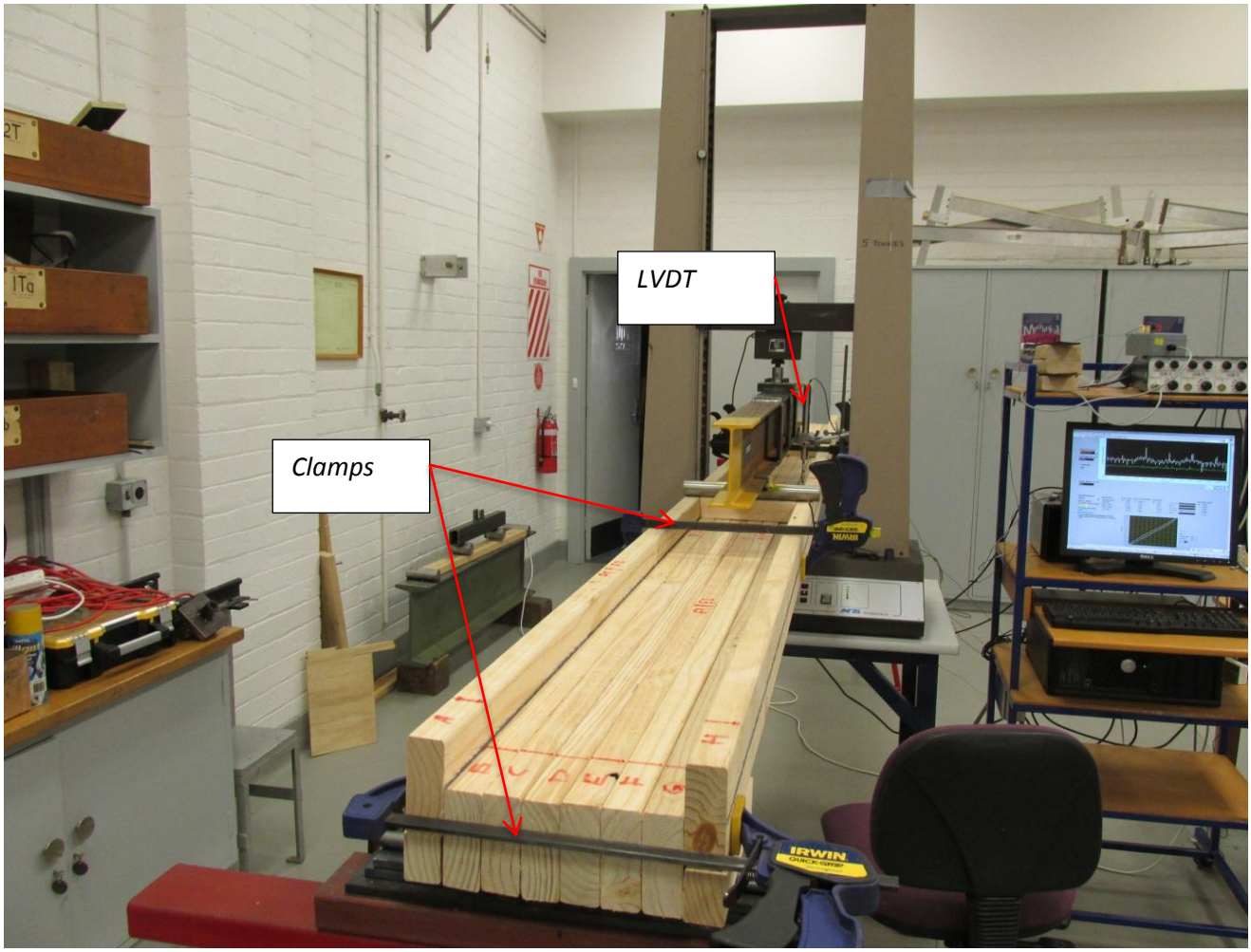

Figure 4.2. Test of clamped beams.

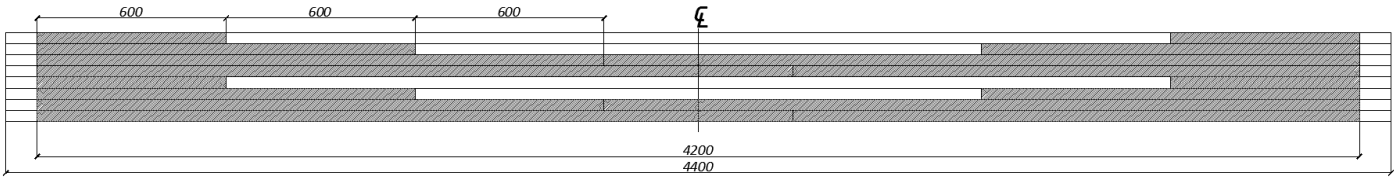

Figure 4.3. Stepped pattern and locations of butt joints.

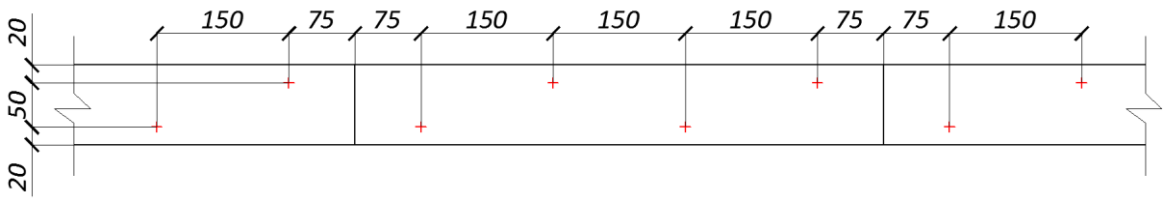

Figure 4.4. Nailing pattern.

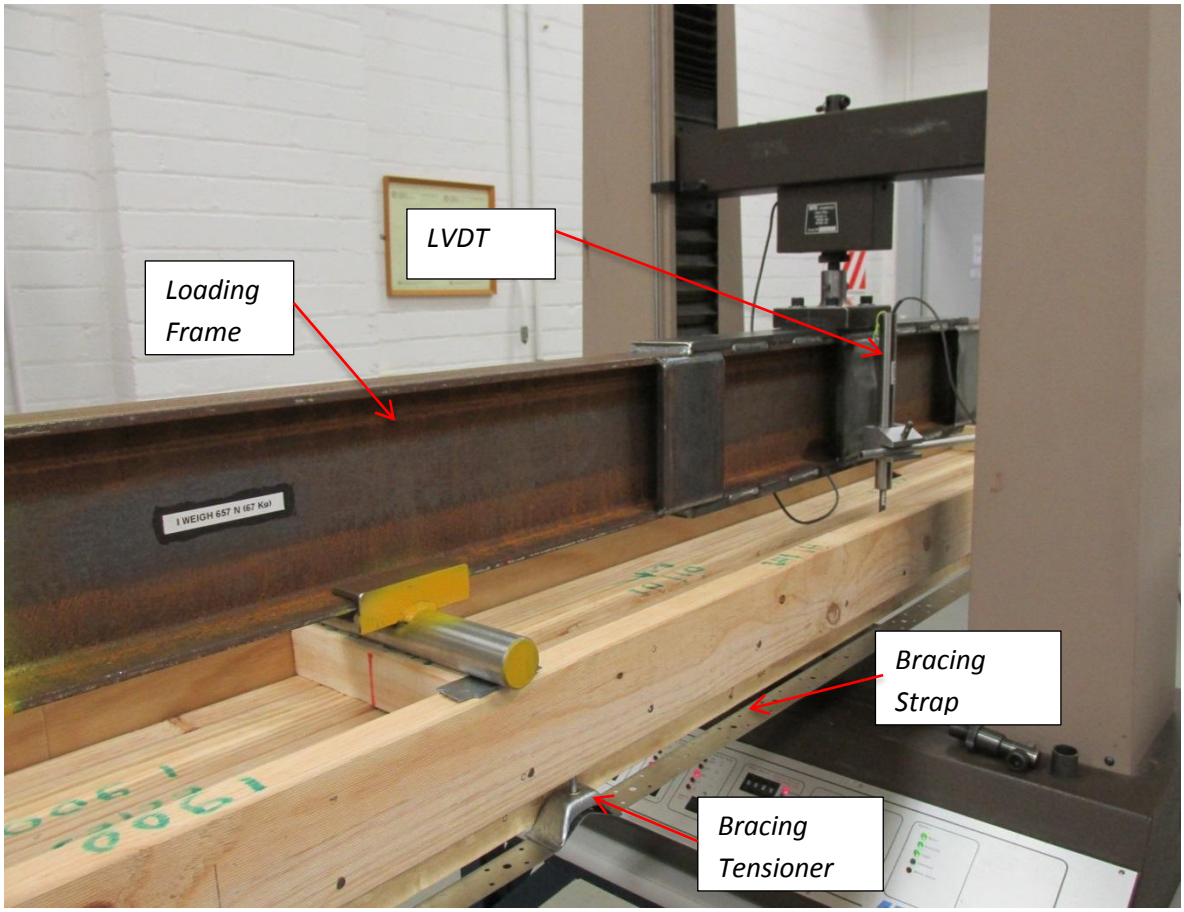

Figure 4.5. Testing of post-tensioned timber panels.

4.3.1. Test of clamped panels

Prior to testing the jointed (nailed) and the nailed post-tensioned panels, each configuration was clamped together and tested in order to provide a basis for deflection comparison (Fig. 2). The results were consistent and are presented in Table 4.1.

Table 4.1. Results of testings of clamped and jointed (nailed) panels

Panel	Maximum deflection under 130% of serviceability load for clamped panels, mm (average of 5 loading cycles)	Maximum deflection under 130% of serviceability load for jointed panels, mm (average of 5 loading cycles)
P-1	9.9	9.3
P-2	9.7	9.1
P-3	9.9	9.6
P-4	11.0	10.2
P-5	11.1	10.6
P-6	10.3	9.8
AVERAGE ± StdDev	**10.32±0.60**	**9.77±0.56**

4.3.2. Test of jointed (nailed) panels (before post-tensioning)

The second stage of testings included the test of nailed panels. The clamped lamella slabs were disassembled then butt joints were introduced (splices) and finally, individual lamellas were subject to mechanical vertical nail lamination, in the same order and orientation as per

the clamped testing (Figure 4.3). As stated by Williams, Bohnhoff, and Moody (1994), the distribution of loads is less uniform and the stress concentrations are higher in asymmetric joint designs, therefore, Shanks (2013) used a 600 mm stepped arrangement giving a minimum splice length of 1800 mm. This approach is also adopted by the American Society of Agriculture Engineers – Design Requirements and Bending Properties for Mechanically Laminated Columns (ANSI/ASAE, 2003). Therefore, a 600 mm stepped pattern and an overall splice length of 1800 mm was adopted for all tested panels (Figure 4.3). The nailing pattern used to vertically connect the timber lamellas was chosen according to the conclusions of Baxter (2014); Hamilton (2014); Snowball (2013), in order to ensure that it was not a limiting factor for the system. The nails used in all testings were gun driven 65 mm x 2.87 bright blue coated, and applied in the pattern shown on Figure 4.4.

Results of this stage of testing are contained in Table 4.1 alongside the results from stage (I) (clamped).

4.3.3. Test of nailed panels after post-tensioning

Post-tension was induced by applying two bracing tensioners to each of two bracing straps (one strap with two tensioners on each side of the panel). The straps were applied to the lower section of the panel and nailed to each end. The tensioners were tightened using a screw bolt (Figure 4.5). This process provokes an elongation of the strap and therefore, induces tensile strain which in its turn compresses the lower section of the timber panel and result in hogging deflections, which were measured during the application of the tensioners using a LVDT. After post-tensioning, each specimen was subject to five loading and unloading cycles similar to the previous stages. The results of these tests (jointed and post-tensioned) are shown in Table 4.2.

Table 4.2. Test results of jointed and post-tensioned panels.

Panel	Hogging (upward) deflection due to post-tensioning (single measurement only) (mm)	Nett maximum (downward) deflection relative to the un-post-tensioned condition under 130% of serviceability load, mm (average of 5 loading cycles after post-tensioning)
P-1	4.8	5.2
P-2	4.7	4.5
P-3	5.1	4.5
P-4	5.2	4.6
P-5	5.3	5.1
P-6	5.0	5.2
AVERAGE ± StdDev	**5.02 ± 0.23**	**4.85 ± 0.35**

4.3.4. Discussion of static loading results

Results shown in Table 4.3 are consistent with those obtained by Baxter (2014); Hamilton (2014) when testing control MGP 10 panels formed of 8 similar lamellas with a span of 4200 mm. It is worth mentioning that the deflection limit set by Standards Australia Limited (2002) is L/300 or 14 mm for this case. As expected, the process of introducing joints and

nailing the panels has slightly affected the total serviceability deflections, which decreased by around 7-8% on average. Clearly the nails provided additional stiffness through greater interactions between beams (presumably particularly between the raised and non-raised ones) via transfer of shear stresses.

As it can be seen from Table 4.2, the introduction of local post-tensioning proved to be critical for the panel's deflections. The process of post-tensioning has introduced a hogging deflection equal to 5mm on average that is equal almost to 50% of the total deflection under serviceability load for non-post-tensioned panels. This is mainly due to the compression force induced by the straps at the lower area of the panel, which results in compressing the bottom section and tensioning the top section of the timber panel and therefore, creating a hogging (positive) deflection opposite to that resulting from the imposed load. As a result, the value of total deflection under serviceability load is decreased by the value of the hogging deflection and therefore, the post-tensioned panels have 50% less deflections under serviceability loads than the average panels.

It is noted that the increment in deflection due to the loading was essentially the same regardless of whether post-tensioning was used or not, in other words the improvements in the serviceability deflections were predominantly due to the initial negative offset. The straps introduced an eccentric axial load but no additional stiffness. This is also of significance for the dynamic response discussed below – the introduction of post-tensioning did not change the dynamic stiffness, so the vibration frequency was unchanged.

The applied tensioning force in the bottom section of the panel was limited by the tensile strength of the strap. As mentioned before, the bracing straps used in this study were 0.8 mm thick and their maximum measured tensile strength was around 6.1 kN per strap.

Approximate measurements and calculations show that, when applied, a single bracing strap tensioner applied to a strap with ends fully restrained will lead to a 3 mm increment of the total length resulting in around 2.5 kN of force when using 0.8 mm thick by 30 mm wide strap, and therefore, the total tensile force in a single strap with two tensioners is almost 5 kN, ignoring the negligible draw-in of the two ends of the beam as it hogs. If higher spans are involved, or more hogging deflections are desirable, thicker straps (1 or 1.2 mm) may be used to allow more tensile force in the bottom section of the panel.

4.4. Dynamic Response

4.4.1. Background

One of the main advantages of composite flooring systems is the large achievable spans; however, large span flooring is typically limited by its dynamic performance (Pavic & Reynolds, 2002). Hassan and Girhammar (2013); Murray, Allen, and Ungar (2003) suggest that the vertical fundamental frequency is the most significant vibrational response to consider when investigating the frequency response spectrum of an excited floor, since this mode of vibration induces the largest deflections and therefore is most easily perceived by humans. In residential buildings, footfall is the main source of vibration that causes human discomfort, in the form of short term transient oscillations. These transient vibrations are caused by a two phase impulse with the heel drop and toe push off acting as effectively two impulses within one step (Ohlsson, 1991). However, the experimental excitation of a floor does not need to be a footfall; a much smaller magnitude force is suitable and often yields cleaner responses in both frequency and damping ratios (Weckendorf, Zhang, Kermani, & Reid, 2006). A force such as the bouncing of a ball is an ideal test as it excites the floor without affecting the response, since after rebounding it adds no residual mass to the

structure. The large impulse time of the ball bouncing on the floor means that it does not excite the higher modes of vibration, but, as Ellingwood and Tallin (1984) suggest, these higher modes are not of importance to floor dynamic performance.

As Hassan and Girhammar (2013) suggest, the best position to place the sensors for measuring the response is in the centre of the span. This is the position of largest deflection production and the largest and cleanest responses for the panel.

4.4.2. Test setup

The testing method used to determine the dynamic response of the test specimen was similar to Hamilton (2014), and utilised only an accelerometer and a basketball. The accelerometer was placed at the mid-span of the specimen ensuring it is secure and will not move around during excitation. A basketball was then used as the excitation impulse (Figure 4.6). Each test specimen was excited five times, leaving enough time between excitations for the previous vibration to damp out sufficiently to not influence the response to the next impact. The dynamic response was measured for all three testing phases: clamped, jointed and post-tensioned. It is worth noting that, for type of used accelerometer, the data collected is not impacted by the impulse location of the basketball.

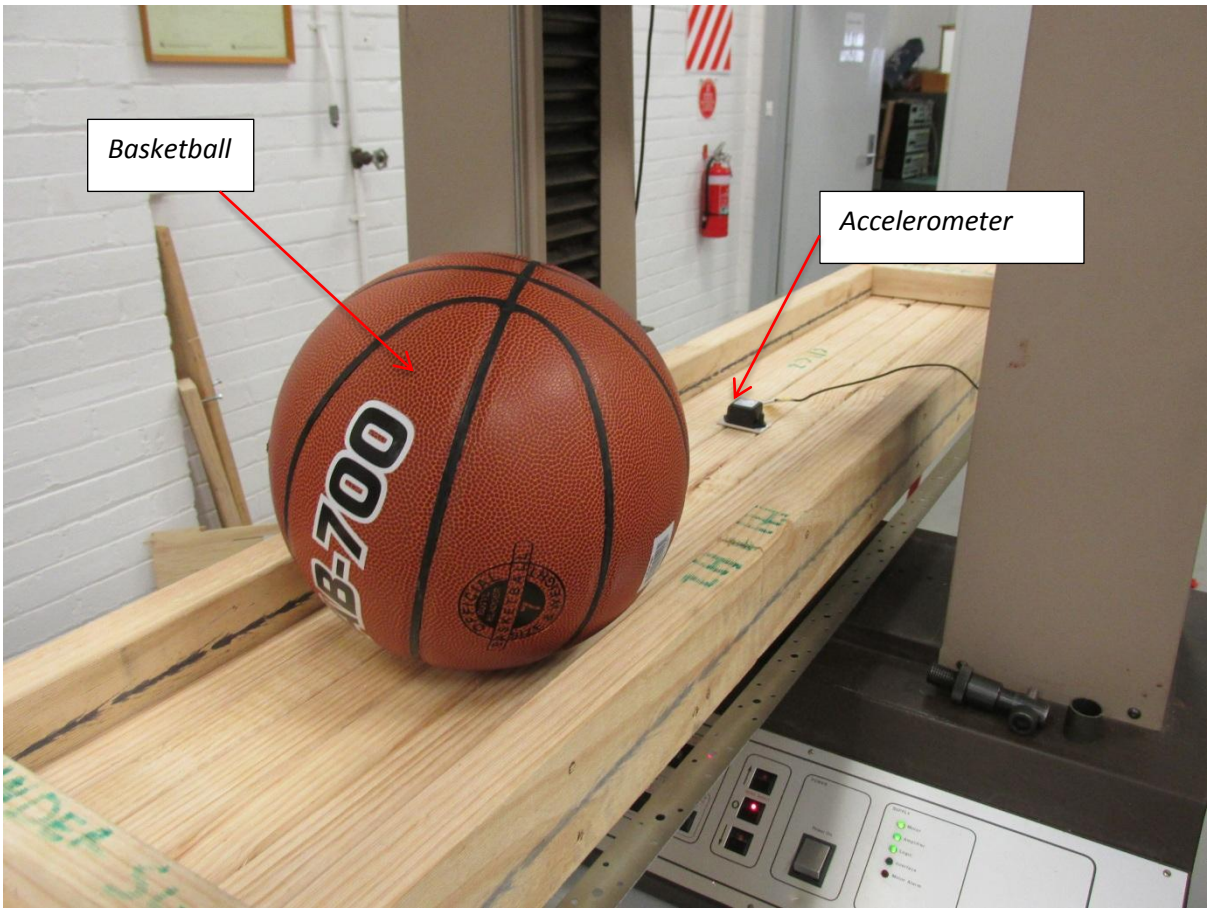

Figure 4.6. Testing of dynamic response.

4.4.3. Dynamic test results

Typical acceleration response of clamped, jointed and post tensioned panels are shown on Figures 4.7, 4.8 and 4.9 respectively.

In each of these graphs initial transients are observed due to the impact from the basketball, containing high frequency modes that very quickly dissipate. This is followed by the classical exponentially decaying oscillations typical of damped free vibration of a single degree of freedom system.

It is noted that in Figures 4.8 and 4.9 there is evidence of 'beating', i.e. superimposed on the general exponential decay there is a slow amplitude modulation pulsing with a period of around 1 second. This indicates that there must be two very similar natural frequencies interacting. This is explained by the fact that once joints were introduced into the beams the composite slab was no longer symmetrical. Thus the left and right sides of the slab had slightly different dynamic stiffness, and so a torsional vibration was set up that interacted with the longitudinal vibration. This will be discussed further below.

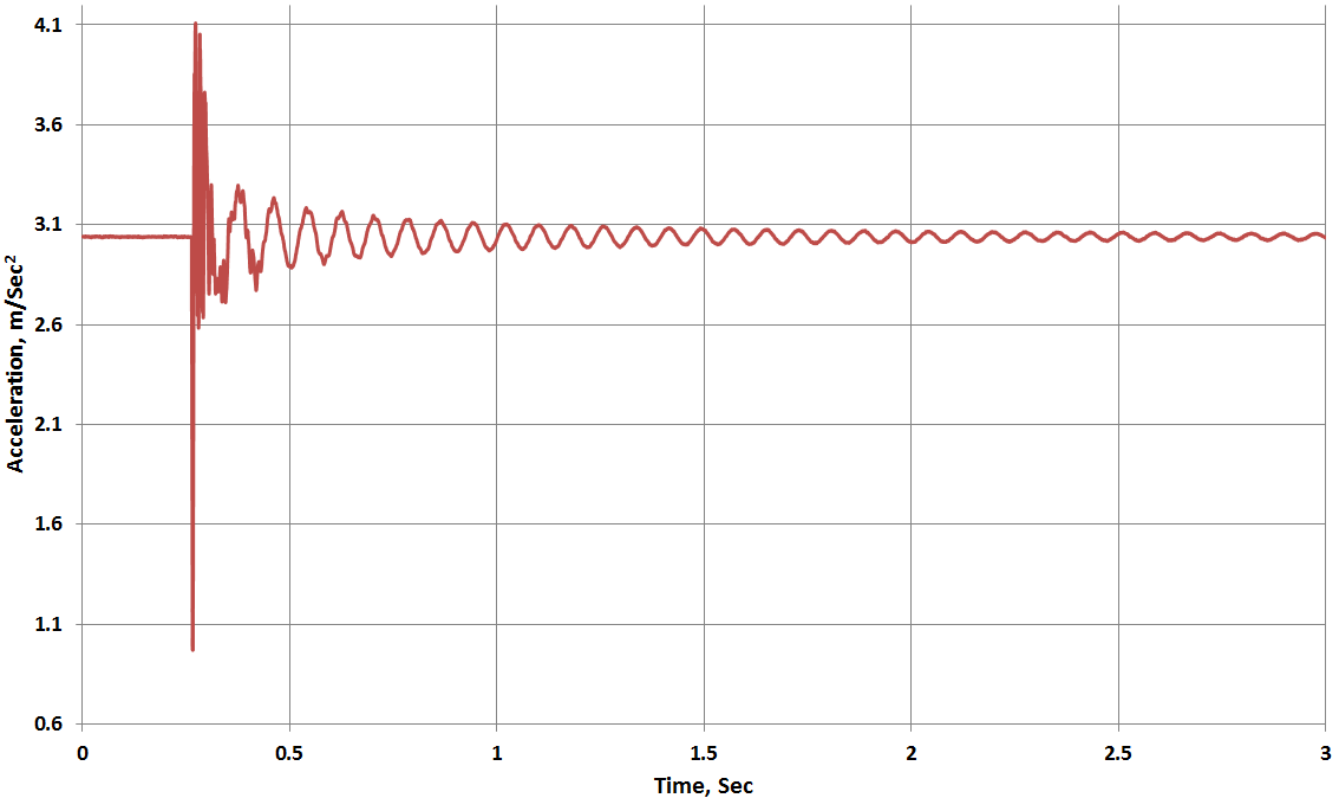

Figure 4.7. Typical acceleration response for a clamped panel (P-2).

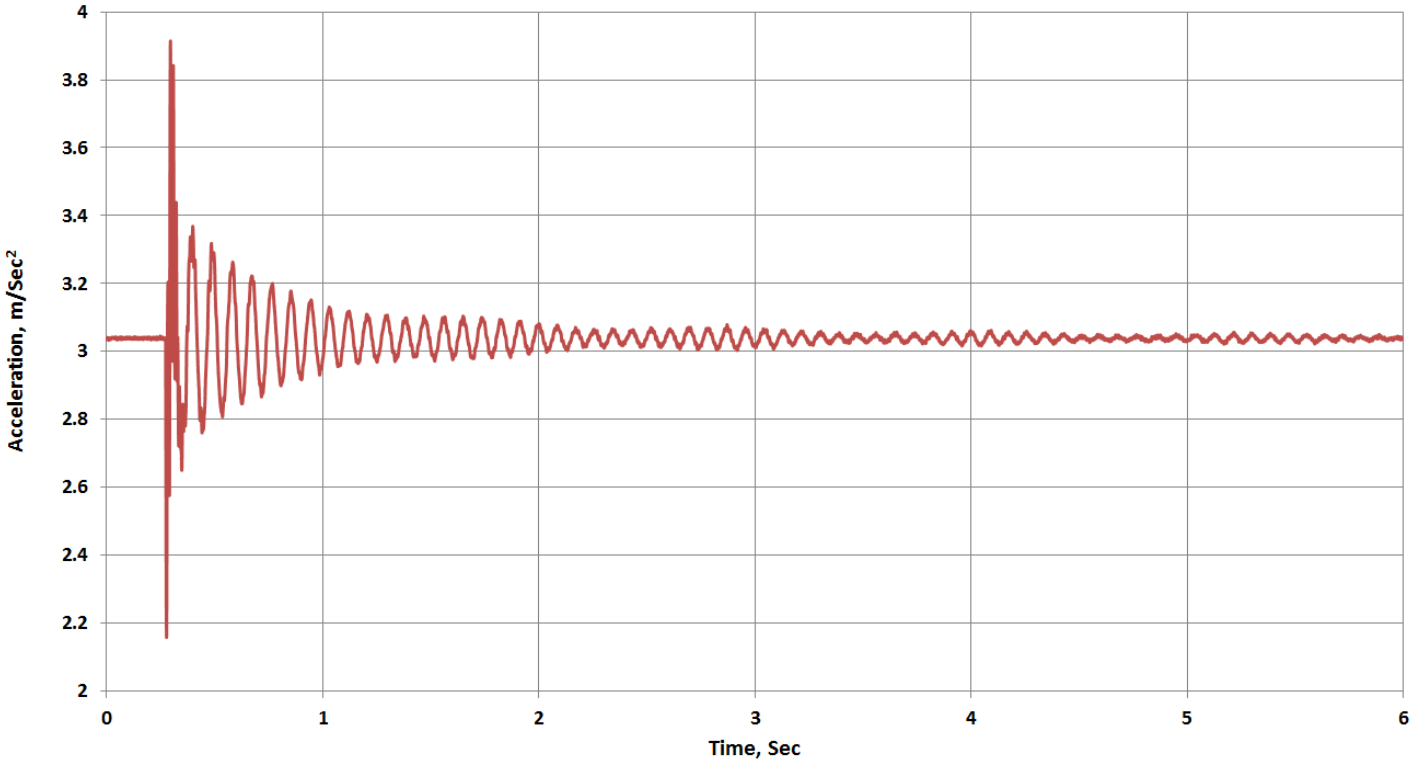

Figure 4.8. Typical acceleration response for a jointed panel (P-5).

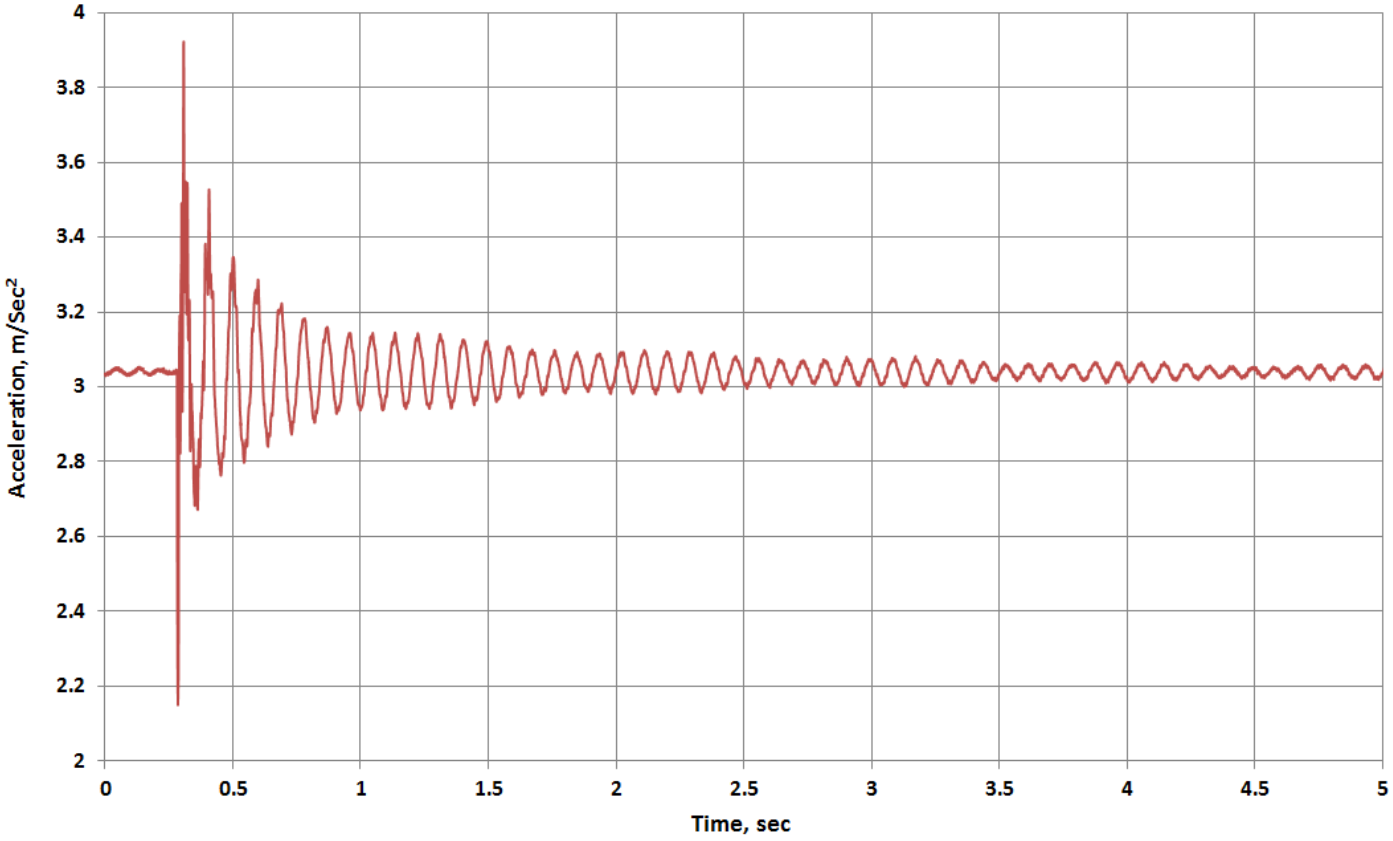

Figure 4.9. Typical acceleration response for a post-tensioned panel (P-4).

The dynamic data analysis was carried out using MatLab. A Fast Fourier Transform (FFT) was taken of the raw data to identify the fundamental frequency. This showed a strong peak located at the fundamental frequency, based on the total duration of each exatiation which was 12 seconds. The damping ratio was determined using the following sequence in MatLab:

The equation for displacement of a vibrating system with linear stiffness and damping response is assumed to follow the form below in Eqn 1 (Thomson, 1993):

$$x = Xe^{-\delta\omega t}\sin(\sqrt{1-\delta^2}\omega t + \varphi) \tag{4.1}$$

where

δ= the damping ratio,

ω= frequency

t= time

φ, X = arbitrary phase and amplitude constants defined by initial conditions

Since the maximum value of the sine term is 1 the magnitude of the oscillations is governed by the following exponential term (Equation 4.2):

$$\boldsymbol{y = Xe^{-\delta\omega t}} \tag{4.2}$$

After differentiating and rearrangement, the damping ratio can be determined from Equation 4.3:

$$\boldsymbol{\delta = -\frac{1}{\omega}\frac{d(\ln(y))}{dt} \approx \frac{1}{\omega}\frac{\ln(\frac{y_1}{y_2})}{t_2 - t_1}}, \tag{4.3}$$

where y_1 and y_2 are amplitudes measured at two times t_1 and t_2 respectively. The results of MatLab data interpretation are presented in Table 4.3 (fundamental frequencies) and Table 4.4 (damping ratio).

Table 4.3. Fundamental frequencies results for all tested panels.

Panel	Fundamental frequency, Hz (average of 5 repetition)		
	Clamped	Jointed (before post-tensioning)	Jointed (after post-tensioning)
P-1	12.5	11.2	11.6
P-2	12.9	11.5	11.7
P-3	13.1	11.7	11.9
P-4	12.3	11.9	11.4
P-5	12.4	11.2	11.3
P-6	12.5	11.7	11.5
AVERAGE ± StdDev	**12.62 ± 0.31**	**11.53 ± 0.29**	**11.57 ± 0.22**

Table 4.4. Damping ratio results for all tested panels.

Panel	Damping Ratio, % (average of 5 repetitions)		
	Clamped	Jointed (before post-tensioning)	Jointed (after post-tensioning)
P-1	4.5	5.1	2.4
P-2	4.1	5.3	2.6
P-3	3.9	5.0	2.3
P-4	4.3	5.3	2.4
P-5	4.5	5.3	2.3
P-6	4.6	5.5	2.5
AVERAGE ± StdDev	**4.32±0.27**	**5.25±0.18**	**2.42±0.12**

4.4.4. Discussion of dynamic loading results

As shown in Table 4.3., the fundamental frequency for the clamped panels was around 12.5Hz, which very similar to the result obtained by Hamilton (2014) when testing control MGP 10 panels over a span of 4200mm. The frequency was found to be slightly lower (around 11.5Hz in average) for jointed panels, which was surprising given that static testing showed the jointed panels to be slightly stiffer, and the clamped panels had the additional mass of the clamp at mid-span. It is noted that the differences in stiffness, mass and natural frequency are all very small, and further speculated that of these the effective stiffness is the slightly in error. It possibly differs slightly from the measured stiffness because of the

asymmetry in the beam, mentioned above in relation to Figures 4.8 and 4.9. With regard to this it may be significant that the LVDT was not placed on the centreline of the slab (see Figure 4.2).

It was also noted that the process of post-tensioning had no effect on the fundamental frequency, as discussed in Section 4.3.4, since it introduces no additional stiffness.

As mentioned before, the conservative nature of the current dynamic requirements placed on flooring systems restricts the achievable spans. Many different design criteria have been proposed to mitigate this issue. The most commonly used is a restriction on the fundamental frequency of the floor. Bernard (2008); Standards Australia Limited (2002); Weckendorf et al. (2006) and many others, specify a minimum fundamental frequency of 8Hz as the defining parameter. Nevertheless, others specified frequencies to be as low as 6Hz or as high as 14Hz (Dolan, Murray, Johnson, Runte, & Shue, 1999). For multi-residential buildings with continuous floors, Hassan and Girhammar (2013) suggest a minimum frequency of 10Hz.

The natural frequency is highly dependent on boundary conditions, span, and added mass (such as of floor coverings). The actual frequency is therefore of little significance, but rather the important observation is that it was not significantly changed by either jointing or post-tensioning. However a simply-supported one-way 4.2 m slab with overhangs will have a low natural frequency, so this is a severe test case and dynamic requirements are likely to be met in a practical application.

The damping ratio results shown in Table 4.4 for clamped and jointed panels before post-tensioning are similar to those obtained by (Hamilton, 2014) when testing control MGP-10

with a span of 4200mm. It is clear that the introduction of post-tensioning has decreased the damping ratio of the tested panels by almost 40% (to around 2.4% on average), which is a close value to that obtained by Worth, Omenzetter, and Morris (2012) when testing post-tensioned laminated veneer lumber building (1.6-2.4%). On the other hand the introduction of joints increased the damping ratio.

This increase of damping ratio is attributed to the introduction of joints, allowing relative movement and frictional dissipation of energy. Likewise the subsequent reduction in damping ratio is attributed to the compressive force in the beam tightening up any gaps or looseness so that energy is not dissipated at the joints. This hypothesis is supported by the observation that the damping ratio was amplitude dependent, being slightly higher in the initial part of the oscillation decay. Furthermore, this effect was less apparent with the post-tensioned specimens.

In spite of the reduction in damping ratio with the use of post-tensioning the obtained ratios are still within the acceptable limits. Durham, Lam, and He (1999); Filiatrault and Folz (2002); Foliente (1995) suggest that, if conservative, 2% of critical damping is still appropriate. Ohlsson (1991) suggests that for light weight floors a damping ratio of at least 1% is desirable and can be reduced to 0.8% for floors with large spans or with a large mass (i.e. low natural frequencies). A higher value of 3% for lightweight floors is suggested by Smith, Hicks, and Devine (2009) who also suggests that for solid timber this value can be reduced down to 1%. Smith et al. (2009) suggest that if the fundamental frequency is at least four times the footfall excitation frequency (which is the case in this study for post-tensioned panels), then the vibration will die out prior to the subsequent footfall and the

excitation will act like a series of independent excitations. Ohlsson (1991) deems this type of vibration to be less perceivable for humans.

It is worth noting, that damping ratios seen under laboratory conditions are very much lower than what would be obtained in a real world application (Murray et al., 2003). This is due to the significant reduction in energy dissipating at connections that the system would be subject to if it were installed in an actual building. This reduction in damping is difficult to estimate because the damping is significantly impacted by the method of construction and the quality of workmanship (Dolan et al., 1999) and by any additional fittings. Because of this, it is impossible to calculate a damping ratio at the design stage or accurately estimate it based on test results. If during the construction stage, it is found that the damping ratio was insufficient then steps can be taken to increase it, such as introducing rubber inserts into the floor (Bernard, 2008).

4.5. Conclusion

This chapter has presented an experimental investigation to understand the behaviour of locally post-tensioned timber panels, in particular their deflections under serviceability loads and their dynamic response. The following can be concluded:

1. The local post-tensioning may be applied using nothing more than a bracing strap and a bracing tensioners, both available in most hardware stores.

2. The application of local post-tensioning can reduce nett deflections under serviceability loads by almost 50%, but in theory further reduction of deflections can be achieved by using thicker bracing straps as post-tensioning elements.

3. The fundamental frequency, which is the most significant vibrational response to consider when investigating the frequency response of timber floors, was not impacted by the post-tensioning process.

4. The application of local post-tensioning has severely decreased the damping ratio of the panels; however its value remained within the acceptable limits and was significantly higher than ratios obtained in other studies involving post-tensioned timber.

5. Using LPT to Restore the Capacity of Severely Damaged Steel Beams

5.1. Introduction

Due to the aging of structures and the increase of traffic loads many steel bridges are experiencing corrosion damage and fatigue cracks in areas of high stress concentration (Deng & Lee, 2009; Kim et al., 2008; Kim & Yoon, 2010; Shahrooz et al., 2002; Wardhana & Hadipriono, 2003). Replacement of these structures is costly and will lead to the interruption to traffic. Therefore various structural repair techniques and strengthening mechanism have been used (Hmidan et al., 2011; Kim & Brunell, 2011; Kim & Harries, 2012; Photiou et al., 2006).

Bolting or welding of steel plates to existing steel beams is one of the most widely used repair techniques (Kim & Brunell, 2011; Tavakkolizadeh & Saadatmanesh, 2003). However there are issues related to this method. For example, the added plates increase the self-weight of the structure. In addition, the welding or bolting process may introduce new stress concentrations in the repaired region, causing a reduction of structural fatigue life (Colombi & Poggi, 2006; Hmidan et al., 2011; Kim & Brunell, 2011; Lenwari, 2006; Nozaka et al., 2005; Roy et al., 2009). Another strengthening method involves applying carbon-fibre reinforced polymer (CFRP), adding sheets bonded to the web or soffit of steel beams. Due to the features of light weight, good durability and ease of handling (Nozaka et al., 2005; Tavakkolizadeh & Saadatmanesh, 2003), use of FRP materials appears to be a convenient and efficient method for increasing the load carrying capacity of the existing beams (Jiao et al., 2012; Kim & Brunell, 2011; Kim & Harries, 2012; Lenwari, 2006; Tavakkolizadeh & Saadatmanesh, 2003).

An alternative of these methods was the technique of external prestressed tendons, which has been applied not only for strengthening of composite steel-concrete beams, , but also for new bridge constructions (Ayyub et al., 1992; Chen, 2005; Chen & Gu, 2004; Nie et al., 2011; Qader et al., 2013; Uy, 2007; W. Xue et al., 2008; W. C. Xue & Li, 2001). This can be achieved by welding end anchorages and using conventional high-strength post-tensioning cables (Refer to Section 2.3 for more details).

This chapter presents an experimental study on the use of the LPT method to strengthen steel beams damaged by severe fatigue cracks. The aims were to investigate the behaviour of locally post-tensioned steel beams in three-point-bending and to examine the effect of the post-tensioning levels on the rigidity and the load carrying capacity of the damaged steel beams. Results were compared with those of beams strengthened by other methods.

5.2. Specimen preparation and test setup

5.2.1. Steel beams

As the objective was to study the effectiveness of repair methods for damaged beams, it was first necessary to induce a consistent form of damage. This was achieved by fatigue loading of the original unreinforced beam under load control with a loading frequency of 7 Hz until a crack developed in the mid-span up to the neutral axis. The proposed repair process could subsequently be conducted and the beams retested. The crack was initialised by a notch at the tensile flange (Jiao et al., 2012).

The steel beams used in the tests were Grade 400 150UB14 with the section dimension of 75 mm in width and 150 mm in height. A total of six beams were tested, each of length 1.4m. Initially, these beams were tested (without the proposed post-tensioned

reinforcement) up to failure under fatigue loading until a crack developed in the mid-span up to the neutral axis, so that the proposed repair process could subsequently be conducted and the beams retested. The fatigue tests were conducted under load control with a loading frequency of 7 Hz.

The material properties of the steel beams, including the yield stress and the ultimate tensile strength, were obtained through tensile coupon tests. The yield stress, the ultimate tensile strength and Young's modulus were 411.6 MPa, 541.3 MPa and 207.4 GPa respectively (Jiao et al., 2012).

5.2.2. Steel Reinforcing Bars

The local pre-stress was applied by deformed reinforcing bars 500N, as normally used for reinforced concrete. They have a normal yield strength of 500 MPa specified in AS/NZS 4671:2001. The reinforcement bar (normal ductility) has a distinctive plastic zone with a uniform strain of 0.050 and an ultimate fracture strain of 0.20. The material properties were verified by tensile tests. Figure 5.1 shows a typical stress-strain curve of a reinforcing bar, where a yield stress of 580 MPa was obtained. In this study bars with diameters of 12 mm and 16 mm and a length of 1200 mm were used. The choice of bars' diameters was based on the variety of reinforcing steel available in Australian market. The reinforcing grade 500N is available in diameters 12, 16, 20 and up to 40 mm. For the given section of the I-beams (150UB14), the 20 mm rebar would be too large to be welded on the sides of the web.

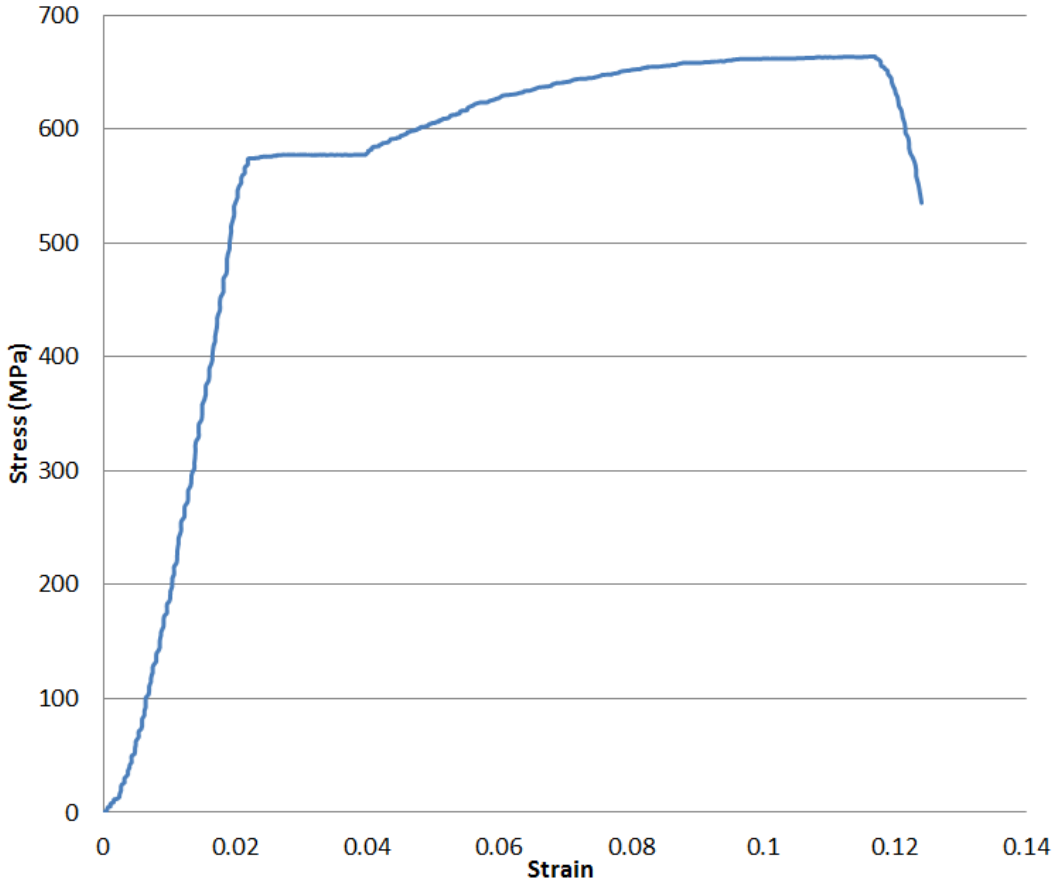

Figure 5.1. Stress-strain relationship of a reinforcing bar.

5.2.3. Specimen preparation and magnitude of tensioning force in reinforcing bars

A typical beam is shown in Figure 5.2. As mentioned above, each prepared specimen contained a crack in the mid-span from the tension flange towards the neutral axis with a depth of 75 mm measured from the top surface of the tension flange. The ratio of the crack depth to the depth of the beam, a_0/h, was 0.5, chosen because it was the most severe damage level that was found in the papers that the results of this study were compared with.

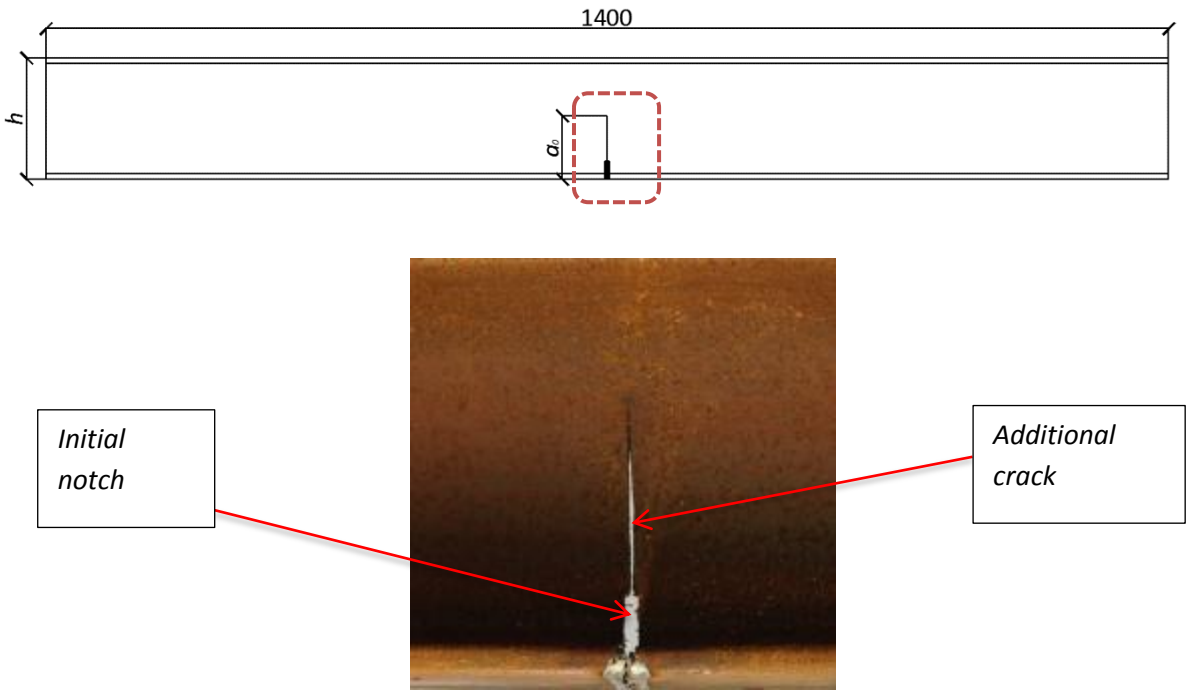

Figure 5.2. Damaged beam.

The damaged beams were repaired using the LPT method. The main concept of this method is to pull the crack together by using a manual screw jack to tension two reinforcing bars, one on each side of the web. The bars were welded to the beam's web at both ends as illustrated in Figure 5.3 (a), at a distance *f* (defined below and in Chapter 3) from the cracked flange such that the bar just touches the flange when it has the desired tension (see Figure 5.3 (c)). Figures 5.3 (b) and 5.4 illustrate the manual screw jack. In this study, the pre-stress was achieved simultaneously for the 2 bars from both sides as shown in Figure 5.4 to prevent lateral torsional buckling. However lateral buckling during the process of post tensioning may be possible in the field if there are imperfections and low quality control.

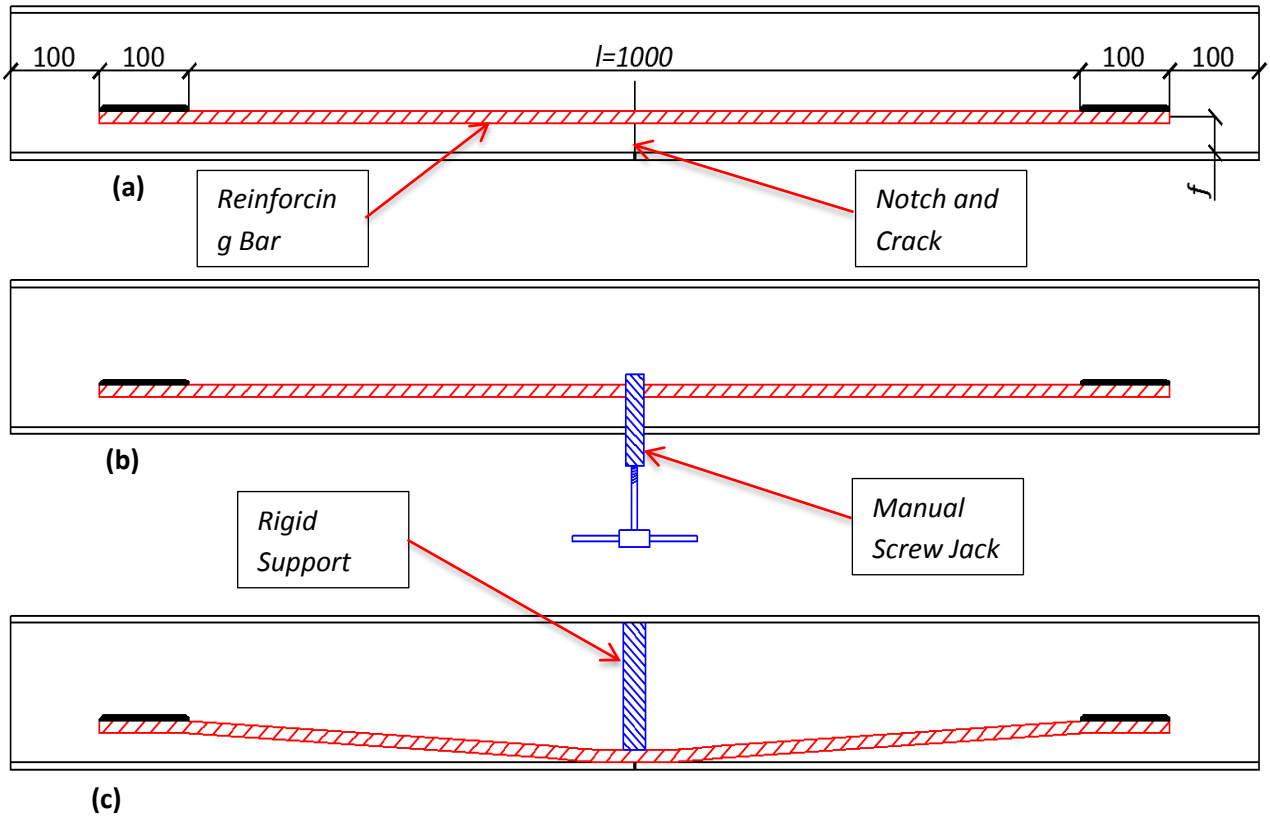

Figure 5.3. The process of LPT. (a) welding the bars (on both sides), (b) pulling the bars using a manual screw jack, (c) fixing the bars in place using a rigid support.

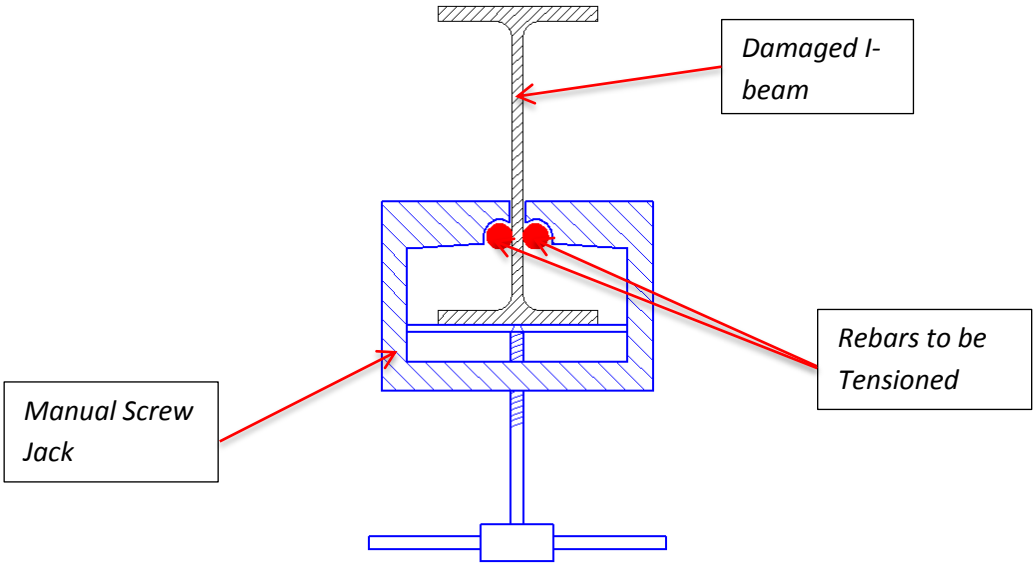

Figure 5.4. Detail of the manual screw jack.

After the bars were pulled to reach the required tensile stresses, a rigid support was inserted between the mid-span of each steel bar and the bottom surface of the top flange to maintain the stresses in the bars. The tensile force in the rebar generated a reverse bending moment in the cracked cross-section that resulted in the closure of the initial crack.

Based on the elastic stress-strain relationship, the vertical displacement (jacking distance) f is calculated using Equation 3.1 (see Chapter 3 and Appendix 2).

Similarly to the local post-tensioned beams, the tensile force N within the reinforcement bars is then calculated using the Equation 3.2.

For example, for a 12 mm diameter reinforcing bar with the cross-sectional area of 133 mm^2, if the level of pre-stress was chosen to be 100% of the yield stress of the reinforcing bar (500 MPa), a tensile force of $N=56.5\ kN$ is needed for the reinforcing bar, achieved by a jacking distance of 35mm based on a reinforcing bar length of $l=1m$. A typical repaired beam (B12-100) is shown in Figure 5.5.

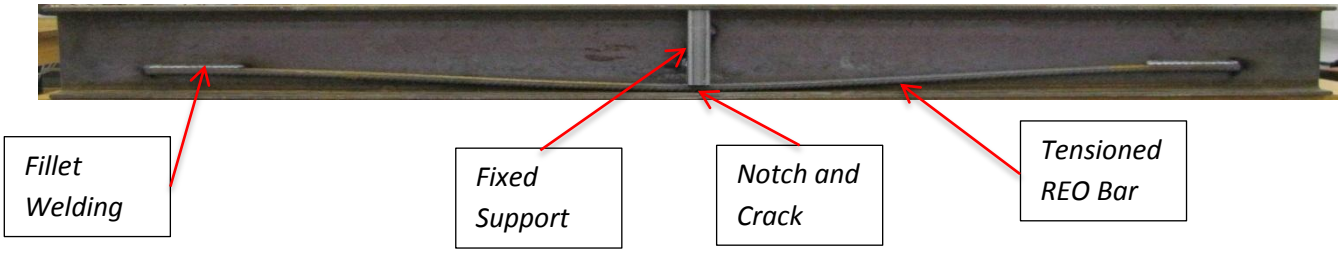

Figure 5.5. Typical strengthened steel beam.

5.2.4. Analysis of forces in the reinforced section

Figure 5.6 shows the jacking force, *F,* and the tensile force, *N,* within a strengthened steel beam after the process of LPT. The jacking force *F*, required to generate the tensioning force *N*, can be calculated using the same principle mentioned in Chapter 3.

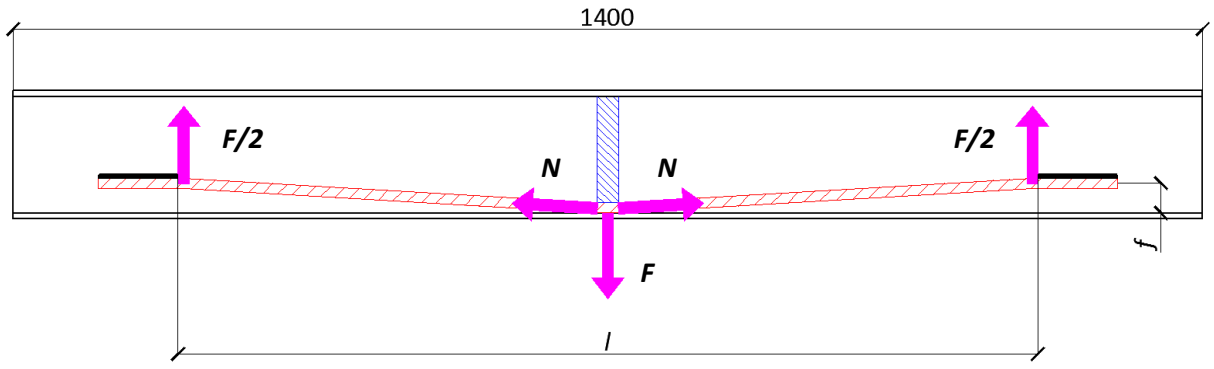

Figure 5.6. The distribution of forces within the beam.

Different pre-stressing forces were applied on each beam in order to highlight the effect of the tensioning force on the beam's overall stiffness and load-carrying capacity. The differences in tensioning levels (force *N*) were achieved by varying the jacking distance *f* and the diameter of reinforcing bar (12 mm and 16 mm were used). Table 5.1 shows the diameter of steel rebar used for reinforcement, the pre-stress and the tensioning force in the steel bars.

Table 5.1. List of specimens.

Beam	Reinforcing bars used (one each side of web)	Level of tensioning in reinforcing bars	Calculated tensioning force *N* (total for the two reinforcing bars) *(kN)*
B16-100	2*N*16	100% (500 MPa)	200
B16-80	2*N*16	80% (400 MPa)	160
B16-50	2*N*16	50% (250 MPa)	100
B12-100	2*N*12	100% (500 MPa)	113
B12-80	2*N*12	80% (400 MPa)	90
B12-50	2*N*12	50% (250 MPa)	56.5

5.2.5. Test Setup

Three-point bending tests were conducted in a universal testing machine with a loading capacity of 1000 kN as shown in Figure 5.7. A beam specimen was simply supported on two roller supports with a span of 1200 mm. To load the beam these supports moved upwards, resisted by a fixed pin support above the mid-span of the beam. The deflections and crack opening were measured using linear digital transducers (LVDTs). LVDT 1 was fixed horizontally in the middle part of the beam to measure the crack mouth opening displacement (CMOD). LVDT 2 was installed at a position measured 360 mm from the centre of the beam, while LVDT 3 was used at the edge support to measure the maximum deflections. Strain gauges were installed on the reinforcing bars to monitor the strains

during the pre-stressing and testing. All strain gauges and LVDTs were connected to an amplifier and a data acquisition system, similar to that used in Chapter 3 (see Appendix 1).

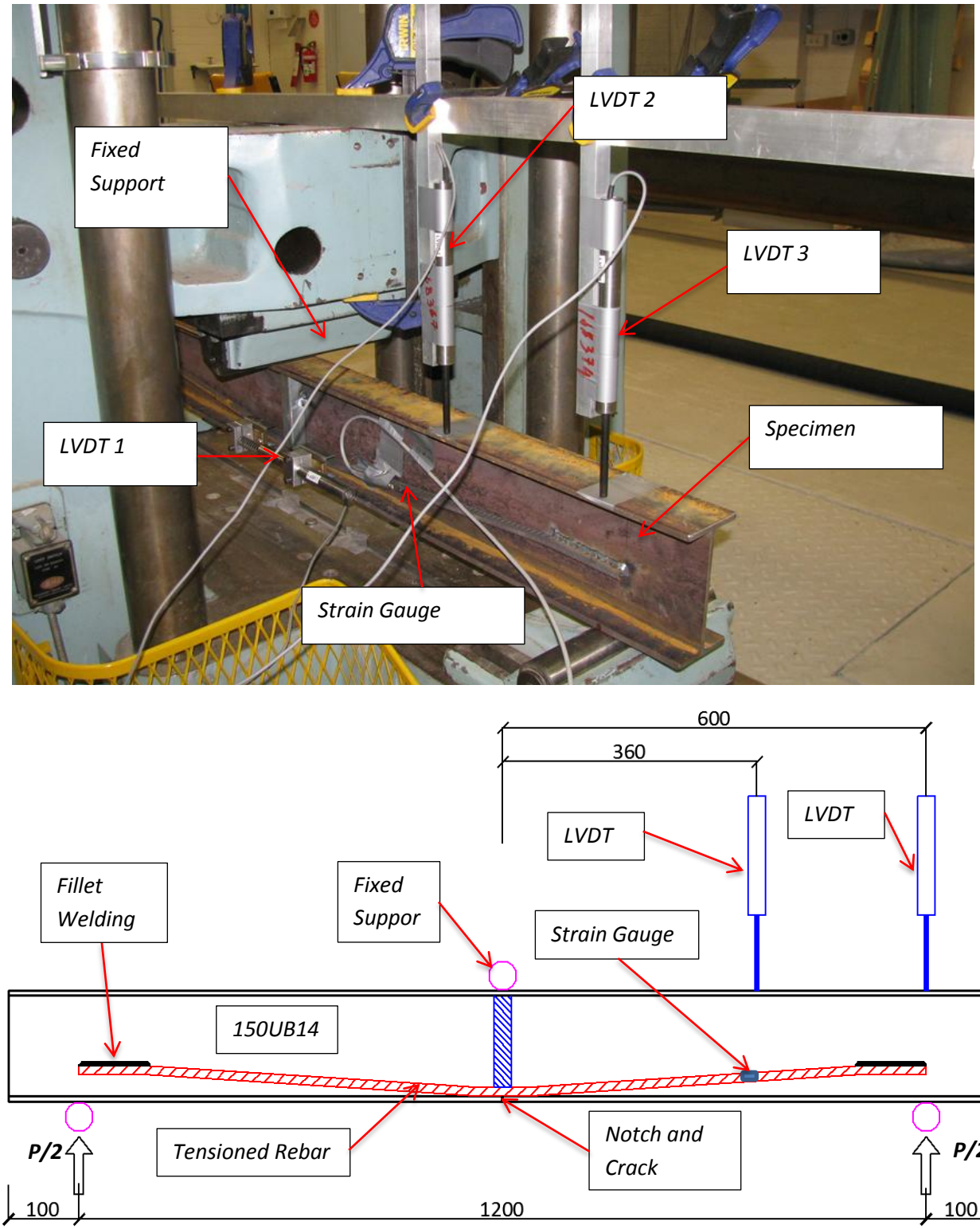

Figure 5.7. Test setup (Note: LVDT 1 omitted for clarity).

5.3. Results and discussion

5.3.1. Failure modes

All beams failed by the yielding of the compressive flange accompanied by the opening of the original crack at mid-span. Figure 5.8 shows the typical failure mode of specimens. Flexural buckling in the compressive flange was also observed but no sign of lateral torsional buckling was observed at failure. The crack opening was accompanied by the yielding of the reinforcing bar.

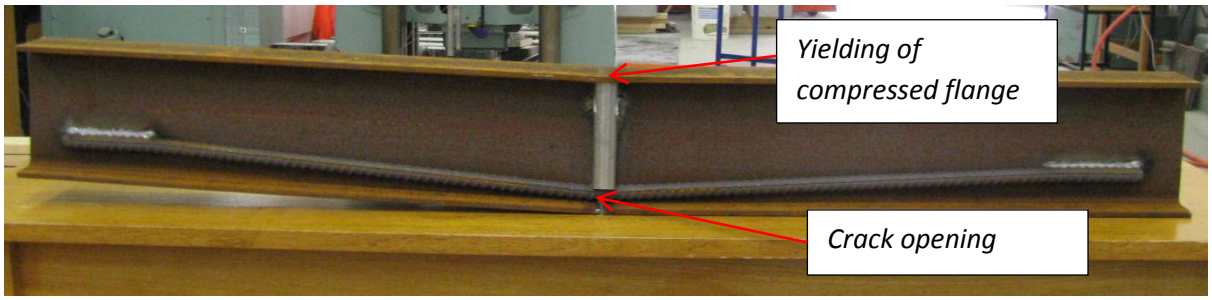

Figure 5.8. Typical failure of specimens (B16-100).

5.3.2. Ultimate loads

The ultimate moments calculated from the ultimate loads and the corresponding post-tensioning forces in the reinforcing bars are listed in Table 5.2.

Table 5.2. Test results

Beam	Tension force *N (kN)*	Ultimate Load P_u, *(kN)*	Ultimate Moment M_u *(kNm)*
B16-100	200	99.1	29.7
B16-80	160	105.9	31.8
B16-50	100	109.4	32.8
B12-100	113	80.9	24.3
B12-80	90	67.3	20.2
B12-50	56.5	72.9	21.9

Figure 5.9 illustrates the behaviour of the beams during loading. In Figure 5.9(a), the deflection recorded by LVDT 3 was plotted against the ratio of M/M_u where M and M_u are the recorded experimental moment and the ultimate moment for each tested beam respectively. It can be seen that high level of pre-stress has helped to restore the beam rigidity. For instance, at a load level of $M/M_u = 0.4$, specimen B16-100, which had 100% pre-stress, showed a deflection of 0.5 mm compared to the deflection of 3.1 mm for specimen B12-50 which had 50% pre-stress. The deflection data are also plotted in Figure 5.9(b) against the ratio of M/M_{ui}, where M_{ui} is the theoretical ultimate moment for an intact beam with the same cross-section (in this case it is equal to 42 kNm). It can be seen that more than 75% of the load-carrying capacity of an intact beam was restored by using ϕ16 bars compared to about 50% for ϕ12 bars. The ultimate load was an average of 74 kN for beams

reinforced with a 12 mm diameter bars (A=113 mm^2) and an average of 105 kN for beams reinforced with 16 mm diameter bars (A=201 mm^2), representing a 42% increase for the larger diameter bars relative to the smaller ones. Nevertheless, it can be noted that the pre-stressing levels for beams reinforced with the same size of bars had little effect on the ultimate load-carrying capacity. This can be explained by the fact that the increment of the reinforcing diameter bar increases the effective area of the tensile flange and therefore, improve the load carrying capacity, while because of the long yield plateau the initial level of post-tensioning becomes irrelevant when considering the ultimate load.

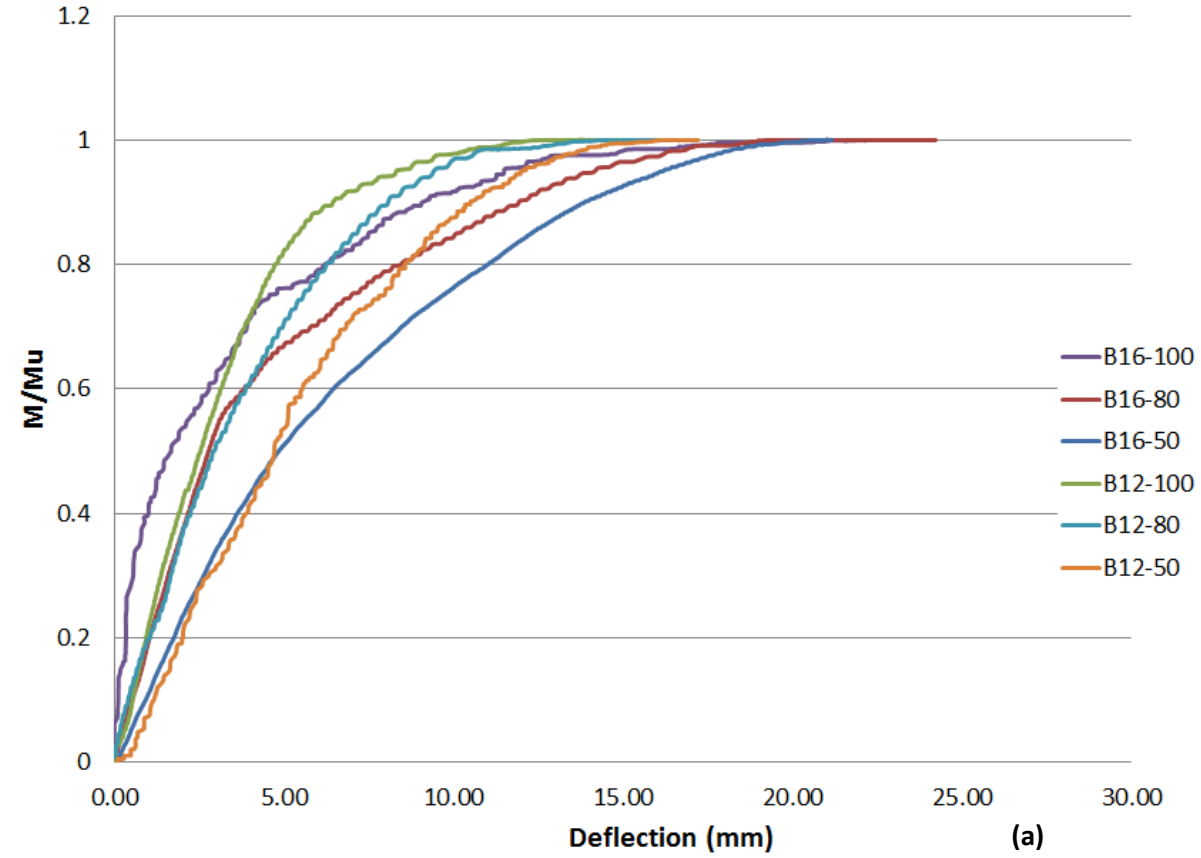

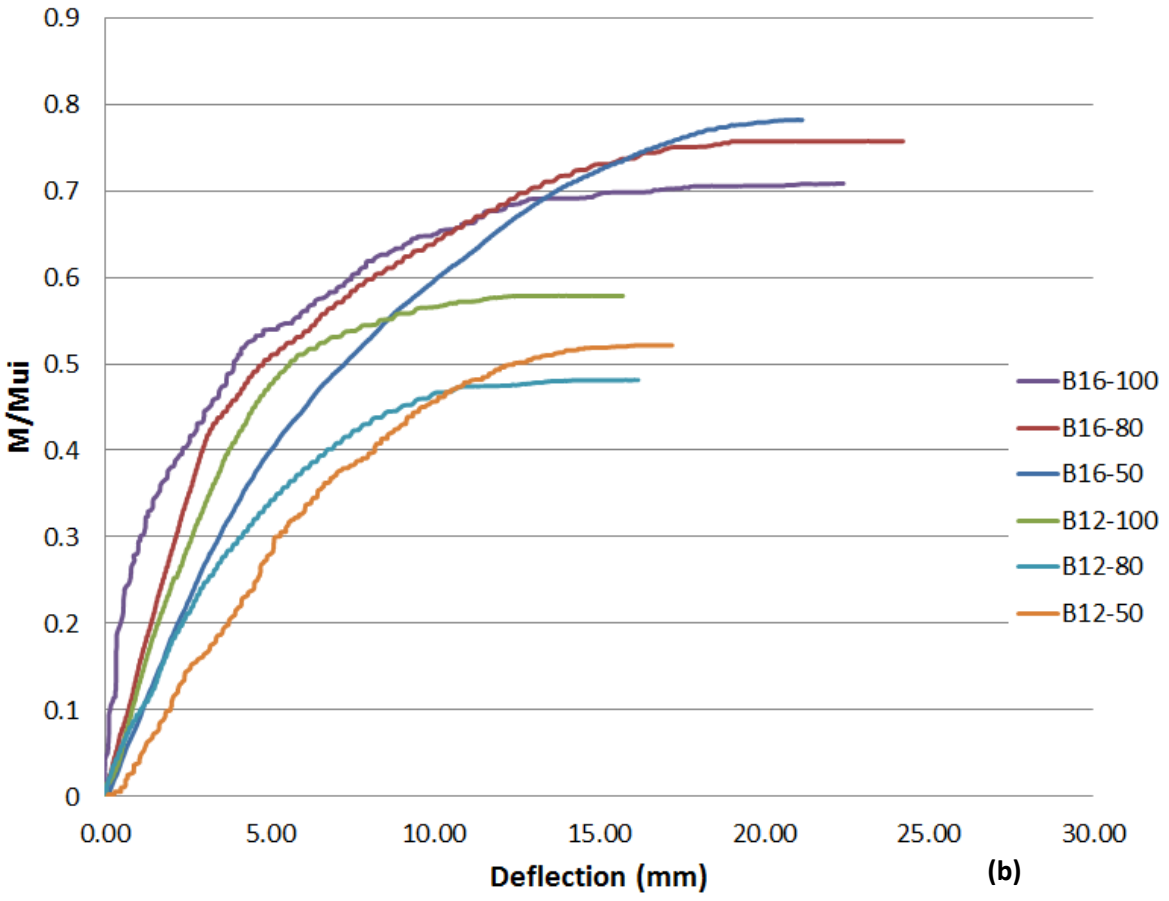

Figure 5.9. Deflections recorded by LVDT 3 against M/M_u (a), and against M/M_{ui} (b).

5.3.3. Strain analysis in rebar

To understand the behaviour of the steel reinforcing bars during testing, strain gauges were applied on pre-stressed bars at a position shown in Figure 5.7. It is expected that, because the bars are slender and essentially in pure tension, the strain would be uniform over both the cross section and length provided it is measured sufficiently far from the bar anchor or loading points.

Results are plotted in Figure 5.10 for specimen B12-100. The measured strain was similar to the theoretical calculated strain. For instance, given that the pre-stress in reinforcing bars in B12-100 was 100% of the nominal yield stress (500 MPa), the calculated initial strain is $\varepsilon=\sigma/E=$ 2500 microstrain, which is similar to the experimental measured initial strain. The strain increased with load increment and exceeded the yield strain of the reinforcing bars; however it should be noted that reinforcing bars used (500N, normal ductility) have a long yield plateau and a uniform strain of 0.050; therefore the steel in the compression flange yielded long before the strain in reinforcing bars reached the hardening phase.

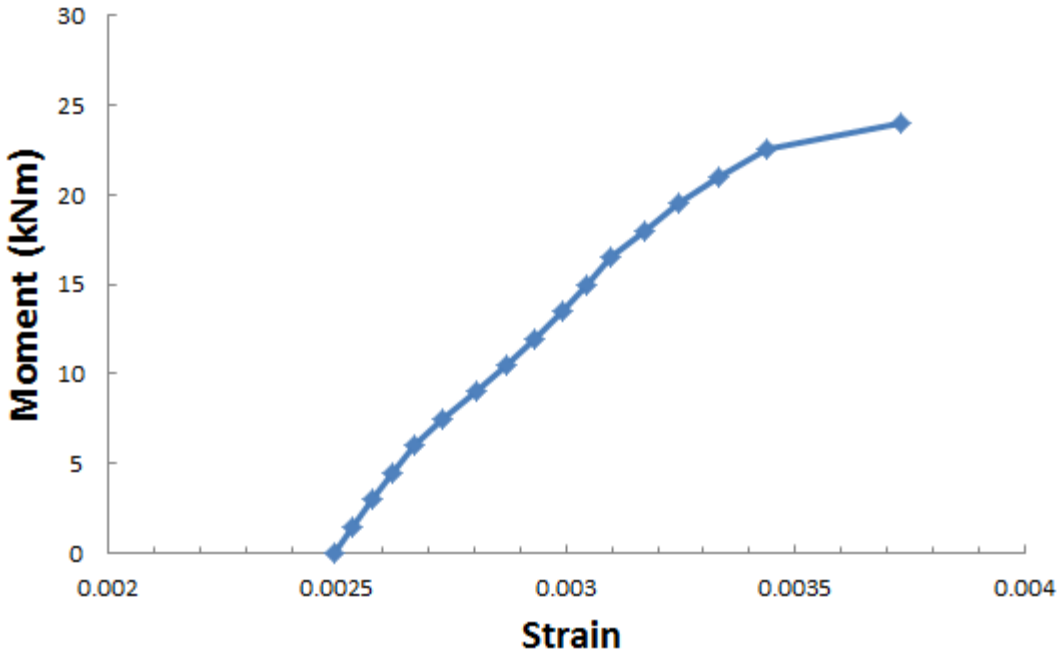

Figure 5.10. Strain behaviour in tensioned reinforcing bars for specimen B12-100.

5.3.4. Creep of post-tensioned bars

Previous studies showed that creep is an important factor when post-tensioning steel is very highly stressed; however, it is of little significance and can be completely disregarded in normal reinforcing steel, which is used in this study (Mosley, Bungey, & Hulse, 2007; Rusch, Jungwirth, & Hilsdorf, 1983).

5.3.5. Comparison with other repair methods

The results were compared to results received by Hmidan et al. (2011); Kim and Brunell (2011). In these tests, Carbon Fibre Reinforcing Polymer (CFRP) was used to repair notched beams which were subject to 3-points and 4-points bending tests respectively (Figure 2.13, Figure 2.14). The beams had almost the same section modulus. The ratio of M_u/Mu_i was plotted in Figure 5.11, were M_u and Mu_i are respectively the experimental ultimate moment for the notched repaired beams and the theoretical ultimate moment for an intact beam

with the same section modulus. The same approach was adopted to determine the experimental ultimate moment obtained by Hmidan et al. (2011); Kim and Brunell (2011).

Figure 5.11 shows that using pre-stress for strengthening damaged beams is more efficient than CFRP, especially in restoring the initial load-carrying capacity (up until 75% for 16 mm diameter bars) when the level of damage is significant ($a_0/h=0.5$).

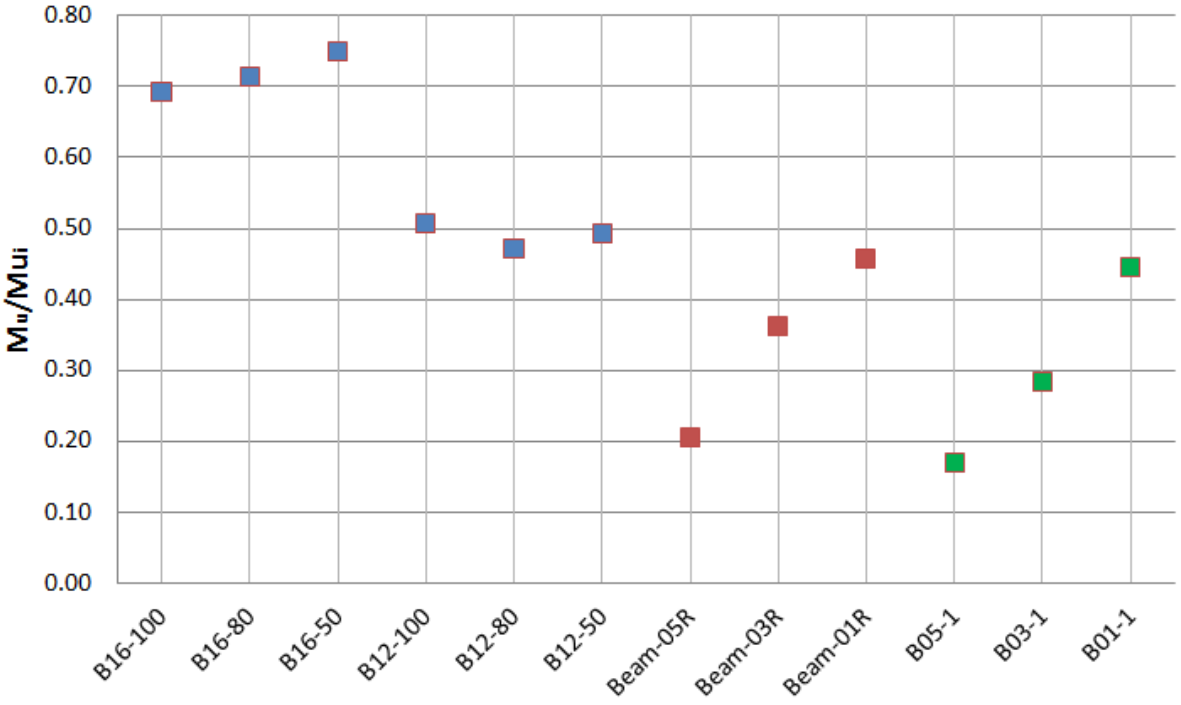

Figure 5.11. Comparison of results of this study (B16-100 to B12-50) with Kim and Brunell (2011) (Beam-05R to Beam-01R) and Hmidan et al. (2011) (B05-1 to B01-1).

5.4. Efficiency of local post-tensioning

The LPT provides both a low cost and easy to operate method to repair damaged steel beams. The only required material to apply this method is reinforcing steel bars, which has a very low cost comparing to materials used in other repairing methods. It is also worth mentioning that LPT does not require any special equipment or personal training other than

as required for welding, which increases its efficiency and reduces its overall cost. Consequently, the LPT can be adopted on almost every restoration site without any previous preparation or material and equipment transportation.

5.5. Conclusion

This chapter has presented an experimental investigation to understand the effectiveness of using pre-stressed reinforcing bars as a method of repairing damaged steel beams. The following can be concluded:

1. Application of local pre-stressed reinforcing bars could restore at least 75% of the load-carrying capacity of the damaged beams, but in theory more if larger bars are used or the bars can be attached to the outside of the flanges.

2. The higher the level of pre-stress in the reinforcing bars, the higher the beam's stiffness.

3. The level of pre-stress in reinforcing bars has negligible effect on the load-carrying capacity of the beam. In order to increase the load-carrying capacity, the diameter of pre-stressed reinforcing bar should be increased.

4. It is simpler and more efficient to use pre-stressed bars than other repair methods, such as applying CFRP, to restore damaged steel beams.

5. Local pre-stress is a cost-effective and easy-to-achieve method of restoring the load-carrying capacity of beams when compared to other repairing methods.

6. Upgrading Steel I-Beams Using LPT

6.1. Introduction

As mentioned in Section 2.3, many steel bridges are rendered structurally inadequate with aging of the structure and the increase of traffic loads (Deng & Lee, 2009; Kim et al., 2008; Kim & Yoon, 2010; Shahrooz et al., 2002; Wardhana & Hadipriono, 2003). Replacement of these structures is costly and will interrupt traffic. Therefore, different structural repairing techniques and strengthening mechanism have been used in modern bridge and structures repair (Hmidan et al., 2011; Kim & Brunell, 2011; Kim & Harries, 2012; Photiou et al., 2006).

Among these repairing and upgrading methods, bolting or welding of steel plates to existing steel beams is one of the most widely used techniques (Kim & Brunell, 2011; Tavakkolizadeh & Saadatmanesh, 2003). However there are issues related to this method. For example, the added plates increase the self-weight of the structure. In addition, the welding or bolting process may introduce new stress concentrations in the repaired region, causing a reduction of structural fatigue life (Colombi & Poggi, 2006; Hmidan et al., 2011; Kim & Brunell, 2011; Lenwari, 2006; Nozaka et al., 2005; Roy et al., 2009). Another strengthening method involves applying carbon-fibre reinforced polymer (CFRP), adding plates or sheets bonded to the web or soffit of steel beams. Benefits are light weight, good durability and ease of handling of FRP materials (Nozaka et al., 2005; Tavakkolizadeh & Saadatmanesh, 2003), and this method appeared to be efficient in increasing the load carrying capacity of the existing beams (Jiao et al., 2012; Kim & Brunell, 2011; Kim & Harries, 2012; Lenwari, 2006; Tavakkolizadeh & Saadatmanesh, 2003).

In addition to these methods, external prestressed tendons have been used to strengthen existing composite steel-concrete beam structures (Albercht & Lenwari, 2008; Ayyub et al.,

1992; Chen, 2005; Chen & Gu, 2004; Nie et al., 2011; Qader et al., 2013; Uy, 2007; W. Xue et al., 2008; W. C. Xue & Li, 2001). This technique involves welding end anchorages and using conventional high-strength post-tensioning cables. Results proved that the initial force in the tendon and its eccentricity significantly affect the strength and stiffness of tested beams (Uy & Craine, 2004). Furthermore, this type of strengthening leads to a 25% increase in load carrying capacity in some cases (Lorenc & Kubica, 2006).

As an alternative to the above mentioned methods, applying prestressing in a localised region within a steel beam is cited in the literature for strengthening existing steel bridges and repairing severely damaged steel I-beams (Shagin, 1996, 2005, 2008). This method increases the stiffness and the load carrying capacity of the steel structural member through adding reinforcing steel bars to a segment of the beam. Prestress is achieved by elevating the steel bars from the soffit of the steel beam by using a manual screw jack that generates a tensile force in the steel bars.

This chapter presents an experimental study incorporating the local prestress method to strengthen and upgrade steel I-beams. The aims of this study are to investigate the behaviour of the locally prestressed steel beams in three point bending and to examine the effect of the prestress levels on the rigidity and the load carrying capacity of steel I-beams. Results are compared with those of beams strengthened with other strengthening methods.

6.2. The local post-tensioning process

6.2.1. Description

The main concept of the local post-tensioning process in this part of the study is to increase the load carrying capacity of a regular steel I-beam by attaching additional reinforcing bars. The reinforcing bars are then tensioned using a manual screw jack.

In this study two bars were attached symmetrically on either side of the beam. Two types of local prestress were: internal and external, shown in Figures 6.4 and 6.5 respectively, differentiated by whether the bars are attached to the web or external flange surface.

Figure 6.1 shows the installation sequence for the internal local post-tensioning type. In this type, the bars were welded to the beam's web at both ends as illustrated in Figure 6.1. After the bars were pulled to reach the required tensile stresses, a rigid support was inserted between the mid-span of each steel bar and the bottom surface of the top flange to maintain the stresses in the bars in a similar way to that used to restore the load-carrying capacity of severely damaged steel beams (see Chapter 3, Section 5.2.3 and Figure 5.4). The tensile force in the rebar generates a reverse bending moment in the mid-span cross section that results in an increase of stiffness and load carrying capacity.

In the external LPT type, the bars were welded to the beam's tensile flange and they were pulled to reach the required tensile strength using a steel plate and a bolt (Figure 6.2).

In addition to the post-tensioned bars, identical steel plates with dimensions of 500 x75 x 6 mm were welded to the centre of the compressive flange of all tested beams, to simulate any additional member attached or welded to these beams in a real roof system (such as a concrete slab in composite beams or a roof top plate).

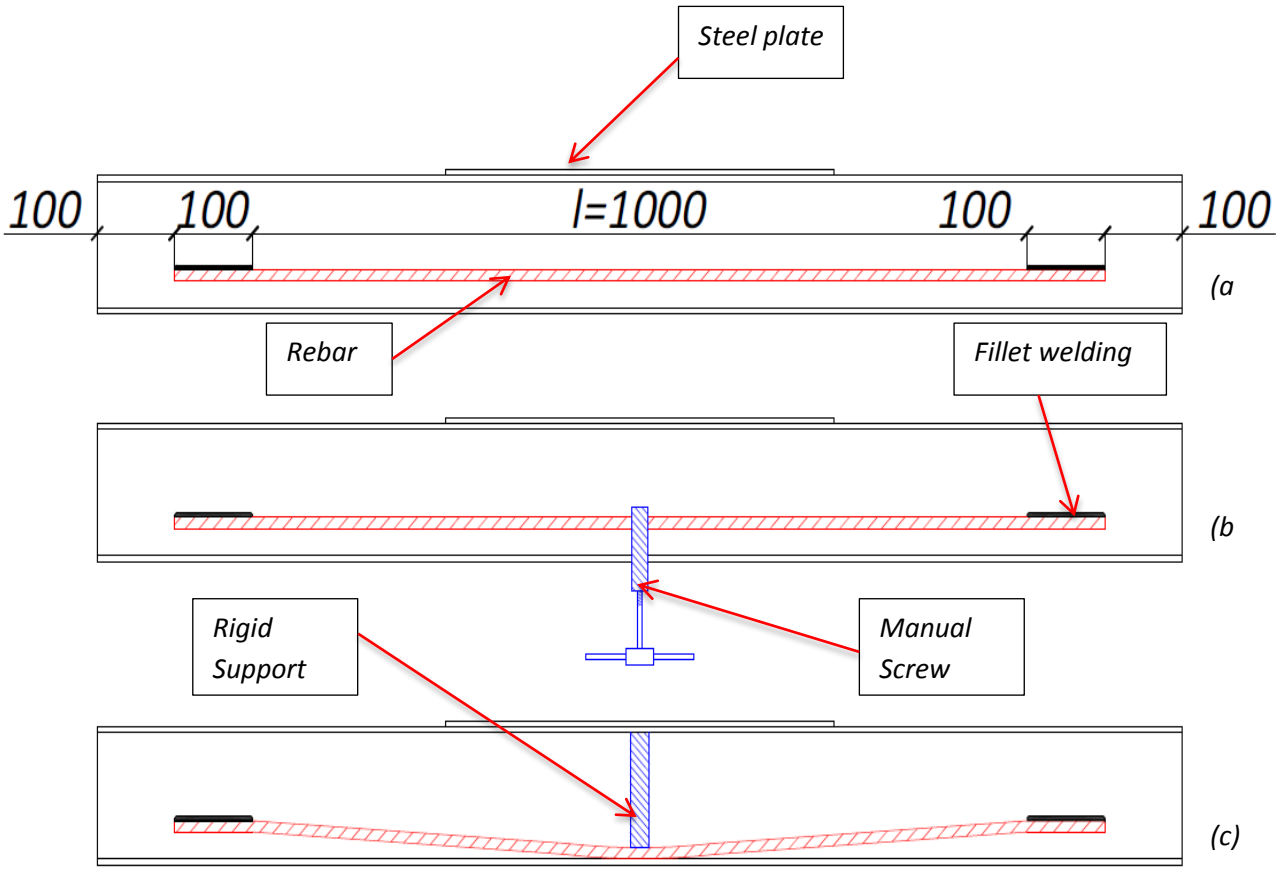

Figure 6.1. The process of LPT: (a) welding the bars (on both sides), (b) pulling the bars using a manual screw jack, (c) fixing the bars in place using a rigid support.

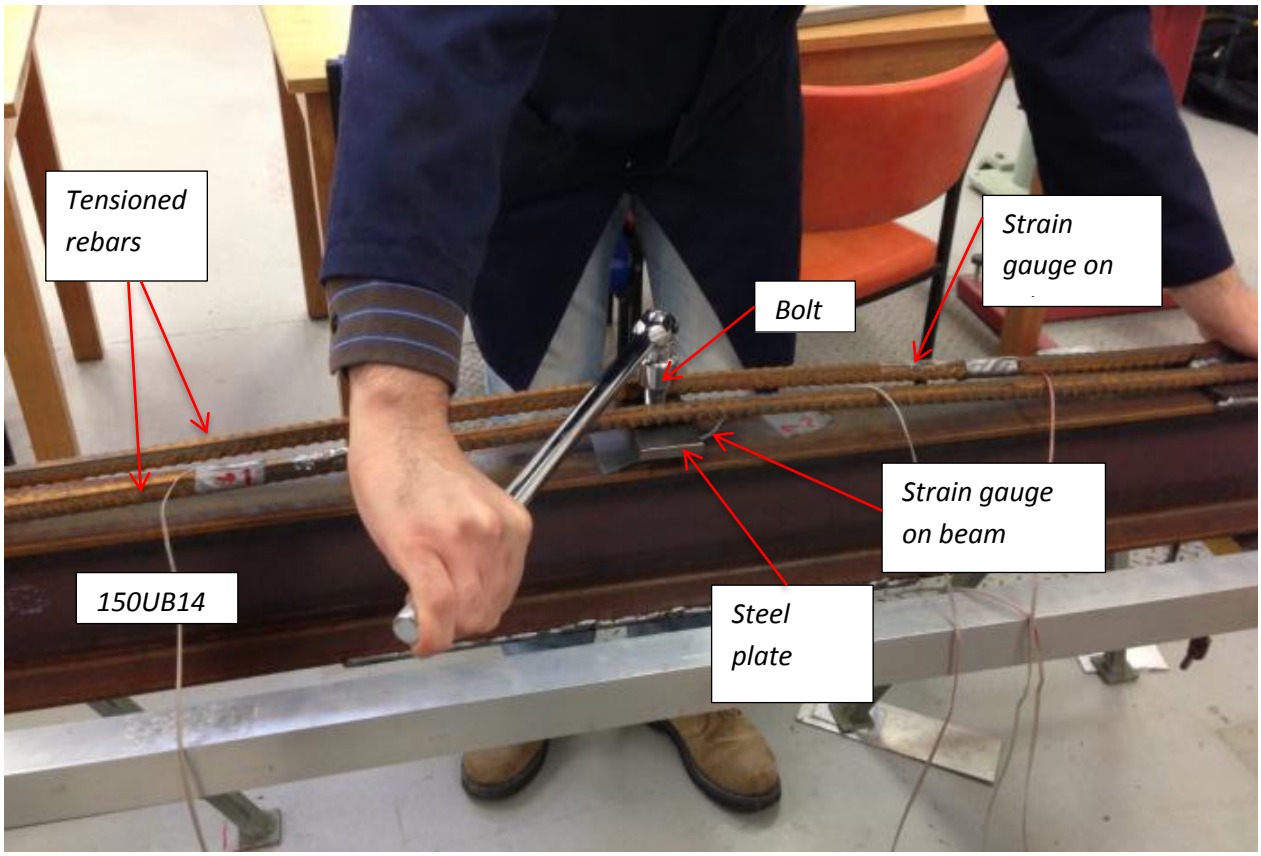

Figure 6.2. The process of post-tensioning an upgraded beam using external LPT (B16-E-2).

6.2.2. Theory

The jacking distance *f,* the tensile force *N* within the reinforcement bars that was generated by the pre-stressing process, and the jacking force *F*, required to generate the tensioning force *N*, where calculated using Equations 3.1, 3.2 and 3.3 respectively (See Chapter 3 and Appendices 2 and 3).

Different pre-stressing forces were applied on each beam in order to highlight the effect of the tensioning force on the beam's overall stiffness and load-carrying capacity. The differences in tensioning levels (force *N*) were achieved by varying the diameter of reinforcing bar (12 mm, 16 mm and 20 mm were used).

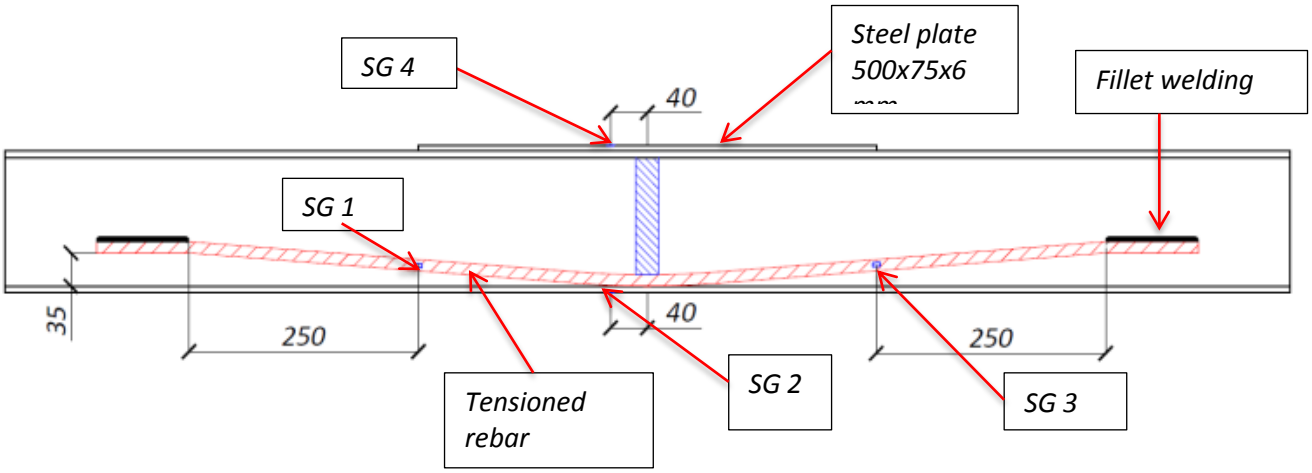

Figure 6.3. Detailed drawing of a beam (B12-I) upgraded using internal LPT

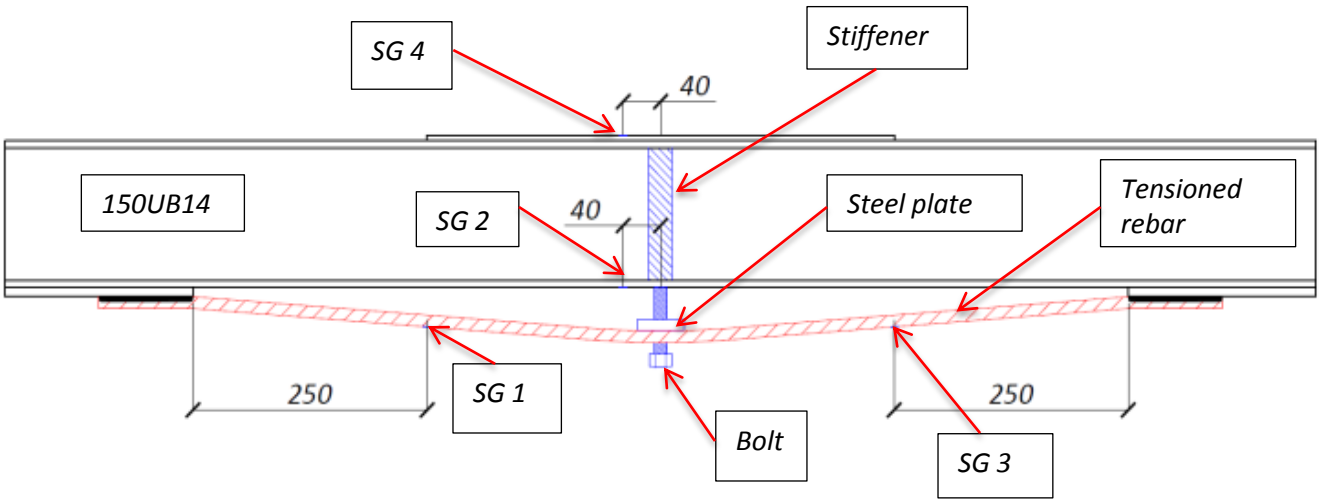

Figure 6.4. Detailed drawing of a beam (B12-E) upgraded using external LPT

6.3. Test procedure

6.3.1. Specimen preparation and properties

The steel beams used in the tests were Grade 400 150UB14. Key geometric properties are an overall depth of 150mm, a flange width of 75mm, flange thickness of 7.0 mm and web thickness of 5.0 mm. The yield stress, the ultimate tensile strength and Young's modulus

were 411.6 MPa, 541.3 MPa and 207.4 GPa respectively, obtained through tensile coupon tests.

Local prestress was applied using deformed reinforcing bars 500N, typically used for reinforced concrete structures. They have a nominal yield strength of 500 MPa specified in AS/NZS 4671:2001. The reinforcement (normal ductility) has a distinctive plastic zone with a uniform strain of 0.050 and an ultimate fracture strain of 0.20. The material properties were verified using tensile tests.

A total of seven beams, each 1.4 m long, were tested. The specimens comprised a control beam (no local prestressing), and examples of both internal and external prestressing using bars of length 1200 mm and diameter 12, 16 and 20 mm (Figures 6.3 and 6.4). Different pre-stressing forces were applied on each beam in order to highlight the effect of the tensioning force on the beam's overall stiffness and load-carrying capacity. The differences in tensioning levels (force *N*) were achieved by varying the diameter of reinforcing bar (12 mm, 16 mm and 20 mm were used). Table 6.1 shows the details of specimen used in this study. For each specimen except for B16-E-2, a stiffener was applied at the loading point to prevent localised buckling as described in the following section.

Table 6.1. List of specimen.

Beam designation	Type of pre-stress	Reinforcing bars used	Calculated tensioning force *N* (for both reinforcing bars) (*kN*)
B12-I	Internal	2*N*12	113
B12-E	External	2*N*12	113
B16-I	Internal	2*N*16	200
B16-E-1	External	2*N*16	200
B16-E-2	External	2*N*16	200
B20-E	External	2*N*20	314
Control	N/A	N/A	N/A

6.3.2. Test Setup

Three-point bending tests were conducted in a universal testing machine with a loading capacity of 1000 kN as shown in Figure 6.5 Each beam specimen was simply supported on two roller supports with a span of 1250 mm. The load was applied through a roller from above in the middle span of the beam. The deflections were measured relative to the mid-span load point using three linear digital transducers (LVDT). LVDT 1 was used at the edge immediately above the moving load point to measure the maximum relative deflection. LVDT 2 was installed at a position 250 mm from the centre of the beam, and LVDT 3 at a position of 450 mm from the centre. Four strain gauges were installed on the reinforcing bars and flanges of beams to monitor the strains during the pre-stressing and testing, as

shown in Figures 6.4 and 6.5 SG 1 and SG 3 were installed on the rebars, while SG 2 and SG 4 were installed on the tensile and compressive flanges respectively, at a position 40 mm away from the mid span (except for B16-I due to technical difficulties). A load cell with a capacity of 1 MN was used to record the load during testing.

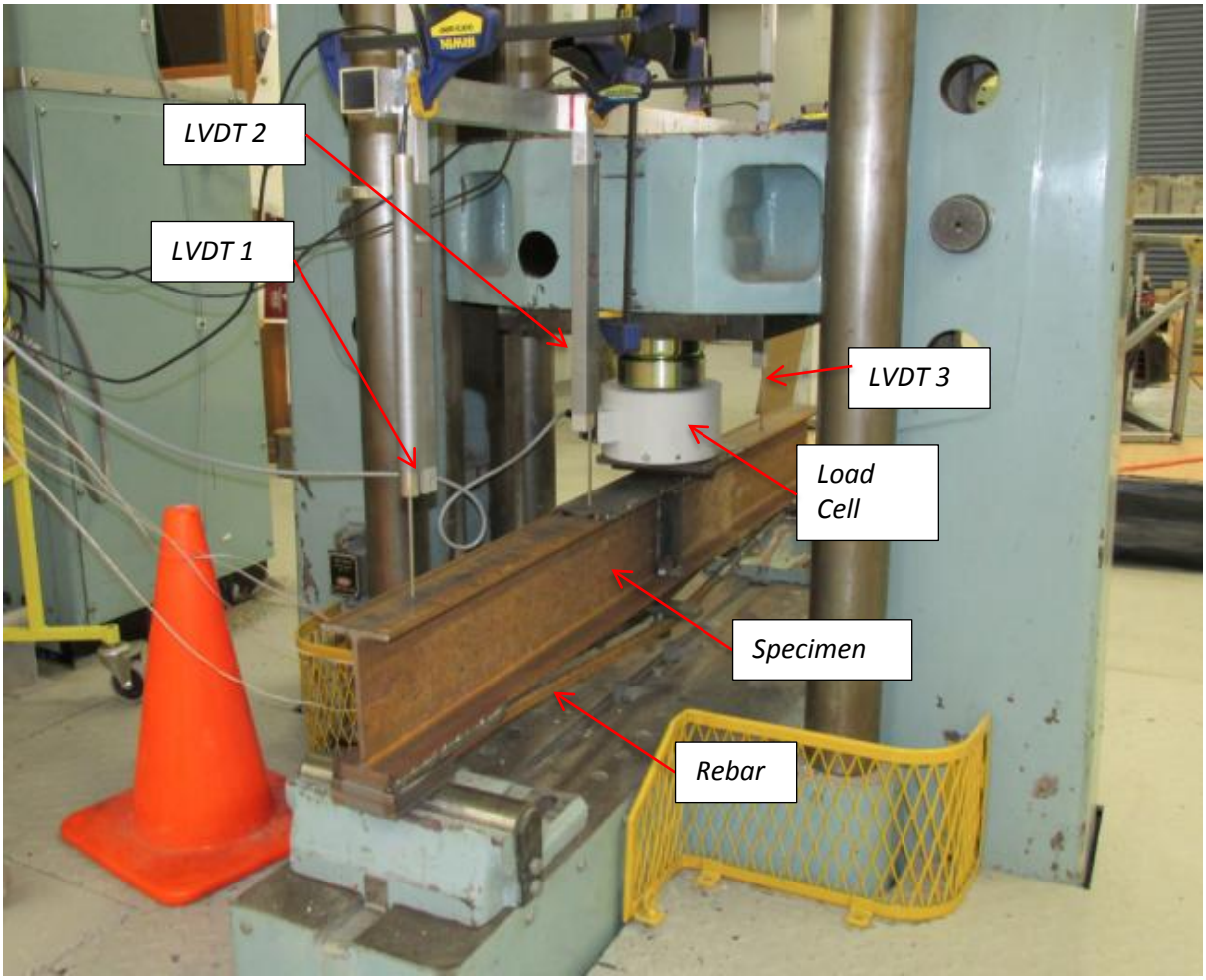

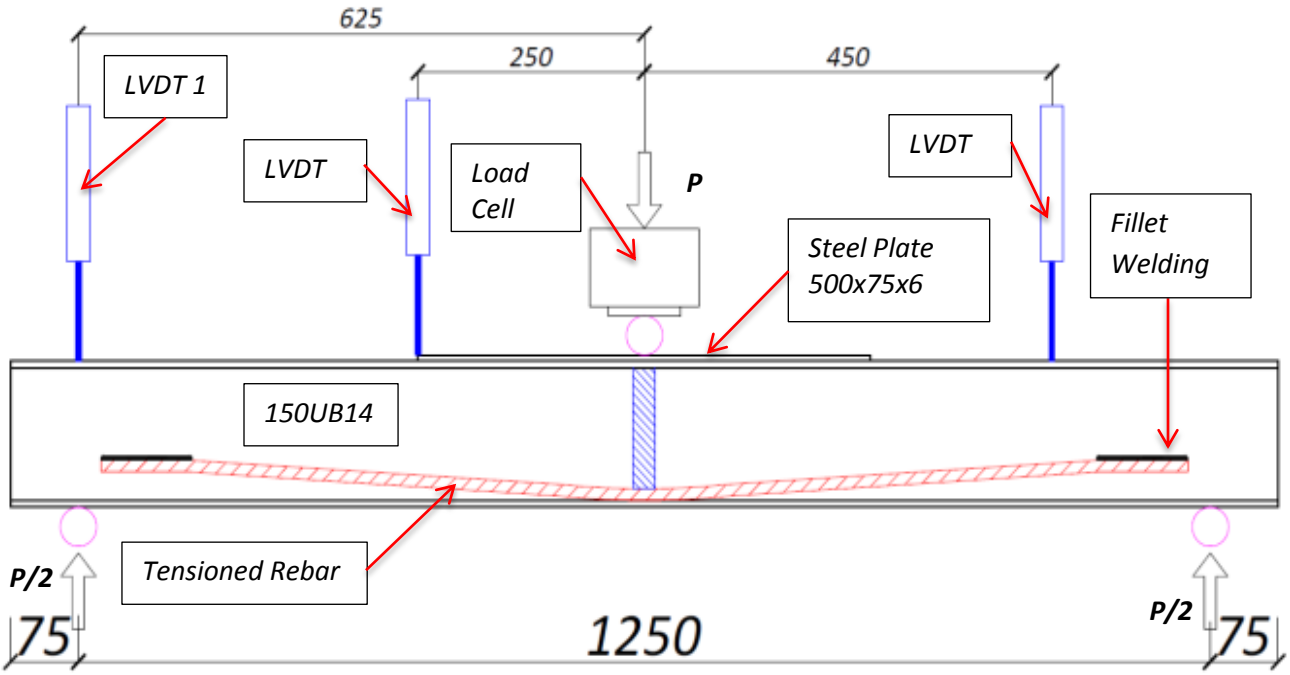

Figure 6.5. Test setup (Top: B16-E-1, Bottom: B12-I).

6.4. Results and discussion

6.4.1. Prestress strain distribution near mid span cross section prior to loading

The process of prestress creates stress in both tensile and compressive flanges of the beam, which is opposite to the stress subsequently generated by load from the testing machine. The magnitude of the opposite initial stress created by the prestress depends on tensile force *N* and the type of local prestress (internal or external). Table 6.2 and Figure 6.6 detail the initial stresses created by prestress in each beam and rebar after finalising the LPT process.

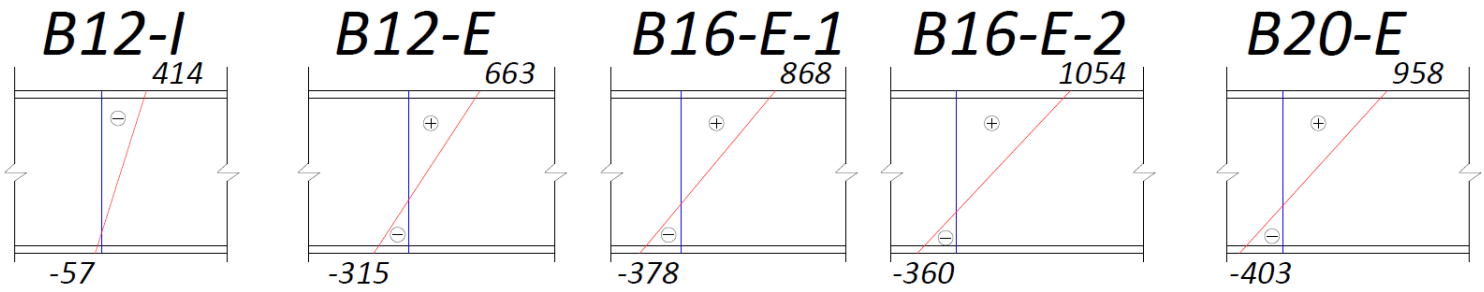

Figure 6.6. Distribution of strain after prestress, based on readings of SG 2 and SG 4.

Table 6.2. Strain in mid span and rebars due to LPT.

Beam	Tensile strain in the compressive top flange (based on the reading of SG 4), *(microstrain)*	Compressive strain in the tensile bottom flange (based on the reading of SG 2), *(microstrain)*	Calculated theoretical strain in each of the reinforcing bar after post-tensioning, *(microstrain)*	Measured strain in the first bar after post-tensioning (based on the reading of SG 1), *(microstrain)*	Measured strain in the second bar after post-tensioning (based on the reading of SG 3), *(microstrain)*
B12-I	414.1	-57.1	2500	2488	2563
B12-E	663.7	-315.9	2500	2495	2446
B16-I	N/A	N/A	2500	N/A	N/A
B16-E-1	868.1	-377.9	2500	2497	2551
B16-E-2	1054.5	-360.2	2500	2558	2502
B20-E	958.5	-403.2	2500	2499	2484
Control	N/A	N/A	N/A	N/A	N/A

It is worth noting that the absence of the stiffener in B16-E-2 allowed more freedom for the tensile flange to generate more compressive initial stress. It is also worth noting that the theoretical strain in bars calculated based on the elastic stress-strain relationship ($E=\sigma/\varepsilon$) and the experimental values measured by SG 1 and SG 3 had insignificant or no differences. During the process of post-tensioning the rebars, the strain in both bars was constantly monitored in real time, to ensure that the value of tensile force is equal in both bars and does not exceed their yield value. This is also vital to avoid any torsion in the beam during post-tensioning and loading. The process of lifting the bars was stopped when the bars

reached the desired jacking distance (vertical displacement) given by Equation 3.1. At this level of post-tensioning, the strain values for each rebar were such as given in Table 6.2.

6.4.2. Behaviour under loading

Table 6.3 lists the yield moment corresponding to the yield load, which was measured based on the strain readings by SG 2 (the corresponding yield strain was 1985 microstrain for the steel, based on the Young's modulus and the yield stress obtained from tensile coupon tests, i.e., *ε=σ/E= 411.6MPa/207.4GPa= 1985 microstrain*). Table 6.3 also lists the ultimate (maximal) load and the corresponding ultimate moment for each of the tested beams (the load was recorded by the load cell). These data are also presented graphically in Figures 6.13 and 6.14 in terms of increase of capacity relative to the control beam.

Table 6.3. Test results.

Beam	Tension force, *N, (kN)*	Experimental Yield Load (Based on the reading of SG 2) P_y, (*kN*)	Corresponding Experimental Yield Moment at mid span, M_y *(kN.m)*	Experimental Ultimate Load (recorded by the load cell) P_u, (*kN*)	Corresponding Experimental Ultimate Moment at mid span, M_u *(kN.m)*
B12-I	113	166.7	52.1	213.7	66.7
B12-E	113	219.5	68.6	251.1	78.5
B16-I	200	N/A	N/A	214.2	66.9
B16-E-1	200	268.4	83.9	304.2	95.1
B16-E-2	200	210.5	65.8	231.2	70.2
B20-E	314	280.9	87.8	323.1	100.9
Control	N/A	125.1	39.1	200.1	62.5

Table 6.3 clearly shows that both internal and external prestress have significantly increased the yield and ultimate loads for tested beams when compared to the control beam. The diameter of rebars directly affected these results. This can be explained by the fact that the reinforcing bar increases the effective area of the tensile flange and therefore improves the load carrying capacity. Table 6.3 also shows that for beams prestressed with the same diameter of rebars, external prestressing was significantly more effective than internal prestressing in increasing both ultimate and yield loads, due to the increase in the depth of the mid-span cross-section. Results also showed that the absence of the stiffener (specimen

B16-E-2) lead to a premature failure of the tested beam due to buckling and a severe decrease in the load-carrying capacity.

Figure 6.9 shows the relative deflections between the mid-span and span end load points during loading of the tested beams. Both types of prestressing increased the stiffness of the tested beams and reduced the deflections; nevertheless, the effect of external post-tensioning was more obvious. For instance, at a moment level of 40 kNm, LVDT 1 showed a deflection of 4.0 mm for B12-I and 3 mm for B16-E-1, compared to 4.5 mm for the control beam.

Figure 6.10 shows the development of the strain in the tensile flange at the mid-span. The initial compressive strain resulted from prestressing as explained previously. It can be seen that the local prestress decreased the strain in the tensile flange and therefore delayed the failure of the tested beams. Once more, the effect was more obvious for beams with external prestress and larger rebar diameters. For example, at a moment level of 34 kNm, the level of strain in the control beam's tensile flange reached 1520 microstrain, while it was 995 and 550 microstrain for B12-I and B12-E respectively. On the other hand, at the same moment level the strain reached only 25 microstrain in the tensile flange for B16-E-1.

A typical strain development in rebars and in the lower tensile flange during the loading process is shown on Figures 6.11 and 6.12 (for B12-I and B20-E respectively). The values of strain (and accordingly stress) remained extremely close during the whole bending test, and therefore, the rebars did not contribute to any torsion in the midspan cross-section of the tested beams. The rebars showed a slow linear increase in strain compared to the strain increment in the tensile bottom flange of the beam, and started to yield almost at the same time when the tensile stress in the bottom flange entered the plastic zone. This indicates

that the bars contribute to the increment of the load-carrying capacity and stiffness of the tested beams during the whole loading process. It is worth mentioning that the rebars showed increased values of yielding stress comparing to that claimed by the manufacturer.

6.4.3. Failure modes

All beams failed due to asymmetrical lateral torsional buckling. Also, local yielding of the tensile and compressive flanges in the mid-span zone was noticed (Figure 6.7). Nevertheless, B16-E-2 failed locally due to the severe buckling of the compressive flange in the mid-span area as shown in Figure 6.8 due to the absence of a stiffener in the mid span.

Figure 6.7. Asymmetrical torsional buckling of B12-E (top left) and B16-E-1 (top right), and yielding (bottom) of B12-E.

Figure 6.8. Local buckling failure of B16-E-2.

6.4.4. Comparison with other repair methods

The results were compared to those reported by other researchers (Colombi & Poggi, 2006; Linghoff et al., 2010; Narmashiri et al., 2011; Yu et al., 2011). In all those tests, Carbon Fibre Reinforced Polymer (CFRP) was used to upgrade and strengthen steel I-beams, which were subject to 3-points and 4-points bending tests (Figure 2.15). For instance, eight Grade 36 ASTM I-beams (150 mm in height and 100 mm in width) were upgraded using three different types of CFRP and then subjected to a 4-points bending test (Narmashiri et al., 2011). The tested I-beams by Yu et al. (2011) were strengthened using FRP laminates. In that study, different thicknesses of adhesives and laminates were applied to the beams to study their impact on the ultimate load carrying capacity. Linghoff et al. (2010) strengthened five HEA180 I-beams using different types of CFRP laminates and epoxy. The beams were tested in static four-point bending. Colombi and Poggi (2006) also used CFRP strips to upgrade three HEA140 I-beams. The beams were subject to a three-point bending test. The strengthening effects in terms of the increase in the ultimate loads were compared as follows.

The ultimate loads of the beams in the present study and three of the above cited studies (Narmashiri et al., 2011) (Yu et al., 2011) (Linghoff et al., 2010) are listed in Table 6.4. The percentage increase in load is plotted in Figure 6.13. It can be seen from Figure 6.13 that up to 60% increase in the load carrying capacity was achieved using the prestressing method in this study. Table 6.5 shows a comparison of the yield loads obtained in this study and in (Colombi & Poggi, 2006) with the percentage increase being plotted in Figure 6.15. It can be seen that the yield load was more than doubled using the LPT method in this study.

Table 6.4. Comparison of ultimate loads from different studies.

Beam (This study)	Experimental Ultimate Load, kN	Increase, %	Narmashiri et al., (2011)	Experimental load capacity, kN	Increase, %	Yu et al., (2011)	Maximum Load, kN	Increase, %	Linghoff et al., (2010)	Increase, %
Control	200.1	**N/A**	F3	184.88	**N/A**	B1	177.1	**N/A**	Ref	**0**
B12-I	213.7	**6.5**	F4	205.54	**11.17**	B2	185.5	**4.7**	1-2	**2**
B12-E	251.1	**25.5**	F10	222.50	**20.35**	B3	200.0	**13.1**	1-3	**17**
B16-I	214.2	**7.1**	F11	230.58	**24.72**	B4	206.9	**16.9**	1-4	**18**
B16-E-1	304.2	**52.1**	F22	238.88	**29.21**	B5	183.6	**3.6**	1-5	**2**
B20-E	323.1	**61.5**	F23	246.42	**33.29**	B6	178.9	**1**		
			F24	246.69	**33.43**					
			F25	255.82	**38.37**					

Table 6.5. Comparison of yield loads.

Beam (This study)	Experimental Yield Load, kN	Increase, %	Colombi and Poggi, (2006)	Yield Load (calculated), kN	Increase, %
Control	125.1	**N/A**	TR0	82.27	**N/A**
B12-I	166.7	**33.2**	TR1	91.82	**11.6**
B12-E	219.5	**75.5**	TR2	91.82	**11.6**
B16-I	N/A	**N/A**	TR3	102.33	**24.4**
B16-E-1	268.4	**114.5**			
B20-E	280.9	**124.6**			

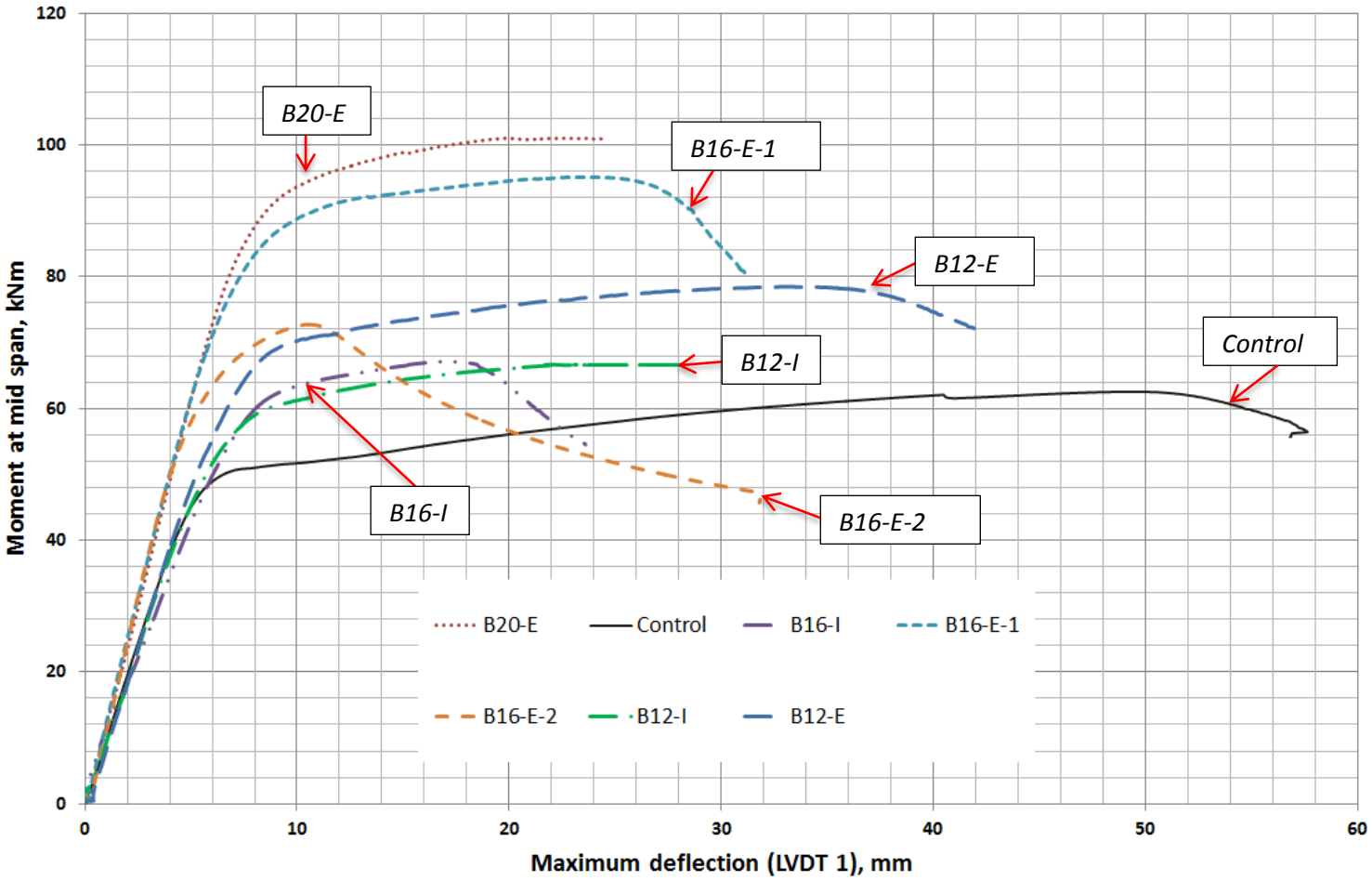

Figure 6.9. Maximum deflections for tested beams.

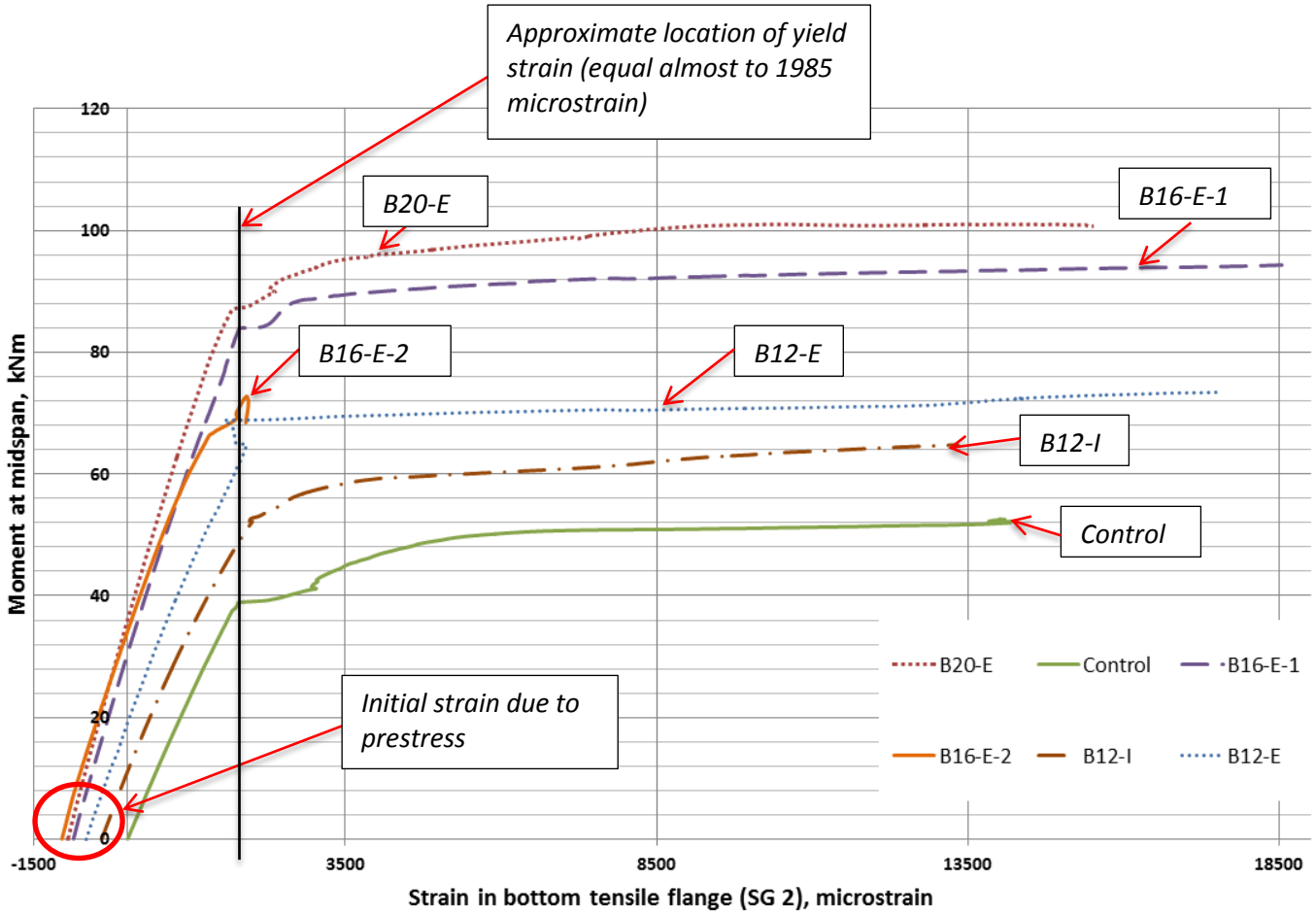

Figure 6.10. Strain development in the tensile flange of tested beams.

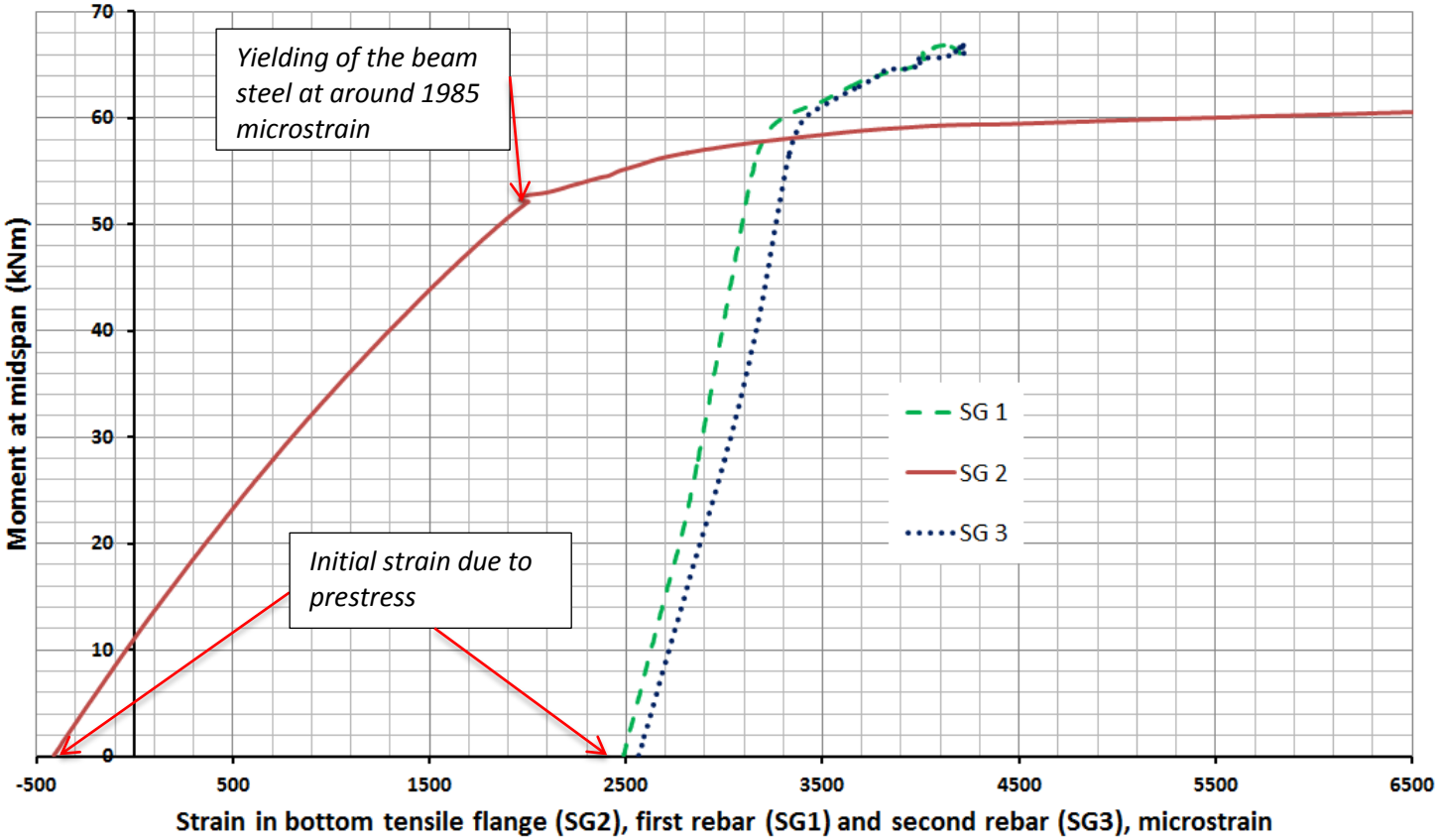

Figure 6.11. Strain development in reinforcing bars and bottom tensile flange for B12-I.

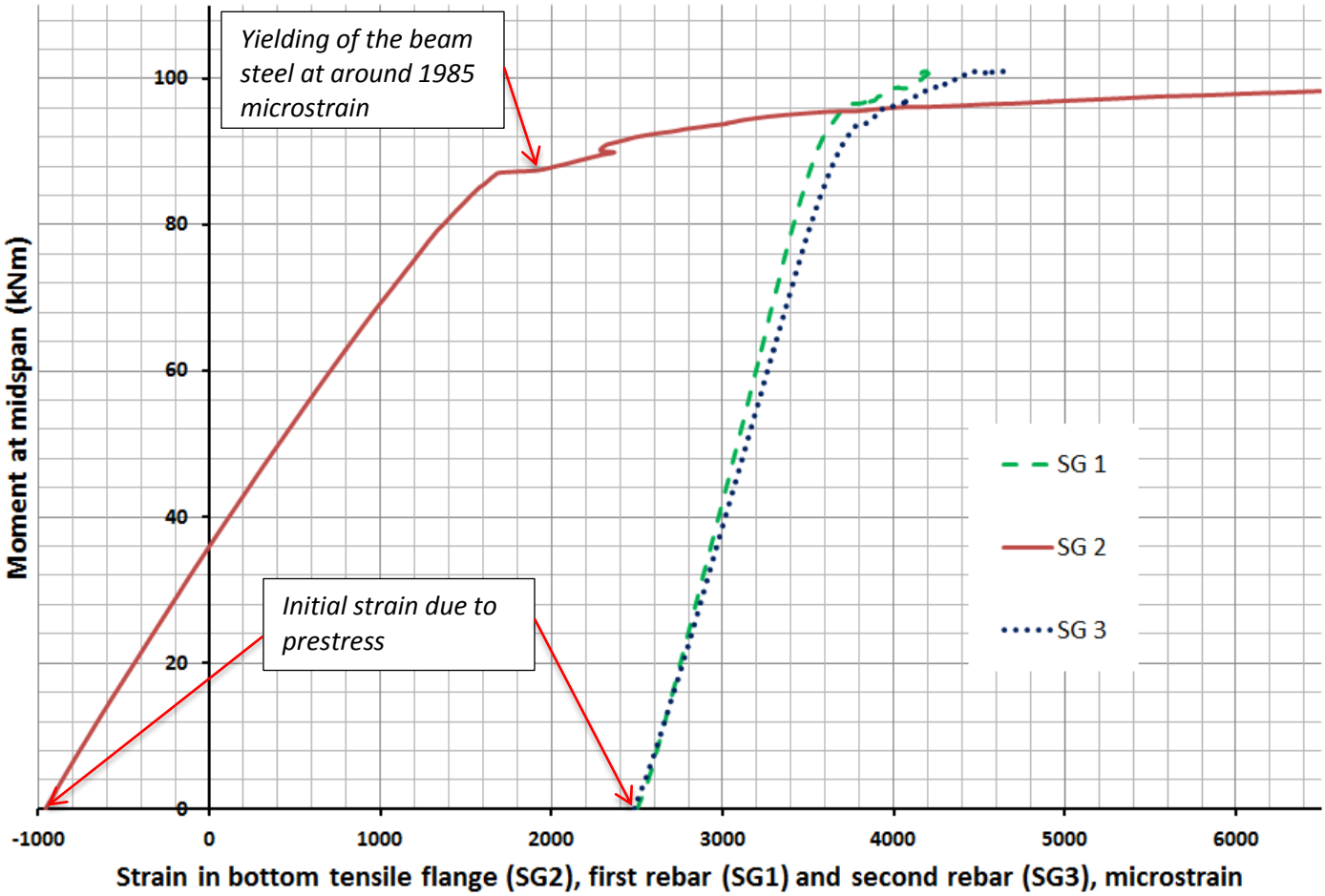

Figure 6.12. Strain development in reinforcing bars and bottom tensile flange for B20-E.

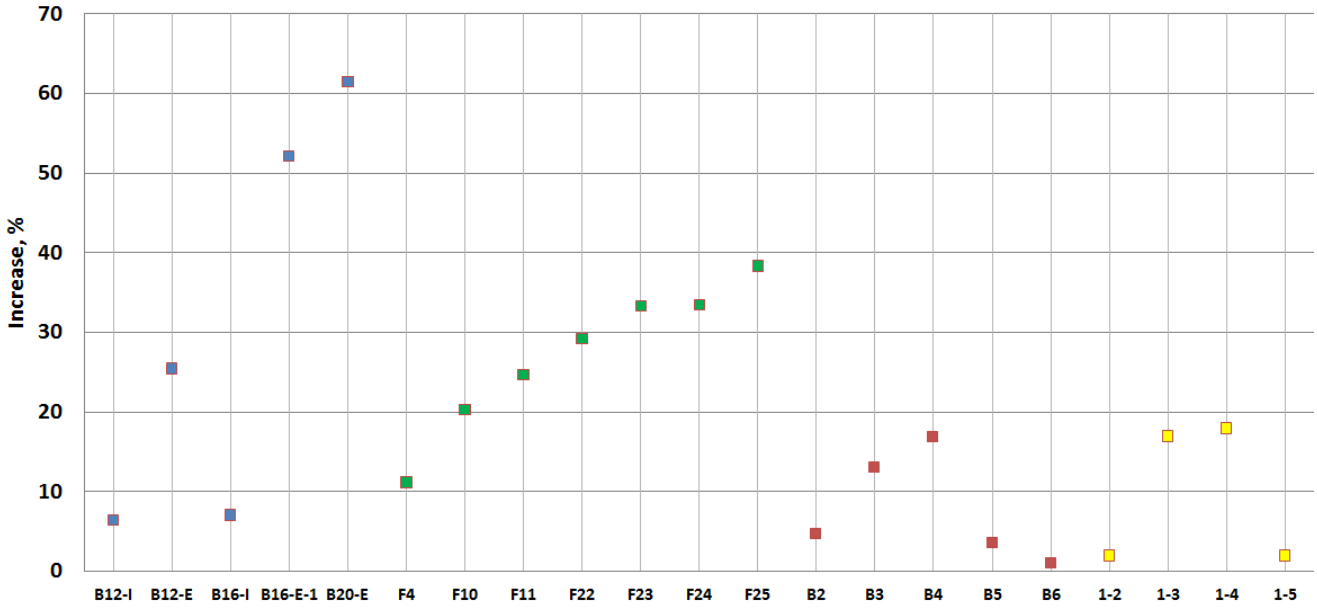

Figure 6.13. Comparison of increments in ultimate loads, for beams tested in this study (B12-I to B20-E), Narmashiri et al. (2011) (F4 to F25), Yu et al. (2011) (B2 to B6), and Linghoff et al. (2010) (1-2 to 1-5).

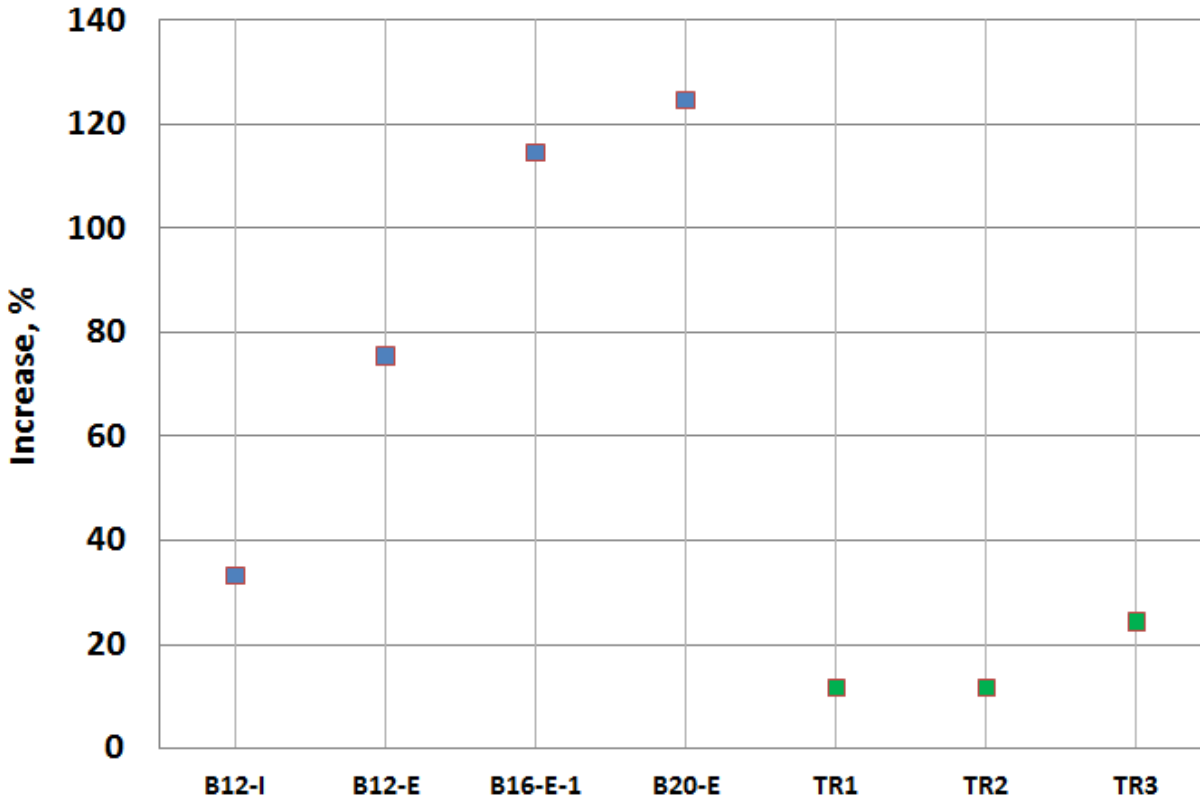

Figure 6.14. Comparison of increments in yield loads, for beams tested in this study (B12-I to B-20E), and in Colombi and Poggi (2006) (TR1, TR2 and TR3).

6.6. Conclusion

This chapter presented an experimental investigation to understand the effectiveness of using pre-stressed reinforcing bars as a method of strengthening and upgrading steel I-beams. The following can be concluded from the test results:

1. Application of local pre-stressed reinforcing bars in conjunction with a stiffener to prevent buckling could add up to 60% of the load-carrying capacity of the steel I-beams.

2. The larger the diameter of rebars used, the higher the beam's stiffness and the load carrying capacity.

3. The external prestress method is more effective in increasing the load-carrying capacity of the steel I-beams than the internal prestress method.

4. The local post-tensioning method is a cost-effective and easy-to-operate method that can be used to increase the load-carrying capacity of beams when compared to other structural strengthening methods.

7. Conclusion and further research

7.1. Final conclusion

This has presented an experimental and theoretical investigation to explore the possibility of using LPT on new and existing structures. The experimental results proved LPT is a low-cost and simple alternative to existing concrete and timber post-tensioning techniques. The results also proved that this innovative technology represents an alternative and a more efficient way to repair and upgrade steel beams when compared to existing repair and upgrade methods.

Unlike conventional post-tensioning methods, LPT is applied only to the critical areas of continuous concrete beams, e.g. above a support or at mid-span. Test results on four large-scale concrete beams proved that LPT effectively increased the crack-resistance of concrete beams – which is the main aim of any prestressing method. Test results also showed that due to its setup and geometrical properties, LPT eliminates the friction losses in prestressing which is a common issue in almost all post-tensioned members. In fact, strain gauges installed on rebars, acting as tensioning rods, showed that the level of post-tensioning increases with further loading of the beam.

After comparing the theoretical and experimental results, it was found that the approach adopted in AS 3600-2009 to predict the cracking moment was not applicable for locally post-tensioned beams, since the forces involved in this process were not considered in the Standard (in particular the jacking force, *F*). A new approach was adopted to predict these moments, considering all forces and their geometrical properties, which proved to give more accurate results.

Also, a design approach for locally post-tensioned beams was proposed along with a numerical design example. This approach is based on the design of conventional post-tensioned beams but with considerations and modifications made to address all the particularities of LPT, such as determining the main forces (*F* and *N*), the jacking distance, *f*, and the void dimensions.

The LPT was applied to timber panels, as part of its application to new structures. Six full-scale timber panels made of butt jointed and nailed timber beams were locally post-tensioned and tested. Results revealed that the application of LPT can reduce deflections under servicability loads by almost half of their values. Moreover, the LPT was achieved using bracing straps and bracing tensioners, both available in most hardware stores and do not require any special skills or training to be used.

After analysing the results and comparing the dynamic behaviour of tested panels beofre and after applying LPT, it was found that the fundamental frequency, which is the most significant vibrational response to consider when investigating the frequency response of timber floors, was not impacted by the post-tensioning process. Nevertheless, LPT significantly affected damping ratio, which significantly decreased; however its value remained within the acceptable limits and was significantly higher than ratios obtained in other studies involving post-tensioned timber. The obtained average damping ratio of 2.4% remains higher than the conservative 2% suggested by many researchers.

Furthermore, LPT was used to restore the load-carrying capacity of severely damaged steel beams. Six repaired beams with different bar diameters and levels of pre-stress were tested under three-points bending. Results showed that the application of LPT bars could restore at least 75% of the load-carrying capacity of the damaged beams when using 16 mm diameter

bars. To compare, a maximum of around 47% was obtained when using CFRP strengthening. The variation of reinforcing bars' diameter (12 and 16 mm) and the level of post-tensioning in these bars (achieved through the variation of jacking distance, *f*) proved that the level of post-tensioning (given by the internal force in bar, *N*) has a direct impact on the beam's stiffness (fixed through a lower level of deflections for the same mid span moment) but has no significant impact on the beam's load-carrying capacity. In order to improve the beam's load-carrying capacity, the diameter of the reinforcing bars used should be increased. The application of LPT in this case requires nothing more than reinforcing bars, welding and a simple manual screw jack, which makes it an effective, more efficient and low-cost alternative of existing repair methods such as CFRP retrofitting.

In addition, as part of applying LPT to existing structure, Upgrading of intact steel beams using LPT was also investigated in this study. Seven intact beams were upgraded and tested under three-point bending, using different configurations of reinforcing steel. Two different types of LPT were used in this part: an internal LPT similar to that used to strengthen and repair damaged steel beams (Chapter 5) and an external one, where the rebars are welded to the beam's tensile flange. It was found that the diameter of reinforcing bars significantly affected the beams' ultimate load-carrying capacity, as found for LPT used to repair steel beams. The application of local pre-stressed reinforcing bars in conjunction with a stiffener to prevent buckling added up to 62% of the load-carrying capacity of the steel I-beams. In contrast, other similar studies involving CFRP showed a maximum of 38% of increase in the overall load-carrying capacity. A significant increase of ultimate yield load (up to 125%) was also observed, which by far exceeds results obtained in other studies.

Test results also showed that the external prestress method is more effective in increasing the load-carrying capacity of the steel I-beams than the internal prestress method; this was mainly due to the fact that beams upgraded using external LPT had more effective depth at mid-span than those upgraded using internal LPT.

Finally, LPT, both external and internal proved to be a cost-effective and easy-to-operate method that can be used to increase the load-carrying capacity of beams when compared to other structural strengthening methods such as CFRP and plates retrofitting.

7.2. Further research

Further research in applying LPT to concrete beams can include preparing and testing full-scale continuous concrete beams, or even large scale roof systems including LPT in the main beams. Such type of testing will not only help understand more LPT, but also will highlight the effect of LPT when applied to a continuous beam in different locations (above support and at mid-span simultaneously). It would be reasonable to assume that, in this case, jacking forces *F* (having opposite directions), will create a couple that counters the bending moment from loading and therefore, further delay the cracking of the beam. Also, testing roof systems (for example, these systems will use cast-in-situ main beams with LPT and precast concrete ribs for the perpendicular direction with a cast-in-situ top concrete slab) will help better understand the overall effect of post-tensioning on moments redistribution in perpendicular directions.

LPT can be used in new composite steel reinforced concrete roof systems. These systems use steel I-beams as a main tensile element, with concrete cast-in-situ concrete slabs (connected to the steel beams with shear studs) as the main compressive element. LPT can be adopted at mid-span in a similar way to that explored in Chapter 6 in the lower section of

the steel beam (both internal and external LPT can be used, however the internal type is more aesthetical when the beam is located inside a building). In the above support area, LPT can be applied externally to the steel beam's top flange before casting the concrete (the bars therefore will be completely embedded in the concrete slab). Such arrangement will significantly increase the overall load-carrying capacity of continuous composite beams and increase the crack resistance of the concrete slab in the above support area, allowing for significant savings in height for multistorey buildings due to reductions in overall ceiling depth.

Additional research can also be done in the area of post-tensioned timber. All panels tested in this study had the same post-tensioning configuration, where a 0.8 mm thick bracing strap was used to implement the LPT. More hogging deflections can be achieved by using thicker straps (1 or 1.2 mm) that allow more tensile force in the bottom section of the panel in an analogous way to that used in strengthenign and upgrading steel beams (Chapters 5 and 6), where increasing the diameter of tensioning rods (reinforcing bars) resulted in an increase of the tensioning force and therefore the level of post-tensioning, however, that may or may not further affect the dynamic response of the panels, therefore further research in this direction is required.

LPT can be adopted for low-grade timber panels. Previous research at UTAS and CSAW showed that control of deflections in low-grade timber can be enhanced by attaching a soffit that acts as a tensile element (Section 2.2). As an alternative, LPT can be used to create initial hogging deflections in these panels and allow them to be used in residential construction. Further testing is required to fully understand the behaviour of such panels.

As for the application of LPT to existing structure, it is recommended to investigate the behaviour of repaired steel beams using LPT under cyclic loading, since the majority of damaged steel beams are located in bridge structures. It is worth mentioning that the researchers already performed a preliminary testing in this area (results were not included in this thesis). Three steel beams were strengthened using LPT and tested under cycling loading. Test results showed absolutely no failure even after 2 million cycles of loadings, which by far, exceeds all cyclic testing results for repaired steel beams, obtained using other strengthening techniques (CFRP and welding in particular). This is mainly due to the geometrical setup of LPT, where the internal force in the bar, *N*, restricts any opening of the crack under loading. However, further investigation is required to fully understand the behaviour of LPT under cyclic loadings.

Further research in this area could also include repair methods incorporating both LPT and CFRP. The CFRP in this case will contribute to the overall load-carrying capacity of the beam, while the LPT will prevent the delamination of CFRP under static or cyclic loadings as well as increase the stiffness and load-carrying capacity of the beam).

Finally, external LPT, where the rebars are fixed to the beam's flange could be also used to repair and restore the load-carrying capacity of steel beams (external LPT was implemented for upgrading steel beams, see Chapter 6).

In this part of the study, no bracing or other restrictions preventing buckling of the compressed beam flange were used in this study. Further testing in this direction is needed to study the effect of the boundary restrictions on the behaviour of the locally post-tensioned beams. This is relevant in particular to beams strengthened using LPT.

Appendices

Appendix 1. Configuration of the data acquisition system used in Chapters 3 and 5.

Strain gauges are connected to the bridge head, so the resistance together with bridge head form a Wheatstone bridge. The bridge head is connected to the strain amplifier, it supplies excitation voltage to the bridge head, and the bridge head then sends back a differential voltage to the amplifier. The amplifier has gain settings on it. This gain is adjusted to ensure that the output voltage from the strain amplifier does not exceed +/- 10 volts to avoid overloading the data acquisition system. The gain is adjusted by shunt calibrating the strain gauge using a precision resistor of 119.880 Ω. The shunt calibration of 120 Ω gauge (used in this study) produces a resistance change of 1000 ppm. To convert this value to equivalent mechanical strain it should be divided by the gauge factor (2.08 for gauges used on concrete and 2.1 for gauges used on steel rebars).

During the shunt calibration the change of output voltage from the strain amplifier is measured. Based on the input limits of the data acquisition and the anticipated levels of strain, the strain amplifier gain is adjusted to limit the output signal to +/- 10 volts.

The data acquisition system used is PCI 6025E (16 channel) supplied by National Instruments.

The values digitised by the data acquisition system are then stored to hard disk using software written in Labview 2012.

The reliability and accuracy of the system are periodically verified using precision voltage sources.

Appendix 2. Calculating the jacking distance *f*

All the calculations are made for the elastic phase, where Hooke's law, Caushy (Normal) strain and simple stress formulate are applicable.

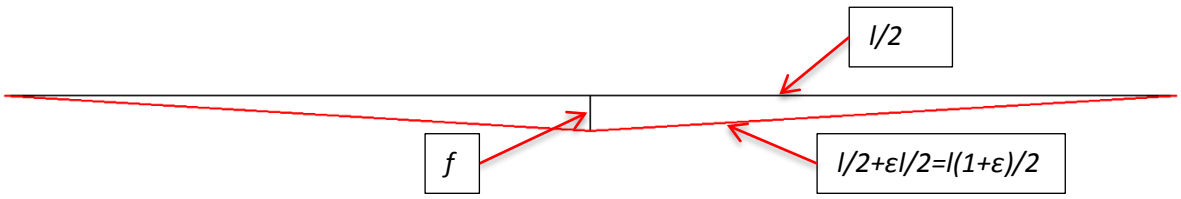

Based on Pythagoras:

$$(\frac{l}{2}(1+\varepsilon))^2 = f^2 + (\frac{l}{2})^2$$

Therefore,

$$\frac{l^2}{4} + \frac{2\varepsilon l^2}{4} + \frac{l^2\varepsilon^2}{4} = f^2 + \frac{l^2}{4}$$

Since $\varepsilon^2 \approx 0$,

$$f = l\sqrt{\frac{\varepsilon}{2}}$$

Based on Hooke's law,

$$f = l\sqrt{\frac{\sigma}{2E}}$$

Appendix 3. Calculating the jacking force *F*

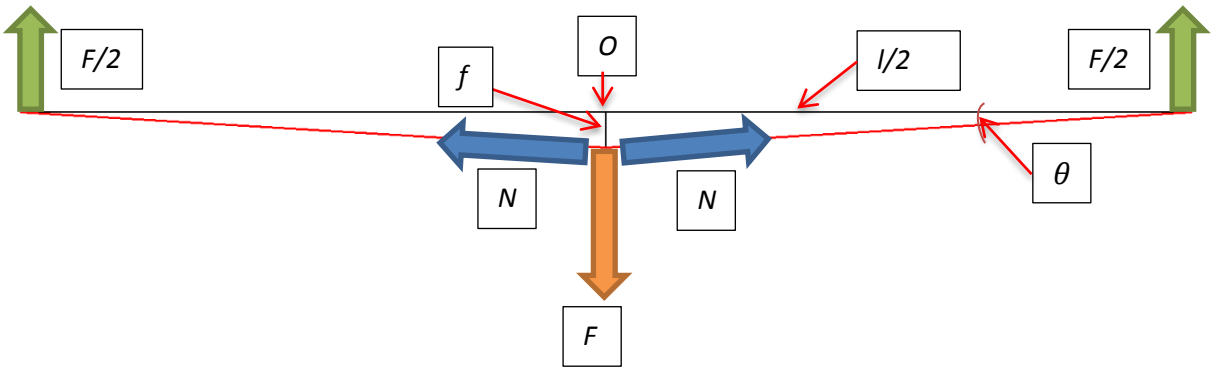

Vertical equilibrium at "O" requires:

$$F = 2sin\theta \cong 2N$$

Since *f*<<*l*

$$F = 2N + \frac{f}{l/2} = \frac{4Nf}{l}$$

Appendix 4. Design of a conventional post-tensioned beam

The same beam considered in Section 3.5 is designed here below using conventional post-tensioning (Figure A.1).

Concrete 28-day strength: $f_c^{'} = 40$ MPa

Concrete strength at transfer: $f_{cp} = 32$ MPa

The cross-section is rectangular with dimensions of *300x500* mm. The section area is $A_g = 150000$ mm^2.

1- Calculation of self-weight:

Self-weight = *0,3x0,5x25 = 3,75* kN/m

2- Choose the serviceability criterion

The beam is designed initially for decompression at mid-span under full dead load, so that the beam will be free of flexural cracks under the permanent load.

Total dead load = *6+3,75 = 9,75* kN/m. The required decompression moment at mid-span is therefore:

$$M_{dec} = \frac{9{,}75.10^2}{8} = 122\ kN.m$$

3- Determine prestressing force and eccentricity

Assuming that at mid-span there will be one 40mm diameter cable and that the maximum available eccentricity will be approximately *e=250-40-40/2=190 mm*.

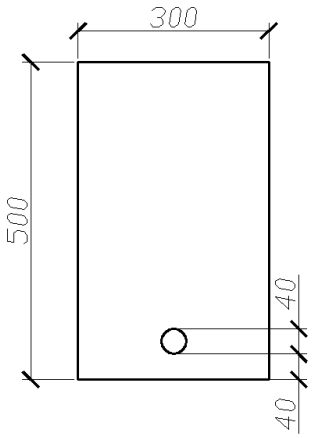

Figure A.1. Cross-section of the designed beam.

The section modulus is calculated:

$$Z = \frac{bD^2}{6} = \frac{300.500^2}{6} = 12{,}5.10^6 mm^3$$

Then the required effective prestressing force is:

$$P_e = \frac{M_{dec}}{e + \frac{Z}{A_g}} = \frac{122.10^6}{190 + \frac{12{,}5.10^6}{150000}} = 446kN$$

4- Prestress losses and cable selection

Assuming that deferred losses total 20 %, the initial prestressing force required at mid-span is:

$$P_i = \frac{446}{0{,}8} = 558kN$$

For cables with parabolic profiles having mean eccentricities varying from zero at each support to 190 mm at mid-span, the average cable slope at the support is

$$\theta = \frac{4e}{L} = \frac{4.190}{10000} = 0{,}076rad = \alpha_{tot}$$

Estimating friction losses taking $\mu = 0{,}2$ and β = 0,016:

At mid-span:

$$\sigma_{pa} = \sigma_{pj} e^{-\mu(\alpha_{tot} + \beta L_{pa})} = \sigma_{pj} e^{-0{,}2(0{,}076 + 0{,}016.5)} = 0{,}97\sigma_{pj}$$

Therefore,

$$P_{ij} = \frac{558}{0{,}97} = 575kN$$

If the design is conducted in a way so that the stress in the prestressing cables at support immediately after transfer *is* $0{,}75f_p$, then the required breaking load of the cables is *575/0,75 = 767* kN.

The breaking load for one 15,2 mm EHT strand is 261kN (provided by VSL), so that the number of strands required is 767/26 = 2,9.

Select one cable with 3 strands of 15,2 mm EHT. The prestressing steel properties are:

Total area $A_p = 430$ mm^2 $f_{py} = 1750$ MPa

Effective stress at mid-span:

$$\sigma_{pe} = \frac{P_e}{A_p} = \frac{446000}{430} = 1037MPa$$

5- Design of reinforcement for M_u at mid-span

$w^* = 1,2.9,75+1,5.9 = 25,5$ kN/m

$M^* = (25,2.10^2)/8 = 315$ kN.m $M_u = M^*/\varphi = 303/0,8 = 394$ kN.m

Given that the lever arm $z=415mm$, the total tensile force required at M_u is:

$$T_{py} + T_{sy} = \frac{M_u}{z} = \frac{394.10^3}{415} = 950kN$$

$T_{py}=430.1750=752,5kN$

Required $T_{sy}=950-752,5=197,5kN$

$$A_s = \frac{197,5.10^3}{500} = 395mm^2$$

Consider $2N16$, $A_s = 400$ mm^2

Analysis of the section gives the following results:

$A_g = 150000$ mm^2 $I_g = 3,12.10^9$ mm^4 $e = 190$ mm

To calculate the cracking moment M_{cr}, it is necessary to calculate the extreme fibre stress due to prestress:

$$\sigma_{ap} = \frac{445900}{150000} - \frac{445900.190.250}{3,12.10^9} = 2,97 - 6,79 = -3,82MPa\ (tension)$$

$$\sigma_{bp} = \frac{445900}{150000} + \frac{445900.190.250}{3,12.10^9} = 2,97 + 6,79 = 9,76MPa$$

$$f'_{cf} = 0,6\sqrt{40} = 3,79MPa$$

And $\sigma_{bp} = 9,76$ MPa

Therefore,

$$M_{cr} = \frac{(3{,}79 + 9{,}76)3{,}12.10^9}{250} = 170kN.m$$

6- Check strength at transfer at mid-span section

The self-weight moment at mid-span is $M_G = 3{,}75.10^2/8 = 47$ kN.m. The initial prestressing force at mid-span, i.e. the force immediately after transfer is *575* kN. During the jacking operation the prestressing force at the section may temporarily exceed this value, and it will be assumed that the maximum jacking force at mid-span is $P_{jm} = 600$ kN.

The extreme fibre stresses are checked first. The tensile stress in the top fibre is:

$$\sigma_a = \frac{-600000}{150000} + \frac{600000.190.250}{3{,}12.10^9} - \frac{47.10^6.250}{3{,}12.10^9} = -4 + 9{,}13 - 3{,}76 = 1{,}37MPa$$

$$\sigma_b = \frac{-600000}{150000} - \frac{600000.190.250}{3{,}12.10^9} + \frac{47.10^6.250}{3{,}12.10^9} = -4 - 9{,}13 + 3{,}76 = -5{,}37 < 0{,}5f_{cp}$$

The section therefore satisfies the AS 3600 approximate “deemed to comply” provision for strength at transfer.

Materials for prestressing: 3 strands 15,2mm EHT, Stressing anchorage type Gc Live End, Dead End Anchorage Type P, Pt-Plus Duct.

Equipment for prestressing: Stressing jack VSLB7, combined mixer and pump unit for grouting.

All materials were chosen form VSL® Catalogues.

Appendix 5. Serviceability load calculation for timber panels

The imposed action, *Q* is defined by AS 1170.1 as a uniformly distributed load of 1.5 kPa. *Q = 1.5×0.28* (width of the panel), *Q = 0.42* kN/m

Therefore the serviceability loading per metre is, $E_d = 0.59$ kN/m

Calculating the moment:

$M = 0.42x4.2^2/8$; *M = 0.93* kNm

The applied load *P* under each pin should then be equal to:

P=3M/L = 0.66 kN and therefore, the total load applied by the testing machine should be equal to *2x0.66 = 1.32* kN.

References

Albercht, P., & Lenwari, A. (2008). Fatigue Strength of Repaired Prestressed Composite Beams. *JOURNAL OF BRIDGE ENGINEERING, 13*(4), 409-417.

Alkhairi, F., & Naaman, A. (1993). Analysis of beams prestressed with unbonded internal or external tendons. *Journal of Structural Engineering, 119*(9), 2680-2700.

ANSI/ASAE. (2003). Design Requirements and Bending Properties for Mechanically Laminated Columns.

ASCE. (2005). *Report card for America's infrastructure*. Retrieved from Reston, VA, USA:

Ayyub, B. M., Sohn, Y. G., & Saadatmanesh, H. (1992). Prestressed Composite Girders. II: Analytical Study for Negative Moment. *Journal of Structural Engineering, 118*, 2763-2782.

Baxter, S. (2014). *Low Grade Solid Timber Systems for Residential Construction.* (Bachelor of Engineering Thesis), University of Tasmania.

Bernard, E. S. (2008). Dynamic serviceability in lightweight engineered timber floors. *Journal of Structural Engineering, 134*(2), 258-268.

Buchanan, A., & Fairweather, R. (1993). Seismic design of glulam structures. *Bulletin of the New Zealand national society for earthquake engineering, 26*(4), 415-436.

Buchanan, A., Palermo, A., Carradine, D., & Pampanin, S. (2011). Post-Tensioned Timber Frame Buildings. *The Structural Engineer, 89*, 17.

CBS, & CBT. (2011a). D-Dalle. In C. B. Technologie & C. B. Structure (Eds.). http://www.cbs-cbt.com.

CBS, & CBT. (2011b). La Dalle O'portune. In C. B. Technologie & C. B. Structure (Eds.). http://www.cbs-cbt.com.

Chen, S. (2005). Experimental study of prestressed steel–concrete composite beams with external tendons for negative moments. *Journal of Constructional Steel Research, 61*, 1613-1630.

Chen, S., & Gu, P. (2004). Load carrying capacity of composite beams prestressed with external tendons under positive moment. *Journal of Constructional Steel Research, 61*, 515-530.

Colombi, G., & Poggi, C. (2006). An experimental, analytical and numerical study of the static behavior of steel beams reinforced by pultruded CFRP strips. *COMPOSITES PART B-ENGINEERING, 37*, 64-73. doi:10.1016/j.compositesb.2005.03.002

Dall'Asta, A., & Zona, A. (2005). Finite element model for externally prestressed composite beams with deformable connection. *Journal of Structural Engineering, 131*(5), 706-714.

Deng, J., & Lee, M. (2009). Adhesive bonding in steel beams strengthened with CFRP. *Proceedings of the Institution of Civil Engineers - Structures and Buildings, 162*, 241-249. doi:10.1680/stbu.2009.162.4.241

Dolan, J., Murray, T., Johnson, J., Runte, D., & Shue, B. (1999). Preventing annoying wood floor vibrations. *Journal of Structural Engineering, 125*(1), 19-24.

Durham, J. P., Lam, H. G. L., & He, M. (1999). *Seismic response of shear walls with oversized sheathing panels*. Paper presented at the 8th Canadian Conference on Earthquake Engineering, Vancouver, Canada.

Ellingwood, B., & Tallin, A. (1984). Structural serviceability: floor vibrations. *Journal of Structural Engineering, 110*(2), 401-418.

Filiatrault, A., & Folz, B. (2002). Performance-Based Design of Wood Framed Buildings. *Journal of Structural Engineering, 128*(1), 29-47.

Foliente, G. C. (1995). Hysteresis Modeling of Wood Joints and Structural Systems. *Journal of Structural Engineering, 121*(6), 1013-1022.

Gilbert, R. I., & Mickleborough, N. C. (1990). *Design of Prestressed Concrete*. London: Unwin Hyman.

Hamilton, J. (2014). *Use of Low Grade Timber in Residential Flooring Systems.* (Bachelor of Engineering with Honours Thesis), University of Tasmania.

Harajli, M., Khairallah, N., & Nassif, H. (1999). Externally prestressed members: evaluation of second-order effects. *Journal of Structural Engineering, 125*(10), 1151-1161.

Hassan, O., & Girhammar, U. (2013). ASSESSMENT OF FOOTFALL-INDUCED VIBRATIONS IN TIMBER AND LIGHTWEIGHT COMPOSITE FLOORS. *International Journal of Structural Stability & Dynamics, 13*(2), 1-26.

Henderson, J., Foster, S., & Bridgstock, M. (2012a). What is Brettstapel?

Henderson, J., Foster, S., & Bridgstock, M. (2012b). Why Use Brettstapel?

Hmidan, A., Kim, Y. J., & Yazdani, S. (2011). CFRP Repair of Steel Beams with Various Initial Crack Configurations. *Journal of composites for construction, 15*(6), 952-962. doi:10.1061/(asce)cc.1943-5614.0000223

Hurst, M. K., & Spon, E. F. (1998). *Prestressed Concrete Design*. London: Routledge.

Ibrahim, A. M. (2010). Parametric Study of Continuous Concrete Beam Prestressed with External Tendon. *Jordan journal of civil engineering, 4*(3).

Jiao, H., Mashiri, F., & Zhao, X. (2012). A comparative study on fatigue behaviour of steel beams retrofitted with welding, pultruded CFRP plates and wet layup CFRP sheets. *THIN-WALLED STRUCTURES, 50*, 144-152. doi:10.1016/j.tws.2012.06.002

Kim, Y. J., & Brunell, G. (2011). Interaction between CFRP-repair and initial damage of wide-flange steel beams subjected to three-point bending. *COMPOSITE STRUCTURES, 93*, 1986-1996. doi:10.1016/j.compstruct.2011.02.024

Kim, Y. J., Green M F., & J., F. G. (2008). Repair of bridge girder damaged by impact loads with prestressed CFRP sheets. *JOURNAL OF BRIDGE ENGINEERING, 13*, 15-23. doi:10.1061/(ASCE)1084-0702(2008)13:1(15)

Kim, Y. J., & Harries, K. A. (2012). PREDICTIVE RESPONSE OF NOTCHED STEEL BEAMS REPAIRED WITH CFRP STRIPS INCLUDING BOND-SLIP BEHAVIOR. *International Journal of Structural Stability & Dynamics, 12*, 1-21. doi:10.1142/S0219455412004628

Kim, Y. J., & Yoon, D. K. (2010). Identifying Critical Sources of Bridge Deterioration in Cold Regions through the Constructed Bridges in North Dakota. *JOURNAL OF BRIDGE ENGINEERING, 15*, 542-552. doi:10.1061/(ASCE)BE.1943-5592.0000087

Klaiber, F. W., Dunker, K. F., Wipf, T. J., & Sanders Jr, W. W. (1988). *Methods of strengthening existing highway bridges*: Washington : Transportation Research Board.

Lago, B., & Dibenedetto, C. (2009). *Use of longitudinal unbonded post-tensioning in multi-storey timber buildings.* (Master of Science, Master Thesis), Technical University of Milan, Milan, Italy.

Lenwari, A. (2006). Debonding Strength of Steel Beams Strengthened with CFRP Plates. *Journal of composites for construction, 10*(1), 69-78. doi:10.1061/(asce)1090-0268(2006)10:1(69)

Linghoff, D., Al-Emrani, M., & Kliger, R. (2010). Performance of steel beams strengthened with CFRP laminate - Part 1: Laboratory tests. *Composites: Part B, 41*, 509-515.

Loo, Y.-C., & Chowdhury, S. H. (2010). *Reinforced and Prestressed Concrete: Analysis and Design with Emphasis on Application of AS3600-2009*: Cambridge University Press.

Lorenc, W., & Kubica, E. (2006). Behavior of composite beams prestressed with external tendons: Experimental study. *Journal of Constructional Steel Research, 62*, 1353–1366.

Mosley, B., Bungey, J., & Hulse, R. (2007). *Reinforced Concrete Design to Eurocode 2*. New York: Palgrave Macmillan.

Murray, T. M., Allen, D. E., & Ungar, E. E. (2003). *Floor vibrations due to human activity*: American Institute of Steel Construction.

Narmashiri, K., Sulong, N. H. R., & Jumaat, M. Z. (2011). Flexural strengthening of steel I-beams by using CFRP strips. *International Journal of the Physical Siences, 6*(7), 1620-1627.

Nawy, E. (2003). *Prestressed Concrete: a Fundamental Approach*. New Jersey: Prentice Hall.

Nie, J., Tao, M., Cai, C. S., & Li, S. (2011). Analytical and Numerical Modeling of Prestressed Continuous Steel-Concrete Composite Beams. *Journal of Structural Engineering, 137*, 1405-1418.

Nozaka, K., Shield, C. K., & Hajjar, J. F. (2005). Effective Bond Length of Carbon-Fiber-Reinforced Polymer Strips Bonded to Fatigued Steel Bridge I-Girders. *JOURNAL OF BRIDGE ENGINEERING, 10*, 195-205. doi:10.1061/(ASCE)1084-0702(2005)10:2(195)

Ohlsson, S. (1991). *Serviceability Criteria, Especially floor vibration criteria*. Paper presented at the International Timber Engineering Conference, Church House Conference Centre, London, United Kingdom.

Palermo, A., Pampanin, S., Buchanan, A., & Newcombe, M. (2005). *Seismic design of multi-storey buildings using Laminated Veneer Lumber (LVL)*. Paper presented at the NZSEE Conference, Wairakei Resort, Taupo, New Zealand.

Pampanin, S., Pagani, C., & Zambelli, S. (2004). *Cable-stayed and suspended post-tensioned solutions for precast concrete frames: the Brooklyn system*. Paper presented at the New Zealand Concrete Society Conference, Queenstown, New Zealand.

Pavic, A., & Reynolds, P. (2002). Vibration serviceability of long-span concrete building floors. Part 1: Review of background information. *Shock and Vibration Digest, 34*(3), 191-211.

Photiou, N. K., Hollaway, L. C., & Chryssanthopoulos, M. K. (2006). Strengthening of an artificially degraded steel beam utilising a carbon/glass composite system. *CONSTRUCTION AND BUILDING MATERIALS, 20*. doi:10.1016/j.conbuildmat.2005.06.043

Priestley, M., Sritharan, S., Conley, J., & Pampanin, S. (1999). Preliminary Results and Conclusions from the PRESSS Five-story Precast Concrete Test-Building. *PCI Journal, 44*(6), 42-67.

Qader, A. H., Agarwal, V. C., & Ibrahim, A. M. (2013). Nonlinear Behavior of Continuous Composite Steel Concrete Beam with External Prestress. *International Journal of Innovative Technology and Exploring Engineering, 3*(7), 76-82.

Rao, P. S., & Mathew, G. (1996). Behavior of externally prestressed concrete beams with multiple deviators. *ACI Structural Journal, 93*(4).

Roy, M., Lang, C., & May, I. M. (2009). Modelling composite repairs to cracked metal structures. *Proceedings of the Institution of Civil Engineers - Structures and Buildings, 162*, 107-113. doi:10.1680/stbu.2009.162.2.107

Rusch, H., Jungwirth, D., & Hilsdorf, H. K. (1983). *Creep and Shrinkage: Their Effect on the Behavior of Concrete Structures*. New York: Springer-Verlag New York Inc.

Sandoz, J.-L., & des Jordils, R. (2004). *Horizontal Timber Slab from 4m to 18 Meters Free Span.* Paper presented at the Proceedings of 8th World Conference on Timber Engineering, Lahti, Finland.

Schaap, B. (2012). *Application of Low Grade Timber in Small Scale Building Systems.* (Bachelor of Engineering Thesis), University of Tasmania.

Sengupta, A., & Menon, D. (2007). *Prestressed Concrete Structures*. Madras: Indian Institute of Technology.

Shagin, A. L. (1996). Locally Post-Tensioned Constructions. *Scientific and Practical Challenges of Modern Reinforced Concrete, 48*, 193-196.

Shagin, A. L. (2005). Local Post-Tensioning of Concrete and Composite Structures. *Scientific and Practical Challenges of Modern Reinforced Concrete, 52*, 107-116.

Shagin, A. L. (2008). Method of Increasing the Load-Carrying Capacity, Crack-Resistance and Stiffness of Cracked Reinforced Concrete Beams. *Scientific Bulletin of Civil Engineering, 41*, 51-58.

Shahrooz, B. M., Saraf, V., Godbole, B., & Miller, R. A. (2002). Response of Slab Bridges before, during, and after Repair. *JOURNAL OF BRIDGE ENGINEERING, 7*(267-275).

Shanks, J. (2013). *Developing low-grade solid-timber systems for residential construction*. Proof of Concept Testing. University of Tasmania.

Smith, A. L., Hicks, S. J., & Devine, P. J. (2009). *Design of Floors for Vibration: A New Approach*. Retrieved from Berkshire, UK:

Snowball, E. (2013). *Behaviour of Lateral Joints in Vertical Nail Laminated Timber Assemblies.* (Bachelor of Engineering Thesis), University of Tasmania.

Standards Australia Limited. (1999). AS 1012.1999 Methods of testing concrete *Method 9: Determination of compressive strength of concrete specimens*. Sydney: SAI Global Limited.

Standards Australia Limited. (2001). AS/NZS 4671:2001 Steel reinforcing materials. Sydney: SAI Global Limited.

Standards Australia Limited. (2002). AS/NZS 1170.0-2002 *Structural Design Actions - General Principles*. Sydney: SAI Global Limited.

Standards Australia Limited. (2009). AS 3600-2009 Concrete Structures. Sydney: SAI Global Limited.

Tan, K. H. (2014). Beam strengthening by external post-tensioning: Design recommendations. *The IES Journal Part A: Civil & Structural Engineering, 7*(4), 219-228.

Tavakkolizadeh, M., & Saadatmanesh, H. (2003). Repair of damaged steel-concrete composite girders using carbon fiber-reinforced polymer sheets. *Journal of composites for construction, 7*(4), 311-322. doi:10.1061/(asce)1090-0268(2003)7:4(311)

Thomson, W. (1993). *Theory of Vibration with Applications* (4th ed.). Suffolk, UK: Chapman & Hall.

Uy, B. (2007). *Modern design, construction and maintenance of composite steel-concrete structures: Australian experiences*. Paper presented at the 1st International Conference on Modern Design, Construction and Maintenance of Structures, Hanoi, Vietnam.

Uy, B., & Craine, S. (2004). Static Flexural Behaviour of Externally Post-Tensioned Steel-Concrete Composite Beams. *Advances in Structural Engineering, 7*, 1-20.

van Beerschoten, W., Palermo, A., Carradine, D., & Law, P. (2012). *Unbonded post-tensioned timber gravity frames for multi-storey buildings.* Paper presented at the Australasian Structural Engineering Conference 2012: The past, present and future of Structural Engineering.

Wardhana, K., & Hadipriono, F. (2003). Analysis of recent bridge failures in the United States. *JOURNAL OF PERFORMANCE OF CONSTRUCTED FACILITIES, 17*, 144-150. doi:10.1061/(ASCE)0887-3828(2003)17:3(144)

Warner, R. F., & Faulkes, K. A. (1988). *Prestressed Concrete*. Melbourne: Longman Cheshire.

Warner, R. F., Rangan, B. V., Hall, A. S., & Faulkes, K. A. (1998). *Concrete Structures*. South Melbourne: Longman.

Weckendorf, J., Zhang, B., Kermani, A., & Reid, D. (2006). *Assessment of Vibrational Performance of Timber Floors*. Paper presented at the WCTE 2006-9th World Conference on Timber Engineering, Portland, OR, USA.

Williams, G., Bohnhoff, D. R., & Moody, R. C. (1994). *Bending properties of four-layer nail-laminated posts*: US Department of Agriculture, Forest Service, Forest Products Laboratory.

Worth, M. L., Omenzetter, P., & Morris, H. (2012). *Ambient and Forced Vibration Testing and Finite Element Model Updating of a Full-scale Post-Tensioned Laminated Veneer Lumber Building*. Paper presented at the 2012 NZSEE Conference, New Zealand.

Xue, W., Ding, M., He, C., & Li, J. (2008). Long-Term Behavior of Prestressed Composite Beams at Service Loads for One Year. *Journal of Structural Engineering, 134*, 930-937.

Xue, W. C., & Li, J. (2001). *Studies on performance of prestressed steel-concrete composite beams*. Paper presented at the Our World in Concrete & Structures, Singapore.

Yu, Y., Chiew, S. P., & Lee, C. K. (2011). Bond failure of steel beams strengthened with FRP laminates - Part 2: Verification. *Composites: Part B, 42*(5), 1122-1134.